CENTER FOR GEOTECHNICAL MODELING

GROUND IMPROVEMENT ISSUES FOR THE POSEY & WEBSTER ST. TUBES SEISMIC RETROFIT PROJECT: LESSONS FROM PHYSICAL MODELING STUDIES

BY

D. P. STEWART
R. W. BOULANGER
I. M. IDRISS
Y. HASHASH
B. SCHMIDT

DEPARTMENT OF CIVIL & ENVIRONMENTAL ENGINEERING
COLLEGE OF ENGINEERING
UNIVERSITY OF CALIFORNIA AT DAVIS

APRIL 1997

1. Report No. Report No. UCD/CGM-97/04	2. Government Accession No.	3. Recipient's Catalogue No.	
4. Title and Subtitle Ground Improvement Issues for the Posey & Webster St. Tubes Seismic Retrofit Project: Lessons From Physical Modeling Studies		5. Report Date April 1997	
		6. Performing Organization Code n.a.	
7. Authors Douglas P. Stewart, Ross W. Boulanger, and I. M. Idriss, Youssef Hashash, and Birger Schmidt		8. Performing Organization Report No. n.a.	
9. Performing Organization Name and Address Douglas P. Stewart, Ross W. Boulanger, and I. M. Idriss Davis, California 95616 and Youssef Hashash and Birger Schmidt Parsons Brinckerhoff Quade & Douglas, Inc. 303 Second St., Suite 700 North, San Francisco, California 94107		10. Work Unit No. (TRAIS)	
		11. Contract or Grant No. 59X797	
12. Sponsoring Agency Name and Address State of California -- Business, Transportation and Housing Agency Department of Transportation Sacramento, California		13. Type of Report and Period Covered Final report	
		14. Sponsoring Agency Code	
15. Supplementary Notes			

16. Abstract

The design of ground improvement work to mitigate liquefaction hazards at the Posey and Webster Street Tubes was complicated by some relatively unique aspects of the project. Therefore, a detailed review of case histories and physical modeling studies was requested to address issues of relevance to the Posey and Webster Street Tubes Seismic Retrofit project. This report addresses "Lessons From Physical Modeling Studies," while a companion report addresses "Lessons From Case Histories."

17. Keywords Liquefaction, stone columns, gravel drains, in-ground walls, centrifuge, shaking table, physical modeling		18. Distribution Statement		
19. Security Classif (of this report) Unclassified	20. Security Classif. (of this page) Unclassified		21. No. of Pages 117	22. Price n.a.

Form DOT F 1700.7 (2-86)

GROUND IMPROVEMENT ISSUES FOR THE POSEY & WEBSTER ST. TUBES SEISMIC RETROFIT PROJECT:

LESSONS FROM PHYSICAL MODELING STUDIES

by
Doug P. Stewart, Ross W. Boulanger, I. M. Idriss
Department of Civil and Environmental Engineering, University of California, Davis, CA

Youssef Hashash and Birger Schmidt
Parson Brinckerhoff Quade & Douglas, Inc., San Francisco, CA

Report No. UCD/CGM-97/04

Center for Geotechnical Modeling
Department of Civil & Environmental Engineering
University of California
Davis, California

April 1997

TABLE OF CONTENTS

1. INTRODUCTION

Due to the difficulty of obtaining detailed field data on the performance of various structures under seismic loading, physical model tests have proven to be a valuable source of data. This is particularly true where liquefaction-induced damage occurs. Shaking table tests performed at increased gravitational fields on a centrifuge, or in the earth's gravitation field in a laboratory, have been used extensively around the world to study soil liquefaction. These studies were initially directed at understanding the development, extent and controlling factors relating to liquefaction, although recently more effort has been directed at assessing the impact of various remediation measures on limiting the effects of liquefaction. These studies have been performed primarily in Japan, and have attempted to simulate the effect of a range of ground improvement techniques.

This report presents a review of available physical model test data relating to the simulation of ground improvement techniques, and their performance in mitigating liquefaction-induced damage. The usefulness and limitations of the modeling techniques are critically reviewed, and the applicability of the data to the planning and design of the liquefaction hazard mitigation program for the Posey and Webster Street Tunnels in Alameda is assessed.

The Alameda Tubes consist of a pair of 37 foot diameter reinforced concrete tubes traversing the channel between Oakland and Alameda. Both tubes were placed in trenches that were backfilled with: (1) loose to medium-dense clean sand along most of the Webster St. tubes; and (2) soft, low-plasticity clay with zones of loose sand, silty sand, and sandy silt along most of the Posey tube.

Initial design proposals for mitigating the potential for liquefaction-induced deformations in the Alameda Tubes involved:

(1)   three rows of stone columns along each side of large lengths of the Alameda tubes; and
(2)   in-ground-walls formed by overlapping jet grout columns along each side of those portions of the Alameda tubes where stone column construction is not feasible.

The design of the ground improvement work, and an evaluation of its expected performance during future earthquakes, is complicated by some relatively unique aspects of this project. Thus, a detailed review of case histories and physical modeling studies was requested to address several issues of relevance to the Alameda Tubes project.

Findings of this study are presented in two companion reports, "Lessons From Case Histories" (Boulanger et al., 1997) and "Lessons from Physical Modeling Studies" (this report). This report is arranged in the following order:

(1) A review of physical modeling principles, scaling relationships and the limitations of the techniques.

(2) A review of the available experimental data broken into sections dealing with (a) experiments without structures, i.e. the effect of ground improvement in isolation; (b)

1-1

experiments with above ground structures; and (c) experiments with below ground structures. At the end of each section a summary of the data is presented, with a comparison between the studies where possible.

(3) A summary of the data relating to different methods of ground improvement, applicability of the data to the Posey and Webster Street tubes, and a discussion on the feasibility of conducting further physical model tests.

Recommendations regarding the proposed ground improvement work for the Alameda Tubes project are outlined by Boulanger, Idriss and Stewart (1997) and have been drawn from the findings presented in this report and the companion report on case histories.

2. MODELING CONSIDERATIONS

2.1. Shaking Table Tests at Unit Gravity

Shaking table tests at unit gravity can be useful to study geotechnical response under seismic conditions. The tests are conducted on models scaled down often no more than 1/10 from the prototype size. By defining the scaling factors for length, density and acceleration, scaling of the fundamental measures of length, mass and time are determined. From these factors, scaling relationships for other properties of the model can be readily derived. The scaling relationships derived in this way for shaking table tests at unit gravity are listed in Table 2.1, where λ is the scaling factor for length. The scaling relationship for time relating to diffusion is derived from the governing equation for consolidation, and is controlled by the reduction in length of drainage paths.

The scaling factors listed in Table 2.1 for time relating to dynamic events ($\sqrt{1/\lambda}$) and to diffusion ($1/\lambda^2$) are different. This conflict can be avoided by the use of a more viscous pore fluid to slow pore pressure dissipation. The non-dimensional time scale for diffusion is $T = c_v t/d^2$, where d is a relevant dimension, and c_v is the coefficient of consolidation of the soil. Thus by use of a more viscous pore fluid, c_v will be reduced, and the time scaling for diffusion will be altered. To equate the time scales for dynamic events and diffusion, c_v must be reduced by a factor $1/\lambda^{3/2}$. For example, a 1/5 ($\lambda = 5$) scale model would require a reduction in model c_v (achieved by an increase in pore fluid viscosity) by a factor of about 11.

Many shaking table studies have used water as the pore fluid, and thus have effectively modeled a more permeable prototype soil than used in the model. Some publications appear to have scaled the input frequency of the shaking motions to achieve a match between dynamic and diffusion time scales. This may appear attractive, but the natural period of the soil and the structure must also be scaled by this factor, and thus some difficulty in interpreting the results may be experienced as the soil's natural period is controlled by its stiffness and dimensions.

In shaking table tests at unit gravity, the soil in the model is confined under low effective stress levels. Therefore, the stress-dependent behavior of soil must be assessed in some way if the results are to be extrapolated to a prototype situation. However, comparison of results between experiments, and the provision of test data for comparison with numerical analysis is valuable. Clearly, the deeper the sample that can be tested on the shaking table, the closer the stress levels will become to those experienced in real field situations, and the more appropriate the extrapolation of results to prototype structures. Several issues relating to soil response under low effective stress levels must be recognized, namely the effects of dilation and liquefaction potential. At low effective stress levels, even relatively loose sands may exhibit dilation during shearing, and this region undergoing dilation may be significantly larger in the model, or not present entirely in the prototype. Additionally, the variation of liquefaction potential with depth may be markedly different, as the gradient of effective stress with model depth is much smaller than in the prototype.

2.2. Centrifuge Model Tests

Due to the well understood stress-dependent behavior of soil, accurate modeling of geotechnical events should be performed with the model experiencing stress levels equivalent to those in the prototype. This will ensure similar soil behavior in the model and prototype. By rotating a scale model in a centrifuge, the centrifugal acceleration field will provide close similarity in self weight stresses throughout the model. This is achieved by reducing the dimensions of the model by a factor of n (the scaling factor), and providing a centrifugal acceleration field of n gravities. The self-weight of the soil is thus increased by a factor of n, and the vertical stress at any depth in the model will be similar to that in the prototype, since at any depth z:

$$\sigma_{v_{model}} = n\gamma\left(\frac{z}{n}\right) = \gamma z = \sigma_{v_{prototype}}$$

This technique is well established internationally, and is being used increasingly in earthquake geotechnical engineering research. Scaling relationships for centrifuge model tests have been published on a number of occasions, Schofield (1980) and Fuglsang and Ovesen (1988) for example, and are summarized in Table 2.2.

Similarly to shaking table tests at unit gravity, the scaling relationships for dynamic (1/n) and diffusion ($1/n^2$) events are in conflict. Following a similar approach to that described in the previous section, using a pore fluid in the model that is n times more viscous than the prototype, the two scaling relationships can both be made equal to 1/n. Sometimes centrifuge tests involving dynamic loading are conducted using water as the pore fluid, and in these cases a more permeable soil than that being used in the experiment is actually being modeled.

2.3. Common Modeling Limitations

There are limitations and qualifying conditions which must be recognized and may be common to all forms of geotechnical model testing. It may be impossible to satisfy all scaling relationships at once, and thus the critical modeling criteria need to be assessed and an attempt made to satisfy these. Some attempts need to be made at addressing the likely differences in model behavior arising from the inability to satisfy the other criteria. This problem is more often encountered with shaking table tests at unit gravity than with centrifuge model tests, due to the difficulty of modeling soil behavior at low stress levels.

While scale models are constructed by reducing the linear dimensions of a prototype structure, soil particle sizes are generally not scaled down as well. This may be particularly significant in centrifuge models, where scale factors of 50 to 100 are common. Thus a fine sand in the model may have a scaled particle size similar to gravel. This argument could be extended to clay size particles in a model that would scale up to represent a fine sand in the prototype. However, this is clearly flawed since the stress-strain behavior of clays and sands are markedly different. The usual approach is to use similar soil in the model as will exist in the prototype. This approach has arisen since it would be expected that there is some critical ratio between the particle size and a major dimension of the model at which particle size effects would cease to become significant. In other words, as the number of soil grains involved in the response of the model becomes larger,

the behavior will approach that of a continuum. On the basis of experimental evidence on shallow foundations, an approximate rule of thumb is that particle size effects will be significant when the ratio of structure dimension to grain size is less than about 15 to 20. However, in some cases the ratio of shear band width to particle size may be important, and this will impose more strict limitations on the exact scaling of results to a prototype situation.

All forms of geotechnical experimental modeling require a container to support the soil, and the effects of this container on the response of the model must be assessed. The container boundaries generally incorporate rigid walls which prevent normal displacements and may or may not allow shear stresses to develop. Additionally, in earthquake simulation experiments the container may inhibit the ability of the soil to deform in the same manner as the prototype soil deposit. To minimize these effects, the containers used in most recent earthquake simulation experiments incorporate flexible side walls to allow the container to deform laterally with the soil layer while having minimal shear stiffness. The containers should also incorporate some means of sustaining complementary shear stresses along the end walls of the container, so that the stress distribution in the model soil deposit is relatively uniform.

Field construction processes are often very important in determining the performance of a constructed facility. Model testing undertaken to study these processes should attempt to reproduce the main features of the prototype. However, the technical difficulty and expense associated with attempting to model field construction procedures may be prohibitive, and therefore it may be necessary to study various aspects of the prototype in isolation. For example, a centrifuge model test examining the effects of stone columns on the response of a structure should ideally include installation of the columns under the correct in situ stress regime so that the compaction induced stresses are modeled correctly. Compaction or installation of stone columns at unit gravity prior to a centrifuge experiment induces small compaction stresses, which are incorrectly scaled upon subsequent spin-up in the centrifuge. Nevertheless, the model tests may still be valuable in assessing the influence of the stiffening and draining effect of the columns as long as the limitations are recognized.

Table 2.1 Selected scaling relationships for shaking table tests at unit gravity

Parameter	Scale factor (model/prototype)
Length	$1/\lambda$
Density	1
Stress	$1/\lambda$
Modulus	$1/\lambda$
Acceleration	1
Time (dynamic)	$\sqrt{1/\lambda}$
Time (diffusion)	$1/\lambda^2$
Frequency	$\sqrt{\lambda}$
Period	$\sqrt{1/\lambda}$

Note: λ is the scaling factor for length.

Table 2.2 Selected scaling relationships for centrifuge model tests

Parameter	Scale factor (model/prototype)
Length	$1/n$
Density	1
Stress	1
Modulus	1
Acceleration	n
Time (dynamic)	$1/n$
Time (diffusion)	$1/n^2$
Frequency	n
Period	$1/n$

Note: n is the scaling factor for length, and the centrifugal acceleration.

3. OVERVIEW OF EXPERIMENTAL DATA

A total of twenty three experimental investigations are summarized in this report, as shown in Table 3.1, grouped by the experimental technique. These comprise sixteen series of shaking table tests at unit gravity, six series of centrifuge model tests and one series of in situ tests. The investigations all relate to the assessment of some form of ground improvement to provide either individually or combinations of: (a) densification; (b) reinforcement or stiffening; or (c) drainage capability. The tests were all conducted on loose and generally relatively clean sand deposits.

The investigations are individually summarized in more detail in tables and figures contained in Appendix A. The tables list the following:

- Type of structure,
- Method(s) of treatment,
- Modeling technique,
- Sample size,
- Base shaking acceleration,
- Base shaking motion and frequency,
- Sand particle size,
- Relative density of the sand,
- Pore fluid used,
- Details about the testing program, and
- Summary of the results.

The investigations are also described individually in the next sections of this report, grouped by the type of structure incorporated in the experiments: (a) none; (b) above ground structures such as tanks and embankments; and (c) below ground structures such as tunnels, pipelines and semi-buried road structures. The studies have been grouped in this way, as those relating to below ground structures are of direct relevance to the Posey and Webster Street Tubes, and are described in more detail. However, tests incorporating other forms of structures are also valuable as they provide indicative data on the likely performance of various ground improvement measures. In some test series, several forms of ground improvement or two types of structures were examined, while one series included both shaking table and centrifuge model tests.

Where possible, the experimental data are presented in prototype units. However, the scaling factor was not reported for many of the shaking table tests at unit gravity. Thus some data are unavoidably presented in model units and then expressed in a dimensionless ratio to allow some comparison with full scale installations.

Table 3.1 Summary of experimental data

No.	Structure type	Relative density, D_r (%)	Method(s) of treatment	Modeling technique	Base acceleration	Reference
1	Surface structure	40	Gravel drains	Shaking table	0.06 g	Tokimatsu and Yoshimi (1980)
2	None and semi-buried road	42 to 58	Gravel drains	Shaking table	0.2 g	Sasaki and Taniguchi (1982a, 1982b)
3	Surface footing	50	Densification	Shaking table	0.1 g	Hatanaka et al. (1987)
4	Manhole	40	• Dewatering • Gravel drains • Gravel drains with sheet pile wall	Shaking table	0.03 to 0.22 g	Yagi et al. (1989)
5	Buried pipeline	30	Compaction	Shaking table	0.08 to 0.12 g	Tohma et al. (1990), Tanaka et al. (1995)
6	Embankment and semi-buried road	60	Stiff impermeable inclusions	Shaking table	0.05 to 0.34 g	Koga et al. (1991)
7	Embankment	40	Compaction	Shaking table	0.2 g	Yanagihara et al. (1991)
8	None	52	In-ground walls	Shaking table	0.5 g	Hamada et al. (1992)
9	Buried utility ducts	26 to 43	None	Shaking table	0.08 to 0.23 g	Tokida and Ninomiya (1992)
10	None and surface structure	26 to 35	Compaction	Shaking table	0.14 to 0.48 g	Taguchi et al. (1992)
11	None and pipeline	26	Gravel drains and compaction	Shaking table	0.06 to 0.3 g	Miyajima et al. (1992), Yoshida et al. (1993)
12	None	22	Sand compaction piles	Shaking table	0.1 g	Akiyoshi et al. (1993), Fuchida et al. (1995)
13	Embankment	60	Quick-lime consolidated briquette piles	Shaking table	0.2 g	Ito et al. (1994)
14	Buried pipelines and manholes	90	Variable extent of loose backfill	Shaking table	0.25 & 0.4 g	Yasuda et al. (1995)
15	None	50	In-ground walls	Shaking table	0.2 to 0.3 g	Kawakami (1996)
16	Tunnel and embankment	42 to 58	Sheet pile walls with and without drainage	Shaking table	0.15 to 0.3 g	Tanaka et al. (1996)
17	Embankment and semi-buried road	60	Stiff impermeable inclusions	Centrifuge test at 30 g	0.18 g	Koga et al. (1991)
18	None	52	Deep cement mixing - grid shaped walls	Centrifuge test at 100 g	0.2 g	Suzuki et al. (1991)
19	None	not stated	Deep cement mixing - grid shaped walls	Centrifuge test at 100 g	0.2 g	Babasaki et al. (1991)
20	Surface footing	34 to 76	Vibrocompaction	Centrifuge test at 50 g	0.17 to 0.36 g	Liu and Dobry (1994), Dobry et al. (1995)
21	Tunnel	35 to 51	• Gravel drains • Sheet pile walls • Sheet pile walls with drainage	Centrifuge test at 50 g	0.2 & 0.5 g	Kimura et al. (1995)
22	Oil storage tank	43 to 49	• Gravel drains • Sheet pile walls • Sheet pile walls with drainage	Centrifuge test at 50 g	0.12 to 0.21 g	Kimura et al. (1995)
23	None	N = 3 to 15	Gravel drains	Insitu test	-	Onoue et al. (1987)

4. EXPERIMENTS WITHOUT STRUCTURES

4.1. Study No. 23

Onoue et al. (1987) performed six in situ tests to assess the drainage capacity of gravel drains. Steel pipes of 1.2 m diameter were first driven slowly to a depth of 11 m. Then gravel drains of diameters between 0.3 and 0.5 m diameter were formed in the center of the soil column enclosed by the pipes to 10m depth. The drains were constructed by augering a hole, and then placing a filter cloth sock enclosing the gravel, to prevent ingress of fines and sand. One test was performed without the filter cloth. The steel pipes were then vibrated vertically to induce liquefaction in the soil surrounding the drains. Permeability data indicated a permeability ratio $k_w/k_s = 400$, where k_w is the permeability of the drain and k_s is the permeability of the soil.

One of the tests was performed without a central drain, and pore pressure measurements indicated that liquefaction of the sand column had occurred. In the tests with central gravel drains, the generated excess pore pressure was found to reduce with increasing pile diameter as the ratio d_w/d_e increased, where d_w is the drain diameter and d_e is the diameter of the tributary volume for the drain (the internal diameter of the steel pipe in this case). At any depth the measured pore pressure was found to be virtually constant with radius, with a very slight gradient towards the drain, indicating significant resistance to flow in the drain.

The in situ drain permeability was also derived from pore pressure recordings during and after vibration. When the filter cloth was not used around the drain, the permeability was found to reduce by about 60 % due to clogging, and liquefaction of the drain itself also occurred.

The test data showed that resistance to fluid flow within the drain (well resistance) was high, and that this should be incorporated in the design method. A derivation of the design equations with the inclusion of well resistance was presented along with a comprehensive guide to the recommended design procedure. The calculation method was shown to yield good agreement between the experimentally measured excess pore pressures. Using this approach, an example calculation was shown for 0.5 m diameter drains of 14 m length, with $k_w/k_s = 1400$. The drain spacing determined from Seed and Booker's (1977) method (ignoring well resistance) was 1.6 m, while inclusion of well resistance in the calculation gave a spacing of 0.95 m. Using a square grid, this suggests that the Seed and Booker approach would lead to an underestimate of the required number of drains by a factor of about 3 in this hypothetical case.

More discussion on the design procedure is given in a companion report, along with design diagrams developed by Onoue (1988) subsequent to the above field study. For cross reference, the drain resistance for full penetration drains is represented by the non-dimensional factor: $L_w = 3.24 (k_s/k_w)(H/d_w)^2$, where H is the length of the drains. $L_w = 0$ corresponds to a perfectly permeable drain, while $L_w = \infty$ corresponds to an impermeable drain. For the field study described here, $L_w = 1$ to 3. Onoue et al. (1987) found that excess pore pressures predicted using Seed and Booker's approach were on average only 8 % of the recorded values.

4.2. Study No. 2

Sasaki and Taniguchi (1982a, 1982b) describe a series of large shaking table tests performed on samples 12 m in length, 2 m in width and 3 m in depth. Four tests were performed: (i) no ground treatment, (ii) a single full penetration gravel drain, (iii) two full penetration gravel drains at 2.4 m spacing, (iv) two half penetration drains at 2.4 m spacing. To simplify later analysis of the tests, the drains were constructed as two-dimensional walls of 0.4 m width across the sample container. These drains comprised a 0.2 m wide core of gravel ($D_{50} = 22$ mm), with a filter shell on either side consisting of fine gravel ($D_{50} = 3.3$ mm). Quoted permeability values indicated a permeability ratio $k_w/k_s = 5000$ for the core, and $k_w/k_s = 500$ for the filter shell. The models were subjected to 0.2 g shaking levels.

Relatively rapid dissipation of pore pressures immediately adjacent to and within the drains was observed during shaking. Although in the untreated areas, sand boils were observed. In the test with a single drain, the zone of dissipation was observed to be limited to about 0.5 m from the center of the drain, or 0.3 m from its edge. It was found that even relatively close to the drains, generation of pore pressure was not slowed or reduced markedly by the gravel drains. However, with two full penetration drains, the soil between the drains experienced a slightly slower rise in excess pore pressure during the shaking event, and faster dissipation after the event. In this region, excess pore pressures were on average about 15 to 20 % lower than in the free field during shaking.

While the drainage walls in these tests are different in geometry from usual installations, and Onoue's (1988) design method can not be directly applied, some attempt can be made to assess the efficiency of the drains. If the wall thickness is used as the approximate drain diameter, then using permeability for the drain core, $L_w = 0.04$. While this calculation is clearly approximate, it suggests that drain resistance was slight in these tests.

As part of the same series of tests, two models were tested with semi-buried road structures; these are described in section 6.1 below.

4.3. Study No. 8

Hamada et al. (1992) reported a shaking table test on a sample of liquefiable sand containing a rigid in-ground wall across the full width of the sample container, perpendicular to the direction of shaking. The ground surface was sloped at a gradient of 2 %.

The data showed that when the soil liquefied, the pressures acting on the walls were very close to the static liquefied soil pressure (the total stress). The pressure was slightly higher on the upstream face as the soil attempted to flow over the wall, and slightly lower on the downstream face as the ground surface settled and soil flowed away from the wall. In this case, the total external force acting on the wall was relatively small. However, with more steeply sloping topography, or with some other effect such as the surcharge or uplift loading of an adjacent structure, it is possible that much higher forces could be transmitted to the wall.

4.4. Study No. 10

Taguchi et al. (1992) described a series of four shaking table tests examining behavior at the boundary between a liquefied soil deposit and a non-liquefied region within it. The non-liquefied region was formed from a relatively dense sand. The models comprised: (i) a loose deposit of fine sand with a central region at higher density; (ii) a loose deposit of fine sand with a central region of denser coarse sand; (iii) an entire deposit of dense fine sand; and (iv) the same arrangement as (i), but with thin rubber sheets at the dense/loose boundary to prevent water flow between the two regions. The shaking events comprised about 50 cycles of a sinusoidal motion.

In the models (i), (ii) and (iv), the loose deposit liquefied rapidly. Where water flow was not prevented, pore water pressures in the dense region rose gradually during the shaking event, reaching as high as $\Delta u/\sigma'_v = 0.8$ near to the boundary with the loose deposit, and reducing with distance from the boundary. The rate at which excess pore pressures in the dense region rose was found to reduce as the distance from the loose/dense boundary increased. When an impermeable barrier was placed at the loose/dense boundary, an excess pore pressure ratio of less than 0.2 was recorded in the dense region. In the model comprised entirely of dense soil, an excess pore pressure ratio of less than 0.05 was observed. The data clearly illustrated that the primary cause of pore pressure rise in the dense region was migration of high pore pressures from the liquefied deposit.

In model (i), surface settlement in the unimproved region was about 4 % of the soil thickness. The settlement reduced to about 3 % of the soil thickness close to the loose/dense boundary, although the reduction was limited to a small zone extending away from the boundary about 25 % of the soil thickness. In model (ii) the boundary between the loose and dense soils could be identified readily since the dense region was comprised of coarser sand. After the test the boundary was found to have displaced outwards due to some loss of lateral constraint when the loose soil liquefied. Over about the upper 35 % of the soil thickness, the outward displacement was greatest and the two sands were found to have mixed together near the boundary.

As part of the same series of tests, three models were tested with a surface surcharge; these are described in section 5.5 below.

4.5. Study No. 11

Yoshida et al. (1992) and (1993) performed two shaking table tests on loose soil ($D_r = 26$ %) with an improved region of soil at one end of the sample container. In one test, this comprised a denser zone of the same soil ($D_r = 52\%$), while in the other test the improved region was composed entirely of gravel. The width of the improved region was twice the loose soil depth and the width of the loose soil deposit was four times its depth. Quoted permeability values indicated a permeability ratio $k_w/k_s = 400$ for the gravel.

The results illustrated that higher excess pore pressures were generated in the unimproved region when improvement was performed by densification. Liquefaction of the unimproved region occurred under 0.1 g shaking levels. When the gravel drainage zone was incorporated, lower excess pore pressures were generated and dissipation was more rapid close to the improved zone.

4-3

Settlement of the soil surface was similar for both treatment methods for 0.1 g shaking levels. Under 0.08 g shaking levels, settlements were lower when the gravel was used. However, this comparison may be affected by the sequence of the input motions applied in the tests. Surface settlements were lower close the improved region, out to a distance away from the improved boundary roughly equal to the depth of loose soil. For a 0.1g event, surface settlements in the unimproved region were about 4 % of the soil depth, while close to the improved boundary, settlements were 2 % with compaction, and 0.5 % for drainage. These differences are likely to be due primarily to differences in stiffness of the two improved regions, since the compacted soil was still relatively loose.

4.6. Study No. 12

Akiyoshi et al. (1993) and Fuchida et al. (1995) performed three shaking table tests; one with no ground treatment, and two with sand compaction piles installed with differing levels of compactive effort. The untreated sand had a relative density of 22 %, while the sand compaction piles themselves had a relative density of 40 to 50 %. The compaction piles were installed to about 60 % of the depth of the sand deposit and at a spacing of 2.8 pile diameters. Almost the entire sample volume was treated in this way.

Limited experimental data were presented. The unimproved model was found to liquefy rapidly during shaking. The model with compaction piles installed with the lower compaction force reached liquefaction more gradually, while the model with the higher compaction force did not liquefy during the test. Numerical analysis was used to study the generation and migration of excess pore pressures and the effect of the lateral extent of the improved area. The analyses suggested the optimum treatment width of about 2 to 2.5 times the treated depth would lead to minimal pore pressure generation within the improved area.

4.7. Study No. 15

Kawakami (1996) performed several shaking table tests on a single in-ground wall extending across the central quarter of the testing container. The soil surface was sloped so that lateral flow around the wall would occur when the soil liquefied during shaking. Forces acting on the wall due to pressure from the liquefied soil were measured, and were found to be close to the total stress, as in Hamada's study. Pressures from flow of liquefied soil were influenced slightly by the initial gradient of the soil surface and the depth of liquefied ground (where a non-liquefiable layer was placed at the surface). The difference in soil pressure acting on the upstream and downstream sides of the wall was generally less than 20 %. Where a soil layer at the surface was not liquefied, the pressure developed in this layer on the upstream face of the wall was somewhat higher, since a passive wedge failure was then generated.

4.8. Study No. 18

Suzuki et al. (1991) performed four centrifuge model tests on loose sand samples containing cellular grid shaped in-ground walls formed by the deep cement mixing method. The width of the cells normal to the direction of shaking was varied. The presented data concentrated on the recorded pore pressure response within the cells formed by the walls. The data illustrated a clear

relationship between the wall spacing across each cell normal to the direction of shaking, and the measured excess pore pressure ratio within the cell. Although there was some scatter in the data, for a fully submerged soil deposit, cell widths of less than the liquefiable soil depth were required to reduce pore pressures and prevent liquefaction. For cell widths less than this value, the excess pore pressures reduced rapidly.

4.9.   Study No. 19

Babasaki et al. (1991) performed two centrifuge model tests using intact soil samples from a field site. One sample was tested without improvement, and cellular grid shaped in-ground walls were constructed using the deep cement mixing method in the other sample. Wall spacing in each cell was varied in the direction of shaking in contrast to Suzuki et al.'s (1991) experiments. The cell width normal to the direction of shaking was equal to the liquefiable soil depth.

The unimproved model liquefied during the 0.2 g shaking event. However, within the in-ground walls, excess pore pressures were lower within each cell, with $\Delta u/\sigma_v' = 0.5$ to 0.6 in each cell. While the data showed that the walls led to a reduction in the generated excess pore pressure, the values were similar for all wall spacings. No distinct relationship between wall spacing and excess pore pressure ratio was evident. These observations coupled with those of Suzuki et al. (1991) suggest that in-ground walls derive their benefit (in terms of reducing generated pore pressures) primarily from the shear stiffness of the walls aligned with the direction of shaking.

4.10.   Summary

The data described in this section can be broadly summarized as:

- Resistance to flow in drains is very important and can be characterized by a drain resistance factor, L_w. Values of L_w as low as 1 to 3 were found to give much greater values of excess pore pressure ratio than predicted by the commonly used approach proposed by Seed and Booker (1977).

- During a shaking event, the effective zone of pore pressure dissipation adjacent to a drainage boundary may be quite narrow, but will depend upon the permeabilities and geometry in any particular situation.

- Densification reduces the magnitude of potential soil strain due to a given shaking event. In one study, a reduction in surface settlement adjacent to a treated area was found to extend out to a distance about equal to the thickness of the liquefiable soil layer, with the reduction in strain reducing with distance from the boundary. However, in another study the reduction in settlement was less significant and more localized.

- The optimum treatment width for densification is suggested to be about twice the treated depth.

- For in-ground walls in gently sloping ground, the lateral stress from flow of liquefied soil is slightly higher than the total stress. However these forces could be dramatically increased by

interaction with an adjacent structure, or from earth pressures from an overlying non-liquefied stratum.

- Cellular in-ground walls appear to derive most of their benefit from shear stiffness of walls parallel to the direction of shaking.

5. EXPERIMENTS WITH ABOVE GROUND STRUCTURES

5.1. Study No. 1

Tokimatsu and Yoshimi (1980) described one of the earliest studies into the effect of gravel drains on soil liquefaction mitigation. A surface structure was placed on loose sand and subjected to small levels of shaking (0.06 g), using a shaking table. One test was conducted without improvement, and one test with a single row of gravel drains adjacent to each side of the structure. It is not clear whether the drains were modeled as a wall, or as individual columns. Permeability of the drainage material was not quoted. The drain width was a quarter of the thickness of liquefiable soil.

Limited data were presented, although it was shown that gravel drains were able to reduce the excess pore pressures beneath the structure to about 30 % of those recorded in the unimproved case. In the test without drains, pore pressures beneath the structure were observed to continue to rise after the shaking event due to migration from the free field. However, with the inclusion of drains, pore pressures began to drop immediately at the end of the shaking event. Pore pressures recorded adjacent to the structure were relatively unaffected by the incorporation of drains, although dissipation after the shaking event was faster. Drains were found to reduce settlement of the structure to about 10 % of the unimproved case, although the magnitude of the settlements was not quoted.

5.2. Study No. 3

Hatanaka et al. (1987) conducted thirteen shaking table tests on samples of relatively loose sand ($D_r = 50$ %) containing a dense block ($D_r = 90$ %) of the same soil, with a concrete structure resting on the surface. The models were subjected to 0.1 g shaking levels. A range of structure sizes and densified areas were tested. Data were presented primarily as plots of the footing settlement versus the extent of the densified region.

The results showed a reduction in footing settlement with increasing width of dense region. The improvement approached a limit when the ratio of width to depth of the dense region equaled 2. Also, the optimum lateral extent of compaction beyond the edge of the structure was identified as being about half of the depth of the compacted region. The improvement in performance was influenced by the width of the structure, and was most dramatic for narrow structures. Minimal footing settlement occurred when the excess pore pressure ratio ($\Delta u/\sigma_v'$) beneath the structure was less than 0.2. Beyond this ratio, the amount of settlement was influenced strongly by the extent of the densified region.

5.3. Study No. 6 & 17

Koga et al. (1991) performed a large shaking table test with an embankment on improved ground, and two centrifuge model tests with an embankment resting on improved and unimproved ground. Ground improvement was incorporated as stiff impermeable inclusions placed into the sand adjacent to the toes of the embankments. The inclusions appear to have been

fabricated from thin steel plate boxes filled with sand, to approximately model some form of stiff impermeable ground treatment; possibly jet grouting or deep cement mixing for example.

Very limited data were presented. In general, qualitative agreement between the two types of tests was observed. During the initial stages of the shaking events, pore pressures beneath the embankment were observed to drop, before gradually increasing during the event to close to the original static value. Liquefaction of soil adjacent to the embankment occurred, while soil below the embankment did not. Improvement adjacent to the embankment had little impact on the measured pore pressures, otherwise no comments were given on the effect of the improvement scheme.

5.4.   Study No. 7

Yanagihara et al. (1991) reported three shaking table tests on embankments resting on a liquefiable layer. One test was performed on unimproved ground, one with a compacted zone beneath the batter slope of the embankment, and one test with a compacted zone adjacent to the toe of the embankment. The unimproved ground was sand of 40 % relative density, while the improved region was compacted to 80 % relative density.

In all tests, liquefaction was observed in the free field soil. In the unimproved test, liquefaction was not observed beneath the embankment, due to the higher effective stress level. With a compacted zone beneath the batter slope of the embankment, liquefaction also did not occur beneath the embankment, although gradual migration of excess pore pressures from the free field into the compacted zone was observed during shaking. With the compacted zone adjacent to the toe of the embankment, a region of liquefaction was observed beneath the batter slope, and dilation of the compacted region was evident. Liquefaction beneath the batter slope led to the development of sand boils through the embankment toe, where the confining stresses were lowest. This in turn gave rise to excessive settlement of the embankment, even though lateral deformations were reduced considerably.

In both tests incorporating ground improvement, the lateral deformations were reduced to about 20 mm at model scale (10 % of the value recorded for unimproved ground). While the scale of the models was not reported, it is likely to be in the vicinity of 1/10. Following the shaking events, the model without improvement and the model with improvement adjacent to the toe could be considered to have failed due to the large deformations. However, with improvement beneath the batter slopes of the embankment, the structure was still in a serviceable state.

5.5.   Study No. 10

Taguchi et al. (1992) reported the results of three shaking table tests with a surface surcharge load resting on dense regions of soil within a loose deposit. The width of the dense region was varied: 1.0, 1.6 and 2.0 times the width of the surface load, with the load positioned centrally. Excess pore pressure data during shaking events was presented.

During the shaking events, pore water pressures were initially observed to drop in the soil below the surface load. Both the magnitude of the negative excess pore pressure and the length of time

it remained negative were found to increase as the width of the dense region increased. After about 5 cycles of shaking, excess pore pressures in the dense soil near to the loose/dense boundary were higher for the wider improved regions, probably because the surface load was further away and thus the effective stress was lower. However, after about 30 cycles of shaking the excess pore pressure distribution adjacent to the loose/dense boundary was found to be virtually identical in all tests, independent of the position of the surface load. In this study the gradual rise in pore pressure in the improved (dense) region was clearly due to migration of excess pore pressures from the liquefied soil.

While it is difficult to draw general conclusions from these data, relatively high excess pore pressures ($\Delta u/\sigma_v' = 0.5$ to 0.8) were recorded in the dense soil within a distance from the loose/dense boundary of about half the liquefiable soil thickness. Further away from the boundary the excess pore pressures approached a plateau at $\Delta u/\sigma_v'$ of about 0.3. For these tests, the optimum treatment width adjacent to the structure could be identified as extending out to about half the liquefiable soil depth away from the edge of the structure. No data were presented to illustrate the effect of improvement width on surface settlement.

5.6.   Study No. 13

Ito et al. (1994) carried out three shaking table tests on embankments resting on a liquefiable sand layer. In two of these tests, quick-lime consolidated briquette (QCB) piles were installed beneath and adjacent to the embankment to 80 % of the soil depth. The piles were placed at a spacing of five pile diameters.

The QCB piles led to slightly reduced accelerations being recorded on the embankment. Soil in the free field liquefied in all tests and led to noticeable deformations near the boundary between the treated and untreated area. Excess pore pressure generation beneath the embankment was reduced to values of about half those recorded in the untreated case, as the stiff piles attracted stress from the weaker surrounding ground. Settlement of the embankment was reduced by the QCB piles to about 10 % of the unimproved value. The settlements with QCB piles were about 3 % of the loose sand thickness.

5.7.   Study No. 16

Tanaka et al. (1996) performed five shaking table tests with embankments on a loose sand layer. The loose sand was underlain by a dense sand stratum. The tests comprised: (i) no improvement, (ii) sheet pile walls below the toes, (iii) sheet pile walls with drainage, (iv) sheet pile walls with drains of reduced flow capacity, and (v) sheet pile walls with tie rods between the heads of the walls through the base of the embankment.

Sheet pile walls led to a moderate improvement in performance of the embankment. Settlement of the embankment was reduced to only about 75 % of the unimproved case by the addition of sheet pile walls. Both the test where a tie rod between the heads of the walls was included, and where free draining elements were incorporated into the wall led to settlements of about 40 % of the unimproved case. Drainage elements of reduced capacity led to performance mid way between the sheet piles without drainage holes and the more freely draining sheet piles.

5.8.   Study No. 20

Liu and Dobry (1994) and Dobry et al. (1995) performed centrifuge model tests with a circular footing resting on the surface of a loose sand deposit. A vibrating tube was inserted on a square grid pattern at unit gravity to densify a region of soil beneath the footing. While this approach was presumably intended to model the field process of vibrocompaction, the confining stresses at unit gravity are small, and thus only relatively small horizontal stresses resulting from compaction can be sustained. Therefore it must be contended that only densification effects are being modeled, not the effects of increasing horizontal stresses.

The depth of the improved region was varied between experiments, while the width of improvement was maintained at 1.6 times the footing diameter. By reference to footing settlements, for this width of improvement the optimum depth of compaction was identified as 1½ to 2 times the footing diameter. However the liquefied soil depth was only 2.7 times the footing width. Higher accelerations were recorded on the footing when the ground was densified. Dilation of soil below the footing was evident during the initial stages of shaking, although gradual migration of excess pore pressures from the free field into the region below the footing occurred during the shaking event. Pore pressures at some locations in the soil were observed to continue to rise after the shaking event, due to stress redistribution and migration of high excess pore pressures. This study also compared the results of tests on unimproved ground using pore fluids of different viscosities, and found that greater positive and negative pore pressures were generated with a higher viscosity fluid. The higher viscosity also led to less settlement occurring during the shaking event, but greater consolidation settlements after the event.

5.9.   Study No. 22

Kimura et al. (1995) described a series of centrifuge model tests of an oil storage tank resting on a loose sand deposit. Seven tests were performed: (i) two with unimproved ground, (ii) one row of gravel drains adjacent to the tank, (iii) three rows of gravel drains, (iv) sheet pile walls, and (v) sheet pile walls with drainage capability. For the gravel drains, $L_w = 3.2$. This was a parallel study to Kimura et al.'s investigation of tunnels, described in section 6.7. The prototype tank width was 7 m.

The magnitude of excess pore pressures generated beneath and adjacent to the tank were about 50 % lower than recorded in the unimproved model in both the test with three rows of gravel drains and also the test with sheet pile walls with drainage capability. Similar pore pressures to those developed in the unimproved model were recorded in the other tests, although high pore pressures were recorded adjacent to the tank where standard sheet pile walls were used. This occurred because the walls were able to carry load from the tank and thus reduced the mean stress in this area. All tests on improved ground performed similarly in terms of settlement reduction, with settlements of about 70 % of the unimproved case. However slightly larger average settlement and much higher differential settlements were observed with only one row of gravel drains. Suppression of lateral displacements (by three rows of drains or sheet piles) was identified as being important in reducing total and differential settlements.

Three rows of gravel drains were found to perform significantly better than a single row, approximately halving the excess pore pressures beneath and adjacent to the tank, and virtually eliminating differential settlements. With three rows of drains the treated width on each side of the structure was just under half the liquefiable soil depth, while with one row the treated width was only 15 % of the soil depth.

5.10. Summary

5.10.1. Comparison of sheet pile wall stiffness

To enable some comparison between various studies incorporating sheet pile walls and extrapolation to field applications, the wall stiffness, length of span through liquefiable soil and fixity conditions need to be accounted for. The maximum deflection of a uniformly loaded beam (δ) is described by the following equation:

$$\delta = \frac{\alpha P l^3}{EI}$$

where α is a factor that varies according to the end fixity conditions and distribution of the load, P is the total supported load, l is the beam span, and EI is the bending stiffness. Separating the effects of load distribution and end fixity, this could be rewritten :

$$\frac{\delta}{l} = \frac{\alpha w (\beta l)^3}{EI}$$

where β varies according to end fixity and w is the distributed load (force/unit length).

Denoting the expression $EI/w(\beta l)^3$ as K_{wall} (ie. $\delta/l = \alpha/K_{wall}$), this factor could be used to characterize the behavior of the walls, where l is the span length in a liquefiable soil layer. The distributed load carried by the wall can be estimated from the applied surcharge pressure from the surface structure, or the buoyancy of a subsurface structure. Values of β can be readily derived from beam deflection solutions, by nominally assigning $\beta = 1$ for a cantilever:

end fixity conditions	β
fixed, free	1
fixed, pinned	0.5
pinned, pinned	0.8

The studies described by Tanaka et al. (1996) and Kimura et al. (1995) are compared using the above approach in Table 5.1 below.

Table 5.1 Comparison of sheet pile wall performance for surface structures

Study No.	Conditions	Estimated K_{wall}	Settlement as % of liquefiable soil thickness	Settlement as % of unimproved case
16	no drainage	7	14	74
	drainage	7	9	52
	no drainage	60	7	40
22	no drainage	8	2	72
	drainage	8	2	69

5.10.2. Summary

The studies described in this section examined the performance of surface structures and can be broadly summarized as:

- In several studies, drains adjacent to the structure gave improved performance, with improvement reducing with increasing shaking event magnitude.

- In one study, three rows of drains rather than one approximately halved excess pore pressure beneath the structure and almost eliminated differential settlements.

- Studies into the effect of densification suggested that the optimum treatment width was about twice the depth of treatment, and that the optimum compaction width beyond the edge of a structure is approximately half the depth of treatment.

- Where densification was performed adjacent to, but not beneath a structure, it was shown that excess pore pressures could be trapped and may lead to sand boils developing if there was insufficient confining stress.

- Sheet pile walls have been studied as a means of providing a barrier to pore pressure migration and to provide an overall stiffening of the soil mass. Settlement reductions of about 25 to 30% were experienced. Adding drainage elements to the walls provided additional benefit in one study. In another study, drainage elements provided little benefit, although in this case the magnitude of settlement without improvement was only about 3 % of the liquefiable soil depth, as opposed to about 18 % in the previous study.

- Increasing the effective stiffness of the sheet pile walls by including tie rods between the heads of the walls gave much improved performance.

6. EXPERIMENTS WITH BELOW GROUND STRUCTURES

6.1. Study No. 2

Sasaki and Taniguchi (1982a, 1982b) reported shaking table tests on a semi-buried road structure, as part of the series of experiments described in section 4.2. The structure was 2 m in width and 1 m in depth, and had an apparent specific gravity of 1.07. The loose soil depth was 3 m. Two experiments were performed, one with no improvement, and one with a gravel drainage mat along the base of the structure and full penetration gravel drains (modeled as walls) installed alongside the structure. The construction detail of the drains was the same as that described in section 4.2, and thus drain resistance was likely to have been small.

The drains were observed to reduce heave of the structure to about 25 % of the unimproved case, although the amount of displacement was still relatively large (5 % of the structure height). Pore pressures were observed to rise at a slower rate and dissipate more rapidly in the vicinity of the gravel drains. The results suggested that while the drainage mat at the base of the road was able to dissipate high excess pore pressures immediately below the structure, the side drains prevented water flow from the free field into the region below the structure.

6.2. Study No. 4

Yagi et al. (1989) described shaking table tests aimed at assessing the impact of liquefaction on manholes situated below the water table. They performed a total of 5 tests examining:
(i) unimproved ground, (ii) dewatering to two levels below the surface, (iii) crushed rock backfill drainage around the manhole, and (iv) crushed rock drainage with sheet pile walls surrounding the manhole on all sides. The crushed rock drainage was only placed along the sides and under the base of the manhole. While permeability values were not quoted, k_w/k_s could be estimated as about 300 on the basis of the particle sizes. Therefore an approximate value of L_w for the drainage components is about 2. The sheet pile walls extended down to a level of three times the depth of the base of the manhole and were rigidly fixed at the bottom of the testing container. The manholes had an apparent specific gravity of 1.13.

In all tests, the soil surface settled, while the manhole generally heaved upward. In the test without any improvement measures, the amount of heave was 205 mm at prototype scale for 0.12 g input motion, and 280 mm for 0.22 g input motion. Where drainage was incorporated around the manhole, the heave was reduced to 20 and 35 mm respectively. Surrounding the manhole with sheet pile walls and providing drainage, led to 5 mm settlement for 0.12 g input motion, and 10 mm heave for 0.22 g input motion. However, this sheet pile arrangement was very stiff, modeling a 50 mm thick steel wall surrounding the manhole and fixed at the base. The estimated K_{wall} for this test is 6000, although this is a lower bound since shear stiffness of the walls parallel to the shaking direction would have dominated the response. The crushed rock drains led to slightly lower generated pore pressures below the manhole. The combination of sheet pile walls with crushed rock drainage was most effective overall, leading to the lowest values and slowest generation of pore pressures in the soil below the manhole.

6.3. Study No. 5

Tohma et al. (1990) and Tanaka et al. (1995) described four tests examining the behavior of two parallel subsurface pipelines. One test was performed on unimproved ground, with a further three tests incorporating a region of dense soil around the pipelines. The dense region extended laterally to 0.6, 0.9 and 1.2 times the soil thickness in these tests. The dense region extended to the base of the testing container.

In all tests, floatation of the pipelines was observed when the excess pore pressure ratio below the pipe reached 0.7 to 0.8. In the unimproved model, liquefaction occurred over the upper part of the soil deposit, however in the improved models the rate of increase and magnitude of excess pore pressures adjacent to the pipelines were reduced. Pore pressures in the dense region continued to rise after the shaking events due to pore pressure migration from the loose liquefied soil. A simple uplift analysis was coupled with the results of numerical predictions of excess pore pressures as the width of the dense zone was varied. This suggested that for a factor of safety against uplift of greater than 1.0, the minimum width of improvement is about 0.5 to 0.8 times the liquefiable soil thickness.

6.4. Study No. 6 & 17

Koga et al. (1991) performed both a shaking table and a centrifuge model test on a semi-buried road structure, as part of the series of experiments described in section 5.3. The method of improvement was similar, with stiff impermeable inclusions placed in the soil deposit at the sides of the structures. In the shaking table test the apparent specific gravity of the road structure was 1.5, while it was 1.7 in the centrifuge test.

Very limited data were presented. During shaking, liquefaction of the entire soil deposit occurred in both tests. Little heave of the structure was recorded; the maximum heave during the shaking table test was about 10 mm prototype scale for shaking events up to 0.2 g. The final settlement of the structure after pore pressure dissipation was described as greater than the measured heave for input motions up to 0.15 g. For a 0.2 g event the settlement was of similar magnitude to the heave, although this may be due to densification of the sand during earlier events. No control test without improvement was reported, however the improvement was obviously successful in limiting heave of the road structures to small levels through partial isolation of pore pressures below the tunnel.

6.5. Study No. 9

Tokida and Ninomiya (1992) performed six shaking table tests on utility ducts buried in a liquefiable soil deposit. Three tests were performed on a square cross-section duct and three tests on a rectangular duct. The cover over the ducts was held constant in each test while the thickness of loose soil below the them was varied.

Vertical heave of the ducts was observed when the excess pore pressure below them exceeded about 0.8. The upward movement was found to reduce with decreasing thickness of liquefiable soil below the structure. Soil deformations observed from the displacement of lines of colored

sand indicated that heave of the structures was caused by flow of liquefied soil from the sides of the duct towards the base of the structure.

6.6. Study No. 11

Miyajima et al. (1992) and Yoshida et al. (1993) performed seven shaking table tests with a subsurface pipeline having two diameters of cover. One test was performed with no ground improvement, while the other six incorporated a single row of gravel drains on each side of the pipeline. The spacing of the drains normal and parallel to the pipe axis was varied between tests. The apparent specific gravity of the pipeline was 1.7. Quoted permeability values indicated a permeability ratio $k_w/k_s = 400$ for the gravel drains, with $L_w = 0.13$.

A reduction in drain spacing was found to reduce the rate of increase and the magnitude of generated excess pore pressures, and to speed the rate of dissipation. However, liquefaction was still able to occur between the drains in most tests. Gravel drains spaced at about two drain diameters appear to have suppressed liquefaction near the pipeline during a 0.2 g shaking event. These effects were slightly more pronounced for spacing in the direction normal to the pipe axis, although this may have been influenced by the location of the pore pressure transducers.

Ground surface settlements were found to reduce with decreasing drain spacing. The effect was observed to be roughly equivalent for spacing in either direction. Heave of the pipeline was about half the pipeline diameter when no improvement was performed. Gravel drains led to a substantial reduction in pipeline heave and a strong correlation with drain spacing along the axis of the pipe. The correlation of heave with drain spacing normal to the pipe axis was less clear, but appears to have been influenced by the effective width of treatment, since the width of soil being drained reduces as the spacing in this direction reduces. The smallest pipeline heave recorded was of the order of 3 % of the pipe diameter.

Dynamic strains recorded on the pipeline were found to increase with increasing excess pore pressure ratio ($\Delta u/\sigma_v'$) measured between the gravel drains. However, permanent strains were much lower in the unimproved case since the pipeline was not fixed at either end and was free to move with the soil.

6.7. Study No. 14

Yasuda et al. (1995) reported a series of tests examining the flotation of pipelines and manholes in homogenous unimproved ground. Only vertical displacement data were presented, illustrating the effect of pipeline specific gravity and soil density. Two tests where subsurface soil displacements were measured and plotted as displacement vectors clearly illustrated the mechanism leading to flotation of the structures. As the pipe or manhole moved upward due to buoyancy, soil adjacent to the structure moved downward and across into the area beneath the structure. The pattern of soil deformation extended further away from the pipeline than from the manhole. The displacement pattern around the manhole was similar in appearance to a bearing capacity failure around the tip of a pile (although in reverse).

In a number of tests, a two stage flotation mechanism was observed where the pipe initially rose rapidly and then slowed, before then heaving rapidly to its final position (often at the surface). This slowing in the rate of upward movement was more distinct for larger diameter pipes, and was attributed to the time required for large soil deformations to occur into the area below the pipe. However, it is also possible that rapid upward displacement of the pipe caused a local reduction in the pore water pressure beneath the pipe, thus reducing buoyancy until additional pore fluid could flow in.

Yasuda et al. (1995) also conducted shaking table tests on buried pipelines and manholes in dense saturated sand. The excavation for the pipe or manhole was backfilled with loose sand. Several tests were conducted, varying the width and depth of the backfilled excavation. In most tests a plastic sheet was placed at the boundary of the backfilled zone to prevent dissipation of excess pore pressures into the surrounding denser soil. In two tests the water barrier was removed to illustrate the effect of pore pressure drainage into the surrounding soil. The apparent specific gravity was 0.75 for the pipeline, and 1.0 for the manhole.

Only vertical displacement data were presented, and in some tests complete flotation of the pipeline occurred. The data illustrated that as the width of the loose backfill region was reduced, heave of the pipeline also reduced. Additionally, as the thickness of loose soil below the pipeline was increased, the pipeline heave increased. Placement of the pipeline directly at the base of the trench led to a heave of less than 10 % of the pipe diameter.

Removal of the drainage barrier for one backfill configuration caused a dramatic reduction in the recorded pipeline heave (from complete flotation to a movement of less than 10 % of the pipe diameter), as pore pressures were then able to dissipate partially into the surrounding soil. However, it is likely that water was used as the pore fluid in these experiments, and thus the rate of drainage may have been artificially high for the type of soil tested.

For the tests incorporating a manhole, the same final value of heave was recorded in all tests: approximately one third of the embedment depth of the manhole. The rate of vertical displacement during shaking was slowed by reducing the width of the backfill and the depth of over excavation, and by allowing drainage to occur. The response of the manholes was distinctly different from the pipelines, since the pipe had soil cover that provided some restraint on movement, but also because of the differences in the pattern of soil deformation during upward movement of the structures.

6.8.   Study No. 16

Tanaka et al. (1996) performed nine shaking table tests with a rectangular shaped tunnel within a loose sand layer. Three different thicknesses of the loose sand were tested for each of the following: (i) no improvement, (ii) sheet pile walls adjacent to the structure, and (iii) sheet pile walls with drainage. The total model soil depth was 0.9 m in all cases, with loose sand depths of 0.55, 0.7 and 0.9 m. Where needed, the loose sand was underlain by a dense soil, with $D_r = 90$ %. The model tunnel was 0.5 m wide by 0.25 m high, with 0.15 m cover, and had an apparent specific gravity of 0.88.

Heave of the tunnel was found to increase as the depth of the liquefiable soil below the tunnel increased. Without ground treatment, increasing the loose soil depth below the tunnel from 0.15 m to 0.5 m (model scale) led to an increase in tunnel heave from about 15 mm (6 % of the tunnel height) to 100 mm (40 % of the tunnel height) for a 0.3 g shaking event. Recorded tunnel displacements are shown in Table 6.1. The addition of drainage capability to sheet pile walls reduced deformations considerably when the loose soil depth below the tunnel was large. However, when the loose soil depth was small, the drains had little effect.

Table 6.1 Measured tunnel heave for a 0.3 g event

Total loose soil depth (m)	Depth of loose soil below tunnel	Estimated K_{wall}	Drainage elements	Heave as % of tunnel height	Heave as % of unimproved case
0.55	0.15	20	No	1.5	27
0.7	0.3	4	No	7	33
0.9	0.5	0.4	No	15	no data
0.55	0.15	20	Yes	2.5	40
0.7	0.3	4	Yes	1	4
0.9	0.5	0.4	Yes	4	no data

Sheet pile wall strains were measured and used to calculate the deformation of the walls. The change in volume due to these deformations was determined and used to estimate the tunnel heave assuming the soil below the tunnel was of constant volume. The measured and estimated heave was similar, however where drainage was incorporated into the walls the calculated heave was higher than the measured value, since soil volume change (contraction) could occur due to excess pore pressure dissipation through the drainage elements. The reverse was true for the walls without drainage, possibly caused by expansion of the soil volume between the walls due to the tunnel buoyancy.

6.9.   Study No. 21

Kimura et al. (1995) described a series of centrifuge model tests of a rectangular cross-section tunnel within a loose sand deposit. Five tests were performed, incorporating unimproved ground, one row of gravel drains, and sheet pile walls with and without drainage capability installed at the sides of the tunnel. This was a parallel study to Kimura et al.'s investigation of oil storage tanks, described in section 5.8. The prototype tunnel dimensions were 5 m width and 3 m height with about 3 m of cover. The apparent specific gravity of the tunnel was 0.85. Gravel drains were formed from a coarse sand contained within a filter sock to provide separation. The quoted k_w/k_s for the drains was 230, and $L_w = 3.2$. For the sheet pile walls the estimated $K_{wall} = 70$.

The model having no improvement and the model including sheet pile walls without drainage both suffered extensive liquefaction during shaking events of 0.2 g magnitude. For these two

tests, accelerations measured on the tunnel were attenuated to about 10 % of the base shaking acceleration, due to loss of soil stiffness. It was found that incorporation of gravel drains led to an attenuation of the tunnel accelerations to about 20 % of the base motion, as less extensive liquefaction occurred. Sheet pile walls incorporating drainage elements led to an attenuation to about 40 % of the base motion initially, although as the shaking event progressed the accelerations increased to about 70 % of the base motion due to pore pressure dissipation through the drainage elements on the walls. With a shaking event of 0.5 g magnitude, the sheet pile walls with drainage responded similarly to the other improvement measures, with tunnel accelerations attenuated to 10 to 20 % of the input motion.

For all tests, except that with the sheet pile walls with drainage, soil below the tunnel liquefied during 0.2 g shaking events, while soil above the tunnel did not. Sheet pile walls with drainage suppressed liquefaction below the tunnel due to the combination of stiffening and draining, although gradual liquefaction above the tunnel occurred because of the higher accelerations transmitted through the structure. With stronger levels of shaking, this test setup responded similarly to the other tests, as the drainage elements were unable to dissipate the generated pore pressures rapidly enough.

The average vertical displacement of the tunnels in each test relative to the initial position is summarized in Table 6.2 below, where upward displacement is positive.

Table 6.2 Summary of tunnel displacements

Treatment method	Magnitude of event	Prototype vertical displacement (mm)	
		After completion of shaking event	After dissipation of pore pressures
1: No treatment	0.2 g	165	150
2: Sheet pile walls	0.2 g	110	-50
3: Gravel drains	0.2 g	85	65
4: Sheet pile walls with drainage elements	0.2 g	-35	-50
5: Sheet pile walls with drainage elements	0.5 g	95	-50

All forms of ground treatment reduced heave of the tunnel during shaking, while sheet pile walls with drainage actually led to settlement occurring during a 0.2 g event. This concurs with the observed differences in pore pressure response, as the drainage elements in the walls were able to reduce the magnitude of the generated pore pressures and allow some dissipation during the shaking event. In the tests where drainage was able to occur during the event (cases 3 and 4 in the table above), small consolidation settlements were recorded. This was also true for the test

without ground treatment, and may be due to continued upward displacement of the tunnel after completion of the event due to buoyancy in the extensively liquefied soil. In the tests where drainage was actually impeded (cases 2 and 5) a large amount of post-event settlement occurred as high pore pressures trapped beneath the tunnel gradually dissipated. The amount of consolidation settlement in these two cases was about 5 % of the liquefiable soil depth below the tunnel.

The difference in deformation behavior can be partially explained by the suppression of lateral soil displacements by the sheet pile walls. In the tests without sheet pile walls, lateral soil displacements from regions to the side of the tunnel into the area beneath the tunnel were measured by observation of lead shot markers before and after the tests. The sheet pile walls were observed to inhibit this movement, although in cases 2 and 5 the toes of the sheet piles deflected inward under the differential pressure developed by the tunnel buoyancy. This was caused by lack of lateral confinement as the surrounding soil liquefied. However, when the drainage elements in the wall were able to function adequately (case 4) the walls did not deflect noticeably since the surrounding soil was stiffer (due to drainage) and provided greater restraint.

Differential vertical displacement across the width of the tunnel was found to be largest in the test involving sheet pile walls without drainage. This is not unexpected, as (i) excess pore pressures were confined by the sheet pile walls and no improvement of drainage was provided, and (ii) the highest consolidation settlements were recorded in this test.

Examination of pore pressure data during each shaking event indicated that heave of the tunnel occurred once the excess pore pressure ratio ($\Delta u/\sigma_v'$) below the tunnel rose above about 0.8.

6.10.   Summary

The studies described in this section have clarified the general behavior of subsurface structure in liquefiable soils during strong shaking events. In several studies, heave of the structure was observed to commence when the excess pore pressure ratio below it exceeded 0.7 to 0.8. Improvement schemes covered in these studies concentrated on gravel drains and sheet pile walls with and without drainage elements. These studies are summarized in Tables 6.3 and 6.4 below.

Performance of the gravel drains in terms of reducing heave of the structures was variable but generally relatively good. The actual improvement in any situation depends on a number of factors, such as relative permeability of the drains to the surrounding soil, the drains' well resistance, the geometry of the problem, the in situ soil conditions, and the structure buoyancy. However it is obvious that relatively free flowing drains were modeled in these studies. Additionally it appears that water was used as the pore fluid in all these experiments, so pore pressure drainage may have been more rapid than might be expected in a field installation in comparable soils.

The performance of sheet pile walls in reducing heave of the structures was also variable. The degree of improvement appears to be influenced by the stiffness of the sheet pile walls through the liquefiable layer. Incorporation of drainage elements into the walls gave rise to a significant reduction in structure displacements.

Table 6.3 Summary of gravel drain studies

Study No.	Structure type	Magnitude of event	L_w	Heave as % of unimproved case	Heave as % of structure height	Comments
2	semi buried road	0.2 g	0.04*	25	5	drain beneath structure also
4	manhole	0.12 g 0.22 g	2* 2*	10 12	1 2	drain beneath structure also
11	pipeline	0.2 g	0.13	6 to 50	3 to 25	improvement depended on drain spacing
21	tunnel	0.2 g	3.2	50	3	

* approximation.

Table 6.4 Summary of sheet pile wall studies

Study No.	Structure type	Magnitude of event	Estimated K_{wall}	Heave as % of unimproved case	Heave as % of structure height	Comments
4	manhole	0.12 g 0.22 g	6000 #	-2 -4	-0.3 -0.5	Wall surrounded manhole on all sides; crushed rock drainage also
16	tunnel	0.3 g	20 4 0.4	27 40 33 4 no data no data	1.5 2.5 7 1 15 4	without drains with drains without drains with drains without drains with drains
21	tunnel	0.2 g 0.2 g 0.5 g	70	67 -20 no data	4 1 3	without drains with drains with drains

\# lower bound due to shear stiffness of side walls
note: negative values indicate that settlement occurred.

7. DISCUSSION AND CONCLUSIONS

A number of ground improvement techniques were examined in the experimental investigations summarized in this report, and included:

- compaction, including vibrocompaction and sand compaction piles;

- deep cement mixing/in-ground walls;

- quick-lime consolidated briquette piles;

- gravel drains; and

- sheet pile walls with and without drainage capability.

The experimental performance of each of these methods depended on the interaction with the type of structure incorporated in the models. Of all the improvement techniques examined, sheet pile walls with drainage capability were found to perform most favorably, particularly where subsurface structures were involved.

7.1. Sheet pile walls

Sheet pile walls as a liquefaction countermeasure have recently been studied in Japan for stabilization of both surface and subsurface structures. The good performance of sheet pile walls under experimental conditions can be attributed to a number of factors, and in summary these include:

- The sheet pile walls provided an increase in stiffness through their bending rigidity, leading to a reduction in shear stress transmitted to the surrounding soil.

- The drainage elements incorporated in the walls allowed relatively rapid dissipation of excess pore pressures near the walls both during and after the shaking events, thus inhibiting the onset of liquefaction.

- The sheet piles provided a barrier to lateral soil displacements, inhibiting movement of soil towards the base of the subsurface structure, and thus limiting or eliminating heave due to buoyancy.

It should be noted that under strong levels of shaking (0.5 g), the sheet pile walls with drainage responded less favorably, presumably since soil liquefaction was more extensive and led to a loss of confinement and fixity of the wall. Removal of drainage elements from the sheet piles led to a dramatic loss of performance, as excess pore pressure dissipation was not assisted, and in fact may have been impeded to some extent. However, the sheet piles still gave an improvement in performance over an untreated site, apart from an increase in differential movement.

The performance of sheet pile walls has been illustrated in this report to be related to the effective wall stiffness, controlled by the bending rigidity of the wall and it's fixity conditions.

Embedment of the walls in a stiff layer and a short span through liquefiable soil has been shown to give rise to improved performance.

7.2. Gravel drains

Several investigations examined the performance of gravel drains in mitigating liquefaction. The general conclusion from all of the studies was that one row of gravel drains may not provide the desired improvement in performance. It was clearly demonstrated that several rows of gravel drains were significantly better than a single row, as the total drainage capacity is increased and a wider band of soil is being drained. However, the drains do not provide the same level of structural support as sheet pile walls and thus are less effective in suppressing liquefaction. The studies concentrated on the improvement of drainage to limit the generation of excess pore pressures, and due to modeling difficulties did not focus on any benefits from compaction associated with installation of the drains. In some studies it was identified that the drains provided a barrier to migration of excess pore pressures in the free field to the region below the structure.

Caution should be exercised in transferring conclusions from the physical models, since all studies appear to have constructed drains having low well resistance. The performance of prototype drains in situ may be dramatically different to that observed in these experiments. Additionally most experiments were conducted with water as the pore fluid, which may have led to better performance due to more rapid pore pressure dissipation than would be expected in the field.

7.3. Densification

Ground improvement by densification was not examined as a means of stabilizing subsurface structures in the reviewed studies. However, densification was examined in isolation and in relation to surface structures. The data indicated that densification should extend beyond the structure to a distance equal to about half the thickness of the liquefiable soil to minimize deformations. For densification in isolation from a structure the optimum treatment width has been estimated as about twice the thickness of the liquefiable soil, to prevent excessive migration of pore pressures from the free field into the densified area.

Studies have shown that the heave of a buried structure is reduced as both the thickness of the liquefiable soil below the structure and the lateral extent of the liquefiable soil beside the structure decrease.

7.4. Applicability of data to the Alameda tubes

Current design proposal for the Posey and Webster Street tubes are understood to involve three rows of stone columns on each side of the tubes, and jet grouting to form in-ground walls where stone column construction is not feasible. Both of these techniques are intended to isolate liquefiable soil below the tube to minimize uplift, while stone columns are expected to also assist drainage to some degree.

The physical model tests reviewed in the report generally involve structures and soil conditions that are very different from those of the Posey and Webster Street tubes. While insight can be gained about likely behavior, considerable judgment is required to translate the results of these studies to the Alameda tubes.

The data include an assessment of isolation walls comprised of steel sheet piles for the stabilization of subsurface structures that are similar in principle to the jet grouted in-ground walls proposed for the Alameda tubes. While stone columns were not specifically studied, some parallels can be found in the behavior of gravel drains and soil densification. Studies have also examined the effect of the extent of liquefiable soil beside and below a buried structure on the magnitude of heave.

7.5. Feasibility of further testing

Physical model testing is a valuable means of assessing geotechnical response under seismic conditions, and could be used effectively in reviewing the likely performance of the proposed ground improvement program for the Posey and Webster Street tubes. This could be performed either on a centrifuge or large laboratory based shaking table.

Additional testing could be designed to examine specific issues related to the site conditions and construction techniques. As described in section 3 of this report, the compaction stresses induced by installation of stone columns could not be modeled correctly without very significant expense for robotic manipulation equipment. Nevertheless, the improvement in drainage and stiffness afforded by the stone columns could be assessed relatively well, although the correlation between the stiffness and permeability of the model stone columns and that of columns constructed in the field would require careful consideration. One issue that could be assessed relatively well is the required lateral extent of ground treatment to achieve the required level of performance. Experimental modeling of jet grouting to isolate liquefiable soil may also be valuable, and would yield very useful data that could improve the level of confidence in design assumptions and performance estimates.

8. REFERENCES

Akiyoshi, T., Fuchida, K., Matsumoto, H., Hyodo, T. and Fang, H.L. (1993) Liquefaction analyses of sandy ground improved by sand compaction piles, *Soil Dynamics and Earthquake Engineering*, 12(5), 299-307.

Babasaki, R., Suzuki, K., Saitoh, S., Suzuki, Y. and Tokitoh, K. (1991) Construction and testing of deep foundation improvement using the deep cement mixing method, Proc. Deep Foundation Improvements: Design, Construction and Testing, ASTM STP 1089, 224-233.

Boulanger, R. W., Idriss, I. M. and Stewart, D. P. (1997) Study of ground improvement issues for the Posey and Webster Street tubes seismic retrofit project. A letter report prepared for Parsons Brinckerhoff Quade & Douglas, Inc., 303 Second Street, Suite 700 North, San Francisco, CA 94107, 5 pp.

Boulanger, R. W., Stewart, D. P., Idriss, I. M., Hashash, Y. and Schmidt, B. (1997) Ground Improvement Issues for the Posey & Webster St. Tubes Seismic Retrofit Project: Lessons From Case Histories, Report no. UCD/CGM-97/03, Center for Geotechnical Modeling, Department of Civil and Environmental Engineering, University of California, Davis.

Dobry, R., Taboada, V. and Liu, L. (1995) Centrifuge modeling of liquefaction effects during earthquakes, Proc. 1st Int. Conf. Earthquake Geotechnical Engineering, Tokyo, 129-162.

Fuchida, K., Akiyoshi, T., Matsumoto, H. and Hyodo, T. (1995) An anti-liquefaction design method for SCP-improved sandy grounds, Proc. 7th Int. Conf. Soil Dynamics and Earthquake Engineering, Computational Mechanics Publications, Boston,155-162.

Fuglsang, L. D. and Ovesen, N. K. (1988) The application of the theory of modelling to centrifuge studies, *Centrifuges in Soil Mechanics*, Balkema, Rotterdam, 119-138.

Hamada, M., Ohmoto, K., Sato, H. and Iwatate, T. (1992) Experimental study of effects of liquefaction-induced ground displacement on in-ground structures, Proc. 4th Japan-US Workshop on Earthquake Resistant Design of Lifeline Facilities and Countermeasures for Soil Liquefaction, NCEER-92-0019, 2, 481-492.

Hatanaka, M., Suzuki, Y., Miyaki, M. and Tsukuni, S. (1987) Some factors affecting the settlement of structures due to sand liquefaction in shaking table tests, *Soils and Foundations*, 27(1), 94-101.

Ito, T., Mori, Y. and Asada, A. (1994) Evaluation of resistance to liquefaction caused by earthquakes in sandy soil stabilized with quick-lime consolidated briquette piles, *Soils and Foundations*, 34(1), 33-40.

Kawakami, T. (1996) Experimental study on countermeasures against liquefaction-induced lateral ground movement by in-ground wall, Proc. 6th Japan-US Workshop, NCEER-96-0012, VII-5.

Kimura, T., Takemura, J., Hiro-oka, A., Okamura, M. and Matsuda, T. (1995) Countermeasures against liquefaction of sand deposits with structures, Proc. 1st Int. Conf. Earthquake Geotechnical Engineering, Tokyo, 163-184.

Kitaura, M. and Miyajima, M. (1985) Analytical and experimental study on behavior of buried pipelines subjected to soil liquefaction, Proc. 2nd Int. Conf. Soil Dynamics and Earthquake Engineering, Springer-Verlag, Berlin, 3.33-3.42.

Koga, Y. and Matsuo, O. (1990) Shaking table tests of embankments resting on liquefiable sandy ground, *Soils and Foundations*, 30(4), 167-174.

Koga, Y., Matsuo, O., Koseki, J., Goto, Y., Kubodera, I., Suzuki, K., Fukada, H. and Okamura, R. (1991) Applicability of the dynamic centrifuge model test method in developing countermeasures against soil liquefaction, Proc. Int. Conf. Centrifuge 91, Boulder, Balkema, Rotterdam, 431-438.

Koseki, J., Koga, Y. and Takahashi, A. (1994) Liquefaction of sandy ground and settlement of embankments, Proc. Int. Conf. Centrifuge 94, Singapore, Balkema, Rotterdam, 215-220.

Liu, L. and Dobry, R. (1994) Seismic settlements and pore pressures of shallow foundations, Proc. Int. Conf. Centrifuge 94, Singapore, Balkema, Rotterdam, 227-232.

Miyajima, M., Yoshida, M. and Kitaura, M. (1992) Small scale tests on countermeasures against liquefaction for pipelines using gravel drain system, Proc. 4th Japan-US Workshop Earthquake Resistant Design of Lifeline Facilities and Countermeasures for Soil Liquefaction, 1, NCEER-92-0019, 381-391.

Onoue, A., Mori, N. and Takano, J. (1987) In-situ experiment and analysis on well resistance of gravel drains, *Soils and Foundations*, 27(2), 42-60.

Sasaki, Y. and Taniguchi, E. (1982a) Large scale shaking table tests on the effectiveness of gravel drains for liquefiable soil deposits, Proc. Int. Conf. Soil Dynamics and Earthquake Engineering, Southampton, 2, Balkema, Rotterdam, 843-857.

Sasaki, Y. and Taniguchi, E. (1982b) Shaking table tests on gravel drains to prevent liquefaction of sand deposits, *Soils and Foundations*, 11(3), 1-14.

Schofield, A. N. (1980) Cambridge geotechnical centrifuge operations, *Geotechnique*, 20(3), 227-268.

Seed, H. B. and Booker, J. R. (1977) Stabilization of potentially liquefiable sand deposits using gravel drains, *J. Geotechnical Engineering Division* ASCE, 105 (GT7), 757-768.

Suzuki, K., Babasaki, R. and Suzuki, Y. (1991) Centrifuge tests on liquefaction-proof foundation, Proc. Int. Conf. Centrifuge 91, Boulder, Balkema, Rotterdam, 409-415.

Taguchi, Y., Ishihara, K. and Kato, S. (1992) Experimental study on behavior of the boundary between liquefied and non-liquefied ground, Proc. 4th Japan-US Workshop Earthquake Resistant Design of Lifeline Facilities and Countermeasures for Soil Liquefaction, 2, NCEER-92-0019, 639-653.

Tanaka, Y., Komine, H., Tohma, J., Ohmoto, K., Tochigi, H., Abo, H. and Fukuda, S. (1995) Area of compaction to prevent uplift by liquefaction, Proc. 3rd Int. Conf. Recent advances in Geotechnical Earthquake Engineering and Soil Dynamics, 1, 269-274.

Tanaka, H., Kita, H., Iida, T. and Saimura, Y. (1996) Countermeasure for liquefaction using steel sheet pile with drain capability, *Sumitomo Metals*, 48(1), 75-83, in Japanese.

Tohma, J., Tanaka, Y., Ohmoto, K., Fukuda, T. and Abo, H. (1990) Study on the ground compaction area as a countermeasure against soil liquefaction for buried pipes, Proc. 8th Japan Earthquake Engineering Symposium, 1, 861-866, in Japanese.

Tokida, K. and Ninomiya, Y. (1992) Experimental study on the uplift deformation of underground structures induced by soil liquefaction, Proc. 4th Japan-US Workshop Earthquake Resistant Design of Lifeline Facilities and Countermeasures for Soil Liquefaction, 2, NCEER-92-0019, 413-423.

Tokimatsu, K. and Yoshimi, Y. (1980) Effects of vertical drains on the bearing capacity of saturated sand during earthquakes, Proc. Int. Conf. On Engineering for Protection from Natural Disasters, Bangkok, Wiley, New York, 643-655.

Yagi, K., Suzuki, T., Hattori, H. and Yoshikawa, M. (1989) An experimental study on the manhole stabilizing techniques against liquefaction, Proc. ASME Pressure Vessels and Piping Conf.: Earthquake Behavior of Buried Pipelines, Storage, Telecommunication, and Transportation Facilities, Honolulu, ASME, New York, 227-237.

Yanagihara, S., Takeuchi, M. and Ishihara, K. (1991) Dynamic behavior of embankment on locally compacted sand deposits, Proc 5th Int. Conf Soil Dynamics and Earthquake Engineering, Karlsruhe, Computational Mechanics Publications, Boston, 365-376.

Yasuda, S., Nagase, H., Itafuji, S., Sawada, H. and Mine, K. (1995) A study on the mechanism of flotation of buried pipes due to liquefaction, Proc. 7th Int. Conf. Soil Dynamics and Earthquake Engineering, Computational Mechanics Publications, Boston,125-132.

Yoshida, M., Kitaura, M., Miyajima, M. and Oishi, H. (1993) Experimental study on a countermeasure against liquefaction for underground pipelines using gravel drain system, *Proc. Japanese Society of Civil Engineers*, 459/I-22(1), 149-153, in Japanese.

9. BIBLIOGRAPHY OF RELATED PUBLICATIONS

Englehardt, K. and Golding, H.C. (1975) Field testing to evaluate stone column performance in a seismic area, *Geotechnique*, 25(1), 61-69.

Iai, S. and Matsunaga, Y. (1992) Analysis of liquefaction induced uplift of underground structures, Proc. 4th Japan-US Workshop Earthquake Resistant Design of Lifeline Facilities and Countermeasures for Soil Liquefaction, 2, NCEER-92-0019, 425-438.

Kuribayashi, E., Kawamura, M., Ieda, R., Aida, M. and Yui, Y. (1985) Experimental behavior of buried pipes during liquefaction of saturated sandy soil, Proc. 1985 Pressure Vessels and Piping Conf. - Seismic Performance of Pipelines and Storage Tanks, 98-4, ASME, 19-24.

Nasu, M., Fujisawa, H., Hikimoto, K., Kaino, T., Fukishima, H. and Asakura, H. (1985) Shaking table tests on liquefaction countermeasure of embankment, Proc. 20th Japan National Conf. Soil Mechanics and Foundation Engineering, 755-756, in Japanese.

Takehara, Y., Tanaka, Y. and Ohira, M. (1980) In situ liquefaction test of ground in which crushed stone drains have been driven, Proc. 35th Annual Conference Japanese Society of Civil Engineers, 3, 263-264, in Japanese.

Tanaka, Y., Kokusho, T., Esashi, Y. and Matsui, I. (1984) On preventing liquefaction of level ground using gravel piles, Proc. Japanese Society of Civil Engineers, 352, 89-98, in Japanese.

Tanaka, Y., Kokusho, T., Esashi, Y. and Matsui, I. (1985) On preventing secondary liquefaction of level ground using gravel piles, Proc. Japanese Society of Civil Engineers, 364, 97-106, in Japanese.

Taniguchi, E., Sasaki, Y. and Ogasawara, H. (1981) Large scale model tests on the countermeasure to liquefaction by gravel drains, Annual meeting of Japanese Society of Soil Mechanics and Foundation Engineering, 633-636, in Japanese.

Yasuda S., Nagase, H., Kiku, H. Uchida, Y. and Kiyota, M. (1992) Shaking table tests on countermeasures against large ground displacement due to liquefaction, Proc. 4th Japan-US Workshop Earthquake Resistant Design of Lifeline Facilities and Countermeasures for Soil Liquefaction, 1, NCEER-92-0019, 367-380.

Yasuda, S., Nagase, H. Kiku, H. and Uchida, Y. (1991) Countermeasures against permanent ground displacement due to liquefaction, Proc 5th Int. Conf. on Soil Dynamics and Earthquake Engineering, Computational Mechanics, Southampton, 341-350.

Zhang, Y., Cai, Z. and Yang, G. (1986) Treatment of liquescent sandy soil foundation by vibro-replacement stone columns method, *Journal of Building Structures*, 7(1), 58-69, in Chinese.

APPENDIX A

**Summary Tables and Figures for Physical Modeling Studies of the
Earthquake Performance of Various Ground Improvement Techniques**

Summary of experimental data

No.	Structure type	Relative density, D_r (%)	Method(s) of treatment	Modeling technique	Base acceleration	Reference
1	Surface structure	40	Gravel drains	Shaking table	0.06 g	Tokimatsu and Yoshimi (1980)
2	None and semi-buried road	42 to 58	Gravel drains	Shaking table	0.2 g	Sasaki and Taniguchi (1982a, 1982b)
3	Surface footing	50	Densification	Shaking table	0.1 g	Hatanaka et al. (1987)
4	Manhole	40	• Dewatering • Gravel drains • Gravel drains with sheet pile wall	Shaking table	0.03 to 0.22 g	Yagi et al. (1989)
5	Buried pipeline	30	Compaction	Shaking table	0.08 to 0.12 g	Tohma et al. (1990), Tanaka et al. (1995)
6	Embankment and semi-buried road	60	Stiff impermeable inclusions	Shaking table	0.05 to 0.34 g	Koga et al. (1991)
7	Embankment	40	Compaction	Shaking table	0.2 g	Yanagihara et al. (1991)
8	None	52	In-ground walls	Shaking table	0.5 g	Hamada et al. (1992)
9	Buried utility ducts	26 to 43	None	Shaking table	0.08 to 0.23 g	Tokida and Ninomiya (1992)
10	None and surface structure	26 to 35	Compaction	Shaking table	0.14 to 0.48 g	Taguchi et al. (1992)
11	None and pipeline	26	Gravel drains and compaction	Shaking table	0.06 to 0.3 g	Miyajima et al. (1992), Yoshida et al. (1993)
12	None	22	Sand compaction piles	Shaking table	0.1 g	Akiyoshi et al. (1993), Fuchida et al. (1995)
13	Embankment	60	Quick-lime consolidated briquette piles	Shaking table	0.2 g	Ito et al. (1994)
14	Buried pipelines and manholes	90	Variable extent of loose backfill	Shaking table	0.25 & 0.4 g	Yasuda et al. (1995)
15	None	50	In-ground walls	Shaking table	0.2 to 0.3 g	Kawakami (1996)
16	Tunnel and embankment	42 to 58	Sheet pile walls with and without drainage	Shaking table	0.15 to 0.3 g	Tanaka et al. (1996)
17	Embankment and semi-buried road	60	Stiff impermeable inclusions	Centrifuge test at 30 g	0.18 g	Koga et al. (1991)
18	None	52	Deep cement mixing - grid shaped walls	Centrifuge test at 100 g	0.2 g	Suzuki et al. (1991)
19	None	not stated	Deep cement mixing - grid shaped walls	Centrifuge test at 100 g	0.2 g	Babasaki et al. (1991)
20	Surface footing	34 to 76	Vibrocompaction	Centrifuge test at 50 g	0.17 to 0.36 g	Liu and Dobry (1994), Dobry et al. (1995)
21	Tunnel	35 to 51	• Gravel drains • Sheet pile walls • Sheet pile walls with drainage	Centrifuge test at 50 g	0.2 & 0.5 g	Kimura et al. (1995)
22	Oil storage tank	43 to 49	• Gravel drains • Sheet pile walls • Sheet pile walls with drainage	Centrifuge test at 50 g	0.12 to 0.21 g	Kimura et al. (1995)
23	None	N = 3 to 15	Gravel drains	Insitu test	-	Onoue et al. (1987)

Study No. 1: Tokimatsu and Yoshimi (1980)

Structure type	Surface structure
Method(s) of treatment	Gravel drains
Modeling technique	Shaking table
Sample size, L, W, H (m)	1.3, 0.2, 0.2
Base shaking acceleration	0.06 g
Base shaking motion	3.5 Hz sinusoidal
Sand particle size	$D_{10} = 0.16$ mm
Relative density, D_r	40 %
Pore fluid	Glycerin
Testing details	One test on unimproved ground, one test with a single row of gravel drains installed adjacent to the structure. Permeability of sand = 5×10^{-5} m/s, permeability of drains not quoted.
Summary of results	- With gravel drains, excess pore pressures beneath the structure were reduced to about 30 % of the unimproved case. - Excess pore pressures adjacent to the structure were relatively unaffected by the drains. - Drains reduced settlement of the structure to about 10 % of the unimproved case.

(all dimensions in mm)
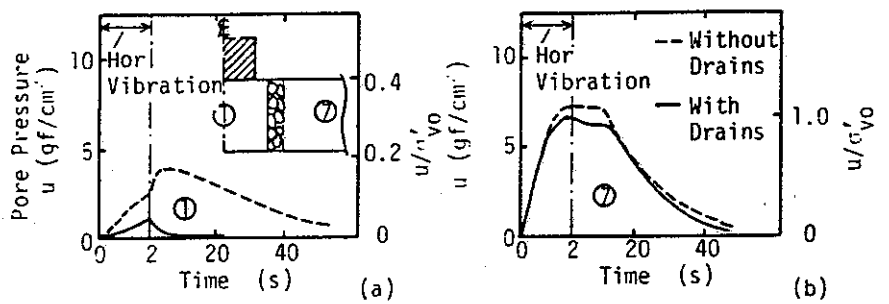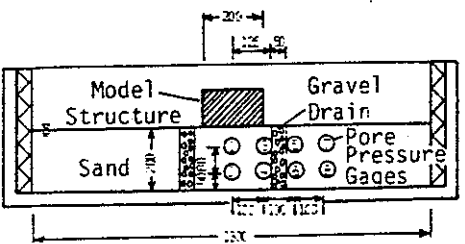
Effect of gravel drains on pore pressure generation and dissipation.
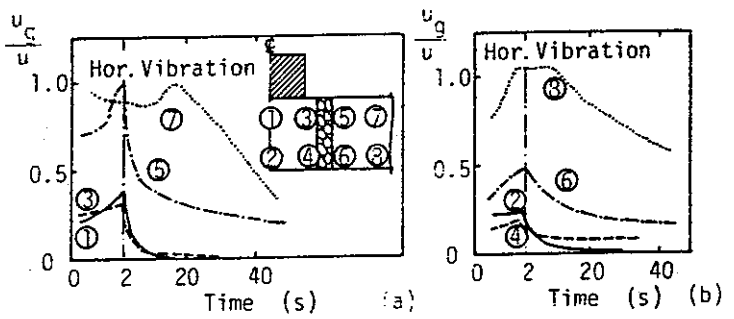
Time histories of the ratio of pore water pressure with gravel drains (u_g) to pore pressure without gravel drains (u).

Figure 1.1 - Study No. 1: Tokimatsu and Yoshimi (1980)

Study No. 2: Sasaki and Taniguchi (1982a, 1982b)

Structure type	None and semi buried road structure
Method(s) of treatment	Gravel drains
Modeling technique	Shaking table
Sample size, L, W, H (m)	12.0, 2.0, 3.0
Base shaking acceleration	0.2 g
Base shaking motion	1 to 24 Hz sinusoidal sweeps and 5 Hz sinusoidal
Sand particle size	D_{50} = 0.28 mm (sand), 22 mm (drain core), 3.3 mm (drain filter shell)
Relative density, D_r	42 to 58 % (unimproved ground)
Pore fluid	Water
Testing details	Two dimensional model with drains modeled as 0.4 m wide walls to assist analysis. Gravel drains incorporated a granular filter shell. Six models tested: (i) unimproved, (ii) one full penetration drain, (iii) two full penetration drains, (iv) two half penetration drains, (v) road structure with no improvement, (vi) road structure with drains. Permeability values: sand = 1.2×10^{-4} m/s, drain core = 0.6 m/s, drain filter shell = 0.06 m/s.
Summary of results	- Pore pressure dissipation observed to occur within 0.5 m of the center of single drain during shaking, sand boils observed in untreated area. - Generation of pore pressure not slowed or reduced markedly by drains, but drainage rate after shaking improved by two full penetration drains. - Soil bounded by two drains experienced slightly slower increase in excess pore pressure during shaking. - Drains reduced heave of semi buried road structure to about 25 % of the unimproved case, but still significant – 5 % of the structure height (drain also along bottom of structure).

MODEL 1

MODEL 2   gravel drain

MODEL 3   gravel drain

MODEL 4   gravel drain

MODEL 5   sand
half buried type road   model

MODEL 6   gravel drain
half buried type
road model

No. 7
gravel

No. 5
gravel

(cm)

excitation

pore water pressure u(kPa)

time (sec)

model 1

model 3

gravel drain

model 4
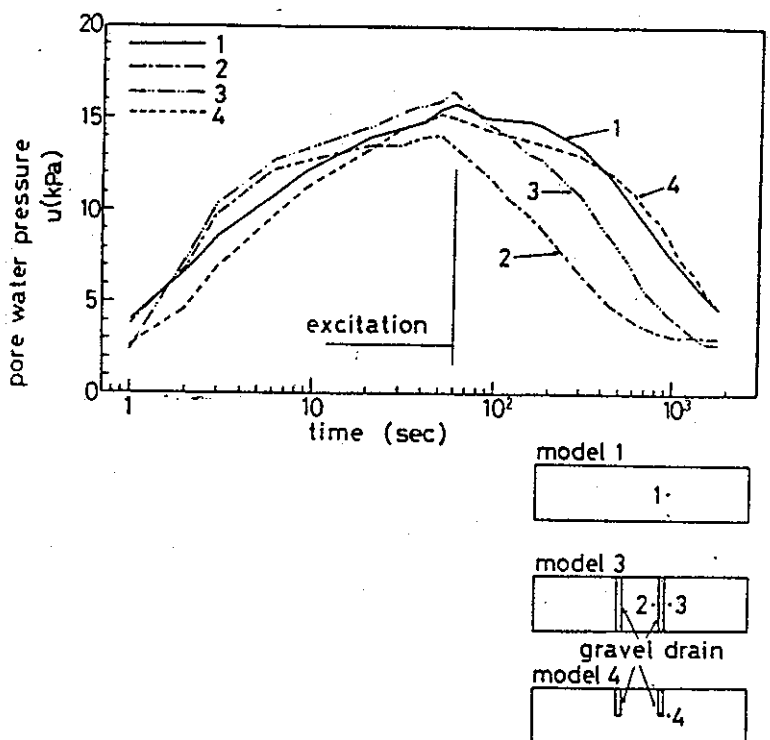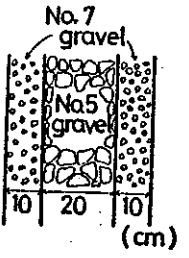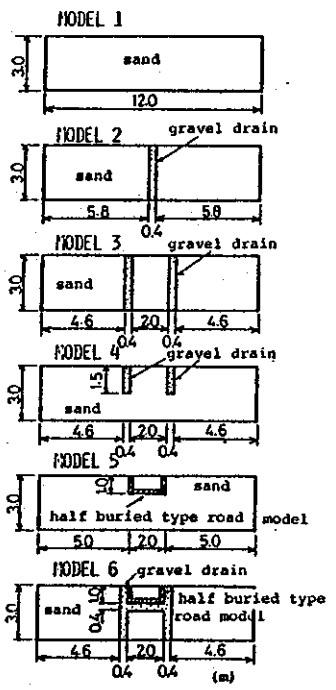
Effect of gravel drains on pore pressure generation and dissipation.

Figure 2.1 - Study No. 2: Sasaki and Taniguchi (1982a, 1982b)
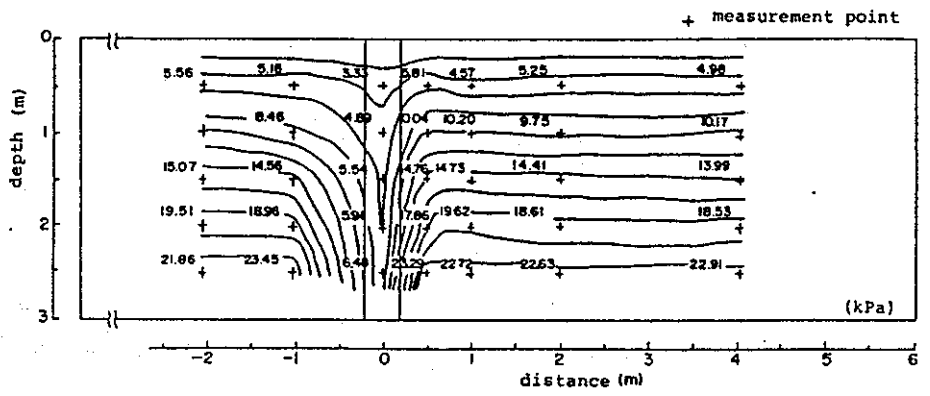
Pore water pressure distribution with gravel drains.
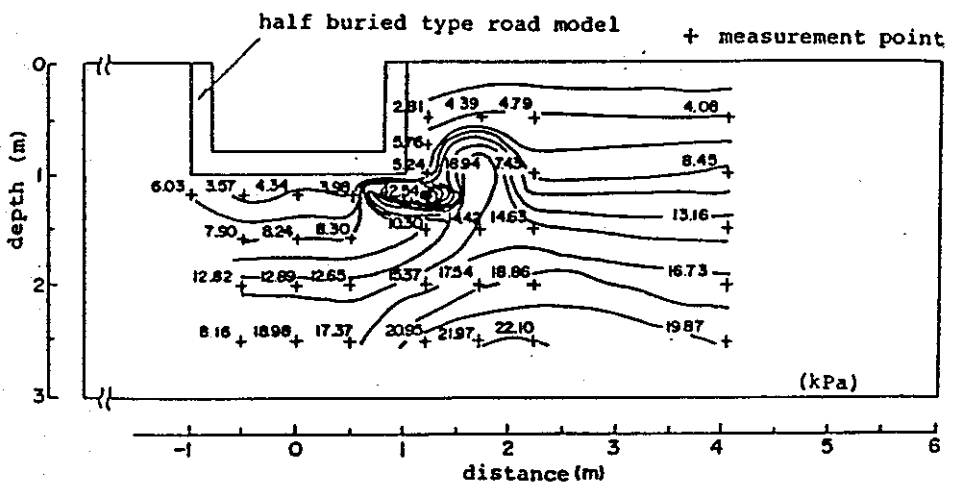
Pore water pressure distribution around semi-buried road structure without gravel drains.

Figure 2.2 - Study No. 2: Sasaki and Taniguchi (1982a, 1982b)
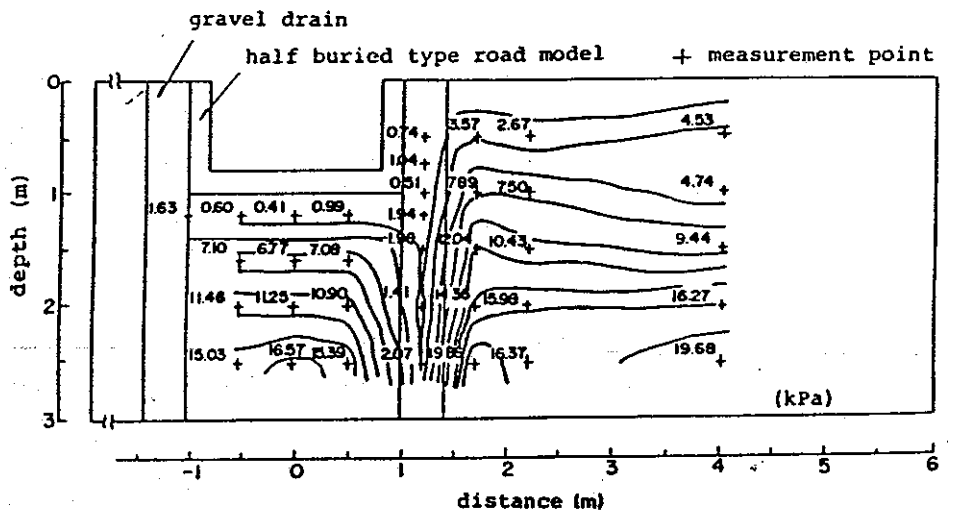
Pore water pressure distribution around semi-buried road structure with gravel drains.
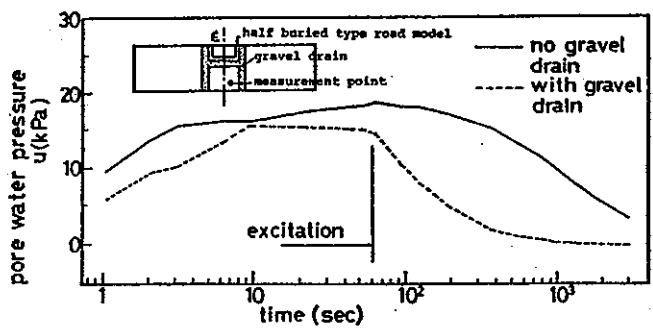
Effect of gravel drains on pore pressure generation and dissipation with semi-buried road structure.

Figure 2.3 - Study No. 2: Sasaki and Taniguchi (1982a, 1982b)

Study No. 3: Hatanaka et al. (1987)

Structure type	Surface footing
Method(s) of treatment	Densification
Modeling technique	Shaking table
Sample size, L, W, H (m)	1.6, 0.285, 0.4
Base shaking acceleration	0.1 g
Base shaking motion	2 Hz sinusoidal
Sand particle size	$D_{50} = 0.2$ mm
Relative density, D_r	50 % (unimproved ground) 90 % (densified region)
Pore fluid	Water
Testing details	Thirteen models covering a range of structure sizes and compaction areas. A dense block of soil placed below each footing.
Summary of results	- Data presented primarily in terms of footing settlement, with little pore pressure data. - Footing settlement reduced with increasing width of dense region, approaching a limit when the ratio of width to depth of the improved region equals 2. - Compaction extending beyond the edge of the footing to about half the compacted depth identified as optimum. - Performance improvement influenced by width of the structure, with most dramatic improvements for narrow structures. - Minimal settlement when excess pore pressure ratio ($\Delta u / \sigma_v'$) beneath the structure is less than 0.2.

|─28.5─|

Accelerometer | Model structure

40 cm

○9 ○5 ○1 — Densified area
○10 ○6 ○2
○11 ○7 ○3 — Loose sand
○12 ○8 ○4

Foam rubber cushion

Pore pressure transducers

|_24_|_16_|____80____|5|
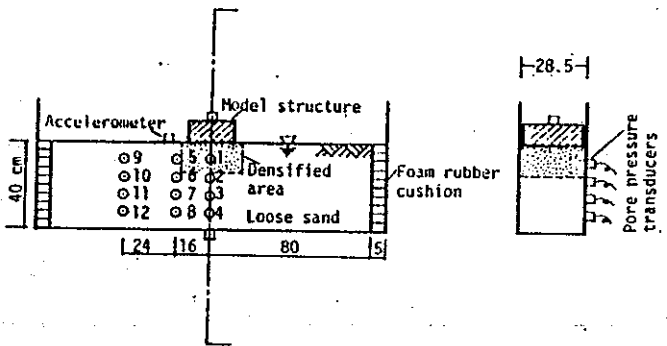
Table 1.   Models tested

A-Series BH*BW=5*10 (dimension:cm)	A1 SW=0	A2 SW=10 SL=0	A3 SW=20 SL=5	BW SL Model structure / BH / Densified area / SU / SD=15	
B-Series BH*BW=10*20	B1 SW=0	B2 SW=20 SL=0	B3 SW=30 SL=5	B4 SW=25 SL=2.5	B5 SW=40 SL=10
C-Series BH*BW=15*30	C1 SW=0	C2 SW=30 SL=0	C3 SW=40 SL=5	D SW=0 BH*BW=10*10	E SW=0 BH*BW=10*40
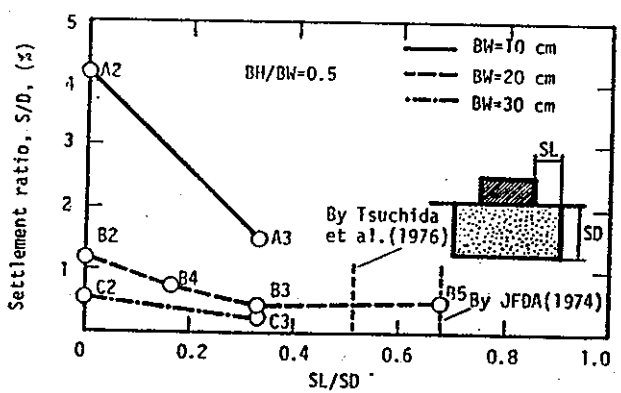
Ratio of settlement to soil depth (S/D) plotted against relative
extent of improved region adjacent to the structure.

Figure 3.1 - Study No. 3: Hatanaka et al. (1987)

Study No. 4: Yagi et al. (1989)

Structure type	Manhole
Method(s) of treatment	- Dewatering - Gravel drains - Gravel drains with sheet pile wall
Modeling technique	Shaking table: 1/5 scale model
Sample size, L, W, H (m)	2.0, 2.0, 1.1
Base shaking acceleration	0.03 to 0.22 g
Base shaking motion	prototype 4.5 Hz sinusoidal.
Sand particle size	$D_{50} = 0.35$ mm
Relative density, D_r	40 % (unimproved ground)
Pore fluid	Water
Testing details	Several tests performed: (i) unimproved ground, (ii) dewatering to two levels below the surface, (iii) crushed rock backfill drainage around manhole, (iv) crushed rock drainage with sheet pile walls surrounding the manhole on all sides. Crushed rock backfill particle size = 5 to 10 mm. Prototype manhole size: 2.84 x 1.95 x 1.84 m (L, W, H) Prototype drain width = 0.3 m. Permeability values not quoted.
Summary of results	- In all tests the soil surface settled, while heave of the manhole generally occurred. - All improvement measures led to reduction in displacement and pore pressure generation. - Sheet pile wall combined with crushed rock drainage led to lowest pore pressure generation below manhole. - Dewatering to the base of manhole and use of crushed rock drains were effective in reducing heave of the manhole, incorporation of sheet pile walls gave best behavior.
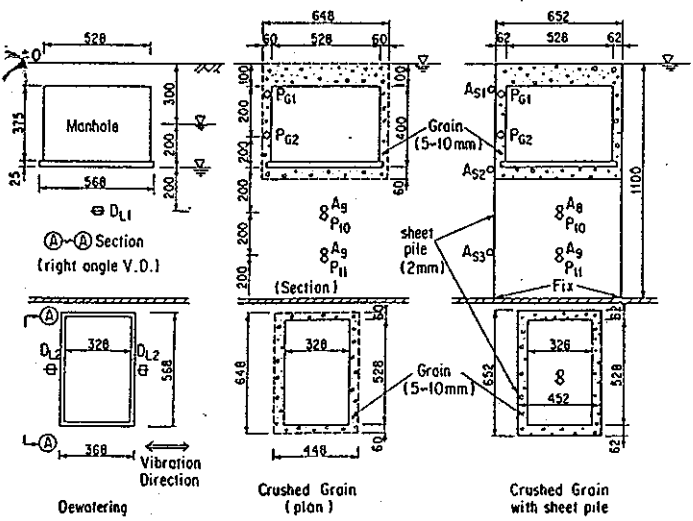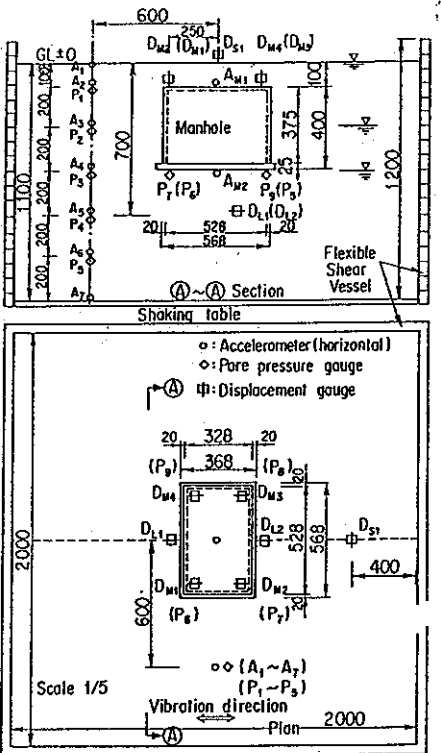
Configuration of the tests.

Figure 4.1 - Study No. 4: Yagi et al. (1989)

Excessive pore pressure (kPa)

(a) Standard (GL±0cm)   (b) Dewatering (GL−30cm)   (c) Dewatering (GL−50cm)

Excessive pore pressure (kPa)

(d) Crushed Grain   (e) Crushed Grain with sheet pile
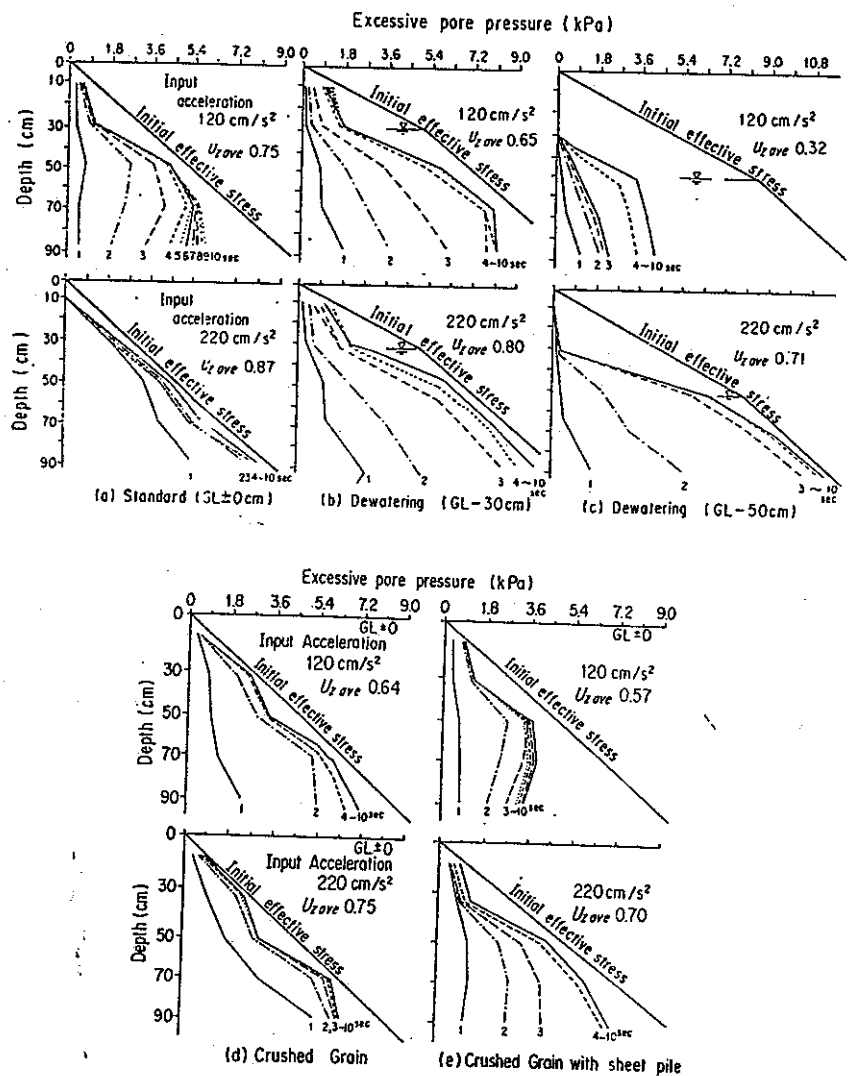
Comparison of pore pressure profiles in each test.

Input Acceleration (cm/s²)	Ground ①		Manhole ②		Relative Settement ② − ①	
	120	220	120	220	120	220
Ground System	−20	−92	—	—	20	92
Combined System						
Standard (GL±0cm)	−27	−89	41	56	68	145
Dewatering (GL−30cm)	−31	−76	25	31	56	107
(GL−50cm)	− 2	−22	2	−22	4	0
Crushed Grain	−22	−16	4	7	26	23
Crushed Grain with Sheet pile	− 3	− 6	−1	2	2	8

unit : mm. +: Floating up. −: Settlement

Figure 4.2 - Study No. 4: Yagi et al. (1989)

Study No. 5: Tohma et al. (1990) and Tanaka et al. (1995)

Structure type	Buried pipelines
Method(s) of treatment	Compaction
Modeling technique	Shaking table: 1/5 scale model
Sample size, L, W, H (m)	6.0, 1.0, 1.0
Base shaking acceleration	0.08 and 0.12 g
Base shaking motion	5 to 10 Hz sinusoidal
Sand particle size	$D_{50} = 0.32$ mm
Relative density, D_r	30 % (unimproved ground) 80 % (improved ground)
Pore fluid	?
Testing details	Twin buried pipelines. One test on unimproved ground, three tests with varying lateral extent of compacted soil: 0.6, 0.9 and 1.2 times the soil depth. Compaction extended to the base of the sample container. Prototype pipe diameter = 0.6 m, pipe specific gravity = 1.03.
Summary of results	- Flotation of the pipelines was observed when the excess pore pressure ratio below the pipe reached 0.7 to 0.8. - With no compaction, excess pore pressure between the pipelines rose rapidly during the shaking event. Liquefaction occurred over the upper part of the sample, with high excess pore pressures throughout. - With compaction, the magnitude and rate of increase of excess pore pressures were reduced. Pore pressures continued to rise in the compacted zone after completion of the shaking event. - High excess pore pressures were measured within the compacted zone, close to the loose soil boundary. - A simple uplift analysis was coupled with the results of numerical predictions of the variation in excess pore pressure with changing geometry of the compacted zone. This suggested that for a factor of safety against uplift of greater than 1.0, the minimum compacted width was 0.5 to 0.8 times the liquefiable soil depth.

Model configuration.

- ● : pore water pressure gage
- ▼ : displacement meter
- ○ : pipe model

(a) Case 1 (No compaction)

(b) Case 2 (B= 60 cm)

(c) Case 3 (B= 90 cm)

(d) Case 4 (B=120 cm)

B:compacted width
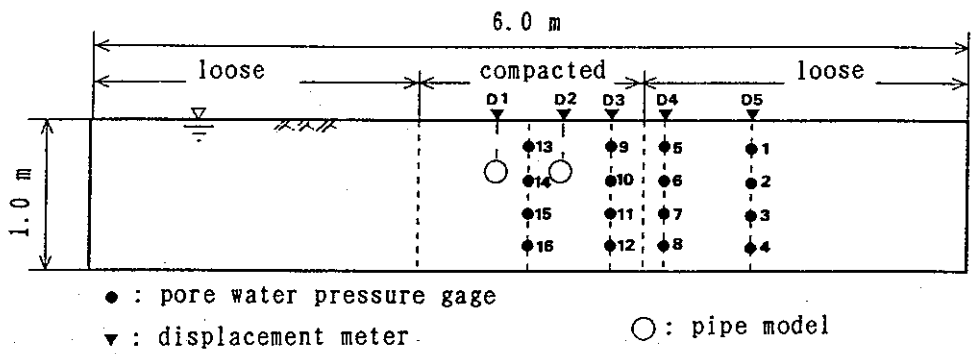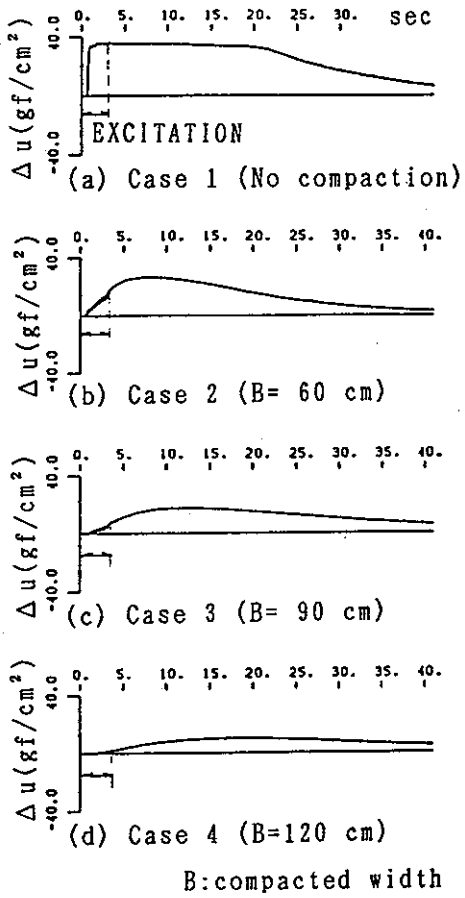
Excess pore pressure between the pipelines with differing widths of compaction.

Figure 5.1 - Study No. 5: Tohma et al. (1990) and Tanaka et al. (1995)
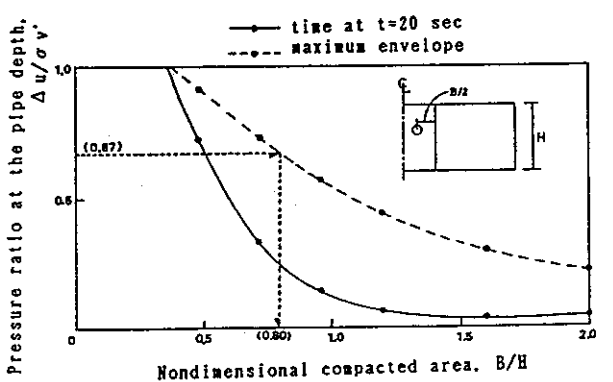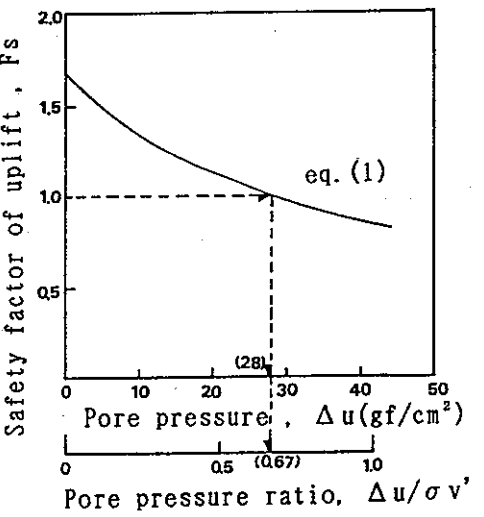
Results of simple analysis aimed at estimating the critical width of compaction.

Figure 5.2 - Study No. 5: Tohma et al. (1990) and Tanaka et al. (1995)

Study No. 6: Koga et al. (1991)

Structure type	Embankment and semi-buried road structure
Method(s) of treatment	Stiff impermeable inclusions
Modeling technique	Shaking table: 1/10 scale model
Sample size, L, W, H (m)	8.0, 1.0, 2.0
Base shaking acceleration	0.05 to 0.34 g
Base shaking motion	5 Hz sinusoidal
Sand particle size	$D_{50} = 0.2$ mm
Relative density, D_r	60 % (unimproved ground)
Pore fluid	Water
Testing details	Embankment with improved regions adjacent to toes; semi buried road structure with improved regions at sides of structure. Improved regions were stiff and impermeable. Apparent specific gravity of semi buried structure = 1.5.
Summary of results	• Limited data presented. • Liquefaction of soil adjacent to the embankment occurred, while soil below the embankment did not. • All soil liquefied in the semi buried road model. • Little heave of the road structure occurred, mainly settlement after the shaking event. • No tests performed without ground improvement, so no comments given on effect of improvement.
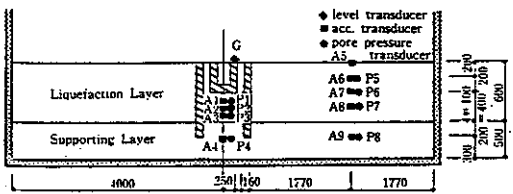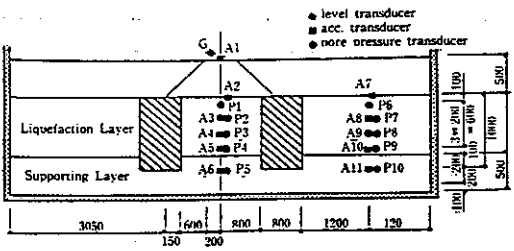
Geometry of models.

Figure 6.1 - Study No. 6: Koga et al. (1991)

Study No. 7: Yanagihara et al. (1991)

Structure type	Embankment
Method(s) of treatment	Compaction
Modeling technique	Shaking table
Sample size, L, W, H (m)	4.5, 2.0, 1.0
Base shaking acceleration	0.2 g
Base shaking motion	2 Hz sinusoidal
Sand particle size	$D_{50} = 0.3$ mm
Relative density, D_r	40 % (unimproved ground) 80% (compacted zone)
Pore fluid	Water
Testing details	• Case 1: embankment on unimproved ground • Case 2: compacted zone beneath toe of embankment • Case 3: compacted zone adjacent to toe of embankment
Summary of results	• Liquefaction in free field in all tests. • Case 1 - no liquefaction beneath embankment. • Case 2 - no liquefaction beneath embankment, gradual migration of excess pore pressure from free field into compacted zone. • Case 3 - limited liquefaction beneath embankment, dilation in compacted zone. • Treatment reduced lateral deformations to less than 10% of unimproved case. • Case 3 - compacted zone confined high excess pore pressures beneath the embankment, and sand boils developed through toe of embankment, leading to excessive settlement.
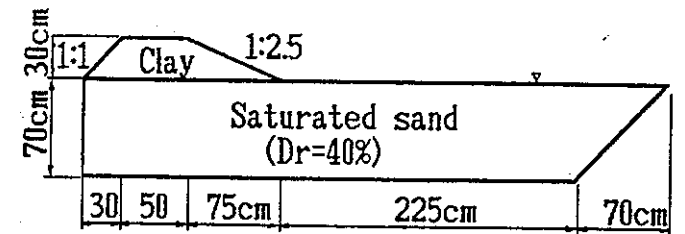
(a) Case 1 Uniform sand deposit
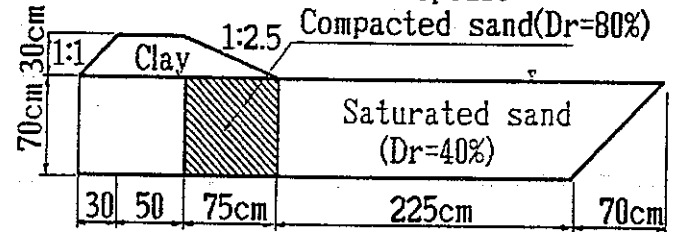
(b) Case 2 Compacted zone beneath the dike
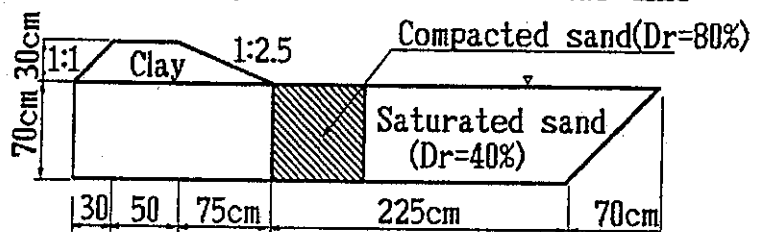
(C) Case 3 Compacted zone in front of the dike
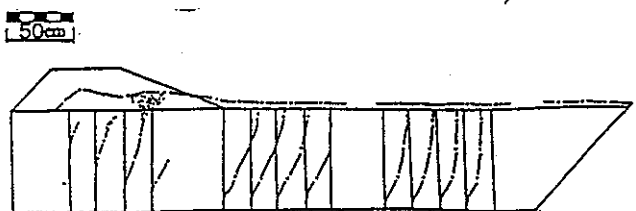
(a) Case 1 Uniform sand deposit
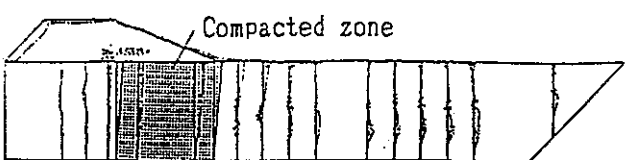
(b) Case 2 Compacted zone beneath the dike
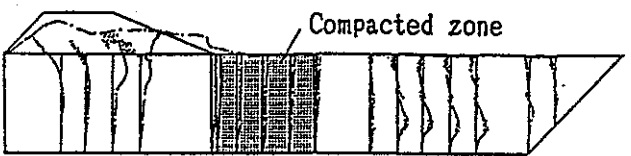
(C) Case 3 Compacted zone in front of the dike

Deformations observed after testing.

Figure 7.1 - Study No. 7: Yanagihara et al. (1991)
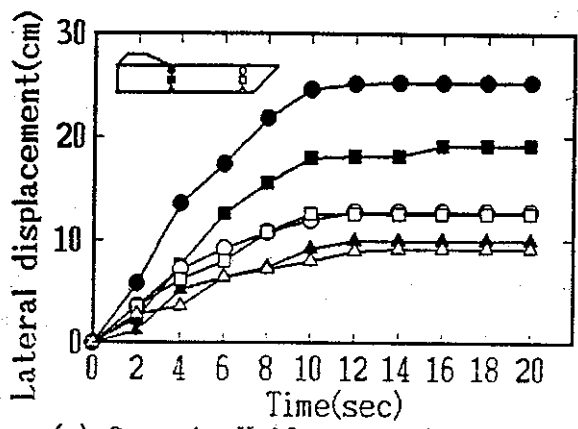
(a) Case 1   Uniform sand deposit
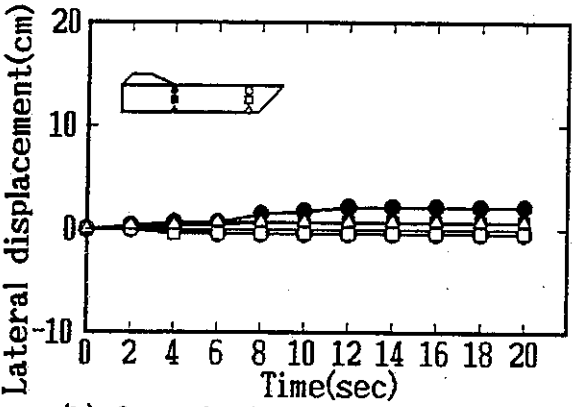
(b) Case 2   Compacted zone beneath the dike
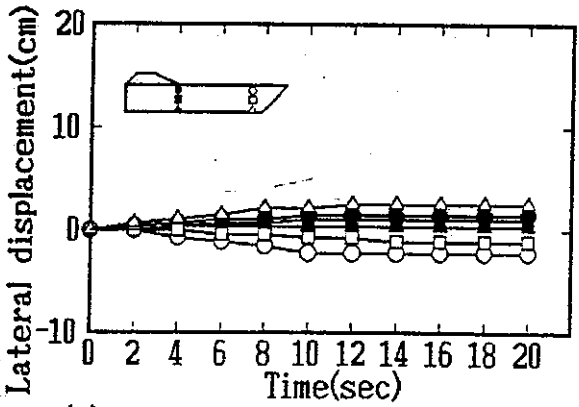
(c) Case 3   Compacted zone in front of the dike

Lateral displacements measured during the shaking event.

Figure 7.2 - Study No. 7: Yanagihara et al. (1991)

Study No. 8: Hamada et al. (1992)

Structure type	None
Method(s) of treatment	In-ground walls
Modeling technique	Shaking table
Sample size, L, W, H (m)	3.0, 0.8, 0.7
Base shaking acceleration	0.5 g
Base shaking motion	5 Hz sinusoidal
Sand particle size	$D_{50} = 0.3$ mm
Relative density, D_r	52 %
Pore fluid	not stated
Testing details	A rigid in-ground wall placed across the full width of the testing container with earth pressure cells on each face. The ground surface had a slope of 2 %.
Summary of results	• When the soil liquefied, the pressures acting on the walls were very close to the static liquefied soil pressure. • The pressure was slightly higher on the upstream face as the soil attempted to flow over the wall.

Gradient of Ground Surface: 2%

Movement of Ground

CP4 CP1
CP5 CP2
CP6 CP3

15 157.5

10 1510

SW1
SW2
SW3

64cm

Loose Sand
Rigid Soil Box

70cm

(b) Elevation

● : Pore water Pressure Meter

■ : Earth Pressure Meter
(cp1~cp6)

RIGID INGROUND WALL

Rigid Soil Box

Direction of Shaking

CP4~6 CP1~3

Loose Sand

● SW1~3

80cm

Movement of Ground

Movement of Ground

300cm

(a) Plan
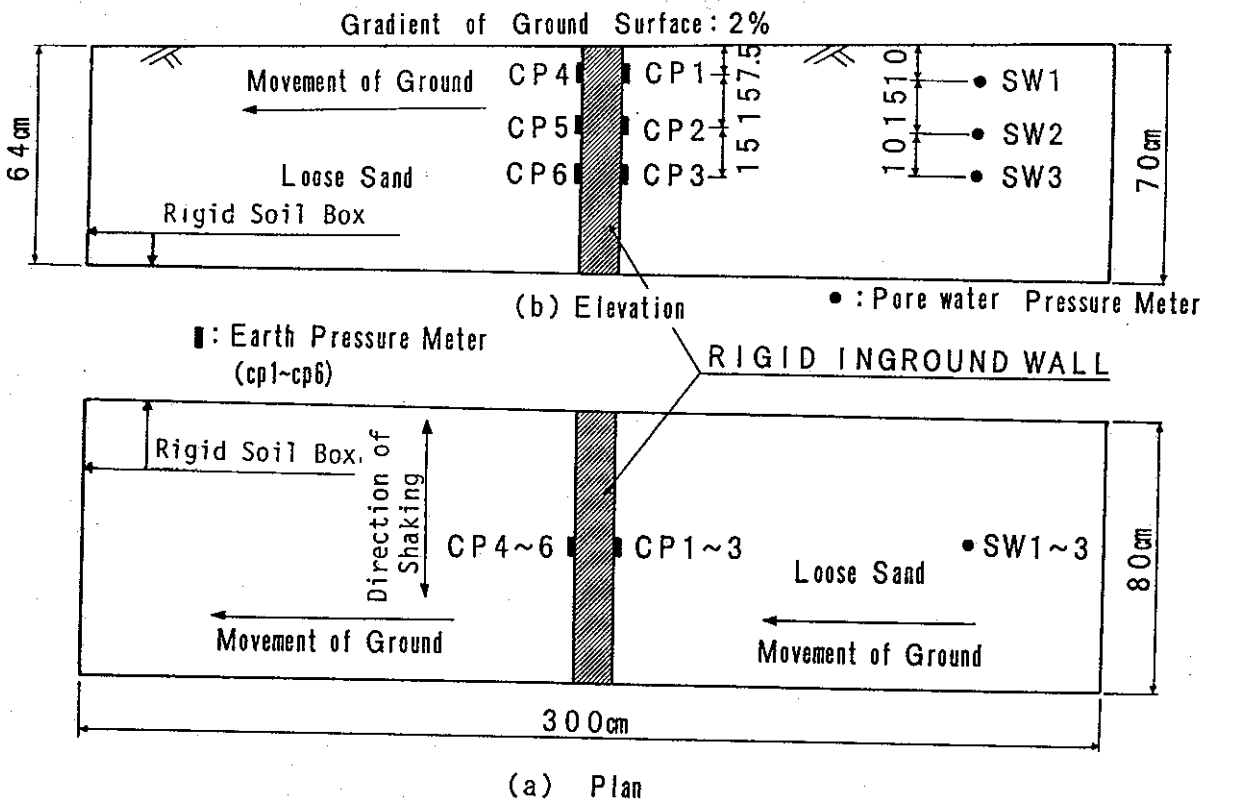
Layout of model.

Figure 8.1 - Study No. 8: Hamada et al. (1992)
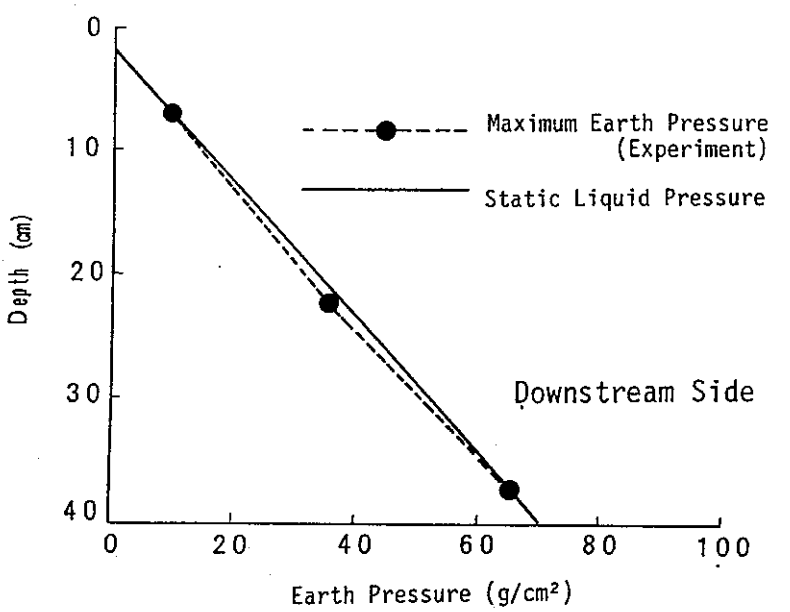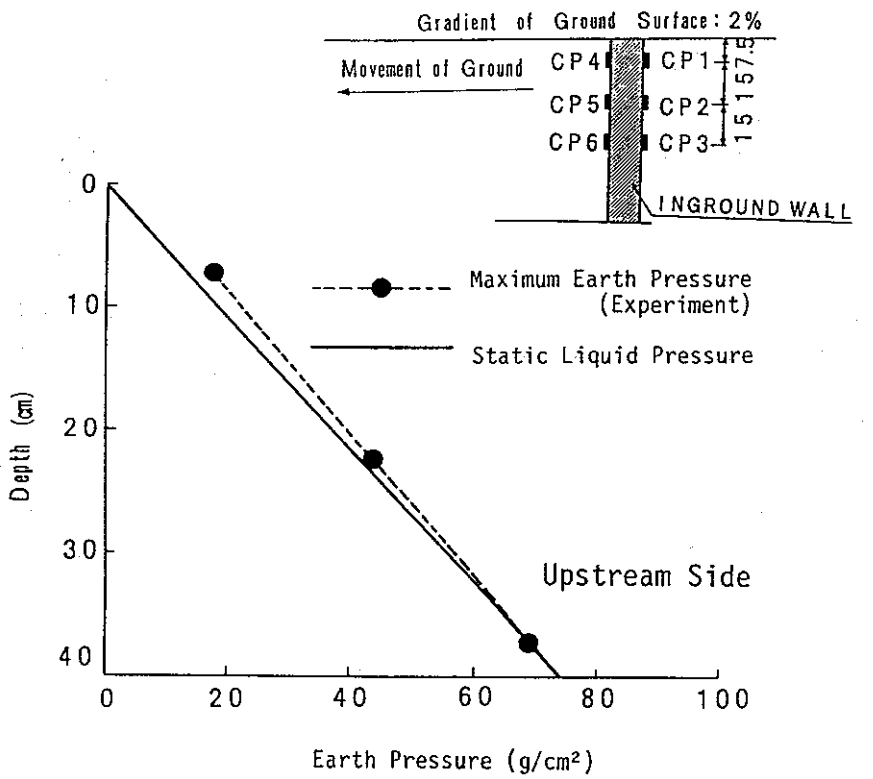
Figure 8.2 - Study No. 8: Hamada et al. (1992)

Study No. 9: Tokida and Ninomiya (1992)

Structure type	Buried utility ducts
Method(s) of treatment	None
Modeling technique	Shaking table
Sample size, L, W, H (m)	1.8, 0.6, 0.95
Base shaking acceleration	0.08 to 0.23 g
Base shaking motion	3 Hz sinusoidal
Sand particle size	$D_{max} = 0.85$ mm
Relative density, D_r	26 to 43 %
Pore fluid	?
Testing details	Two different rectangular cross-section utility ducts: model width = 0.15 and 0.45 m, height = 0.15 m. Three tests with each utility duct. Cover over duct constant at 0.2 m. Thickness of liquefiable soil below duct varied. Specific gravity of small duct = 0.94, for large duct = 0.85.
Summary of results	• Vertical heave of the structure reduced with decreasing thickness of liquefiable soil below the structure. • Observed soil deformations indicated that heave of the structures caused by flow of liquefied soil toward the base of the structure.

Slide wire displacement meters
W=150 2@37.5
W=450 2@112.5

Plates measuring earth pressure
Plate measuring friction

Liquefiable layer
Underground structure model
P1
Non-liquefiable layer
R2 P3 P4 P5

Sponge

W=150 76
W=450 175 50 100 150 150
1800

Direction of excitation
3Hz sine wave

○ Pore water pressure meter
□ Accelerometer
△ Bench mark point

Unit: mm

590

Spaces of measuring instrument

Model No.	Hb1 (mm)	Hb2 (mm)	Hb3 (mm)	Hb (mm)
1	50	—	—	50
2	50	50	—	100
3	100	50	—	150
4	37.5	37.5	—	75
5	100	50	—	150
6	150	100	50	300

Model configuration.

CASE3
CASE2
CASE1

Time histories of vertical displacement of ducts, showing greater heave as the depth of liquefiable soil below the structure increases.

Figure 9.1 - Study No. 9: Tokida and Ninomiya (1992)
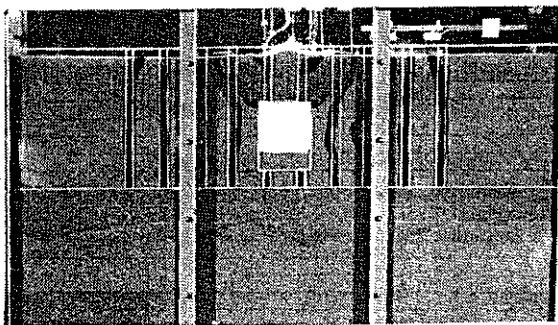
(a) Model 1 W=15cm, Hb=5cm (d) Model 4 W=45cm, Hb=7.5cm
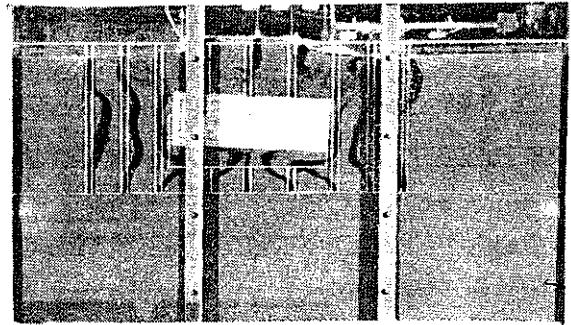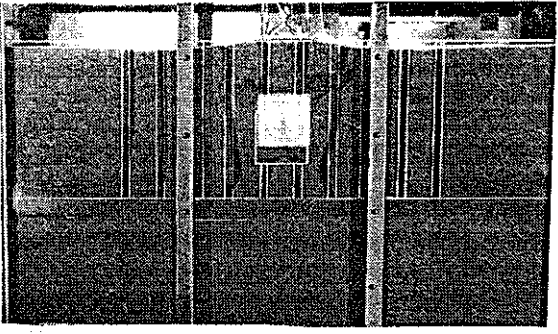
(b) Model 2 W=15cm, Hb=10cm (e) Model 5 W=45cm, Hb=15cm
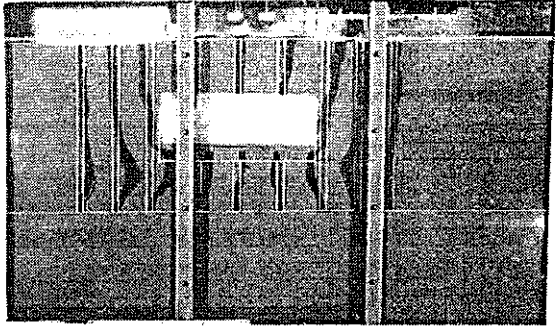
(c) Model 3 W=15cm, Hb=15cm (f) Model 6 W=45cm, Hb=30cm
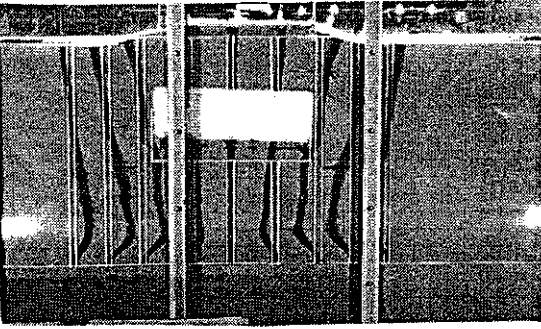
W (Width of the underground structure)
Hb (Thickness of liquefied sand below the underground structure)

Soil and structure deformations after testing.

Figure 9.2 - Study No. 9: Tokida and Ninomiya (1992)

Study No. 10: Taguchi et al. (1992)

Structure type	None and surface structure
Method(s) of treatment	Compaction
Modeling technique	Shaking table
Sample size, L, W, H (m)	4.0, 0.4, 0.55
Base shaking acceleration	0.14 to 0.48 g
Base shaking motion	3 Hz sinusoidal
Sand particle size	D_{50} = 0.22 mm, and 0.7 mm for the improved region in several models.
Relative density, D_r	26 to 35 % (unimproved ground) 70 to 90 % (compacted area)
Pore fluid	Water
Testing details	Four tests with no surface structure, three with a surcharge at the surface. The tests concentrated on behavior at the loose-dense interface, and on migration of excess pore pressures.
Summary of results	• Migration of pore pressures from the loose soil into the dense region was recorded during the shaking events. • Under strong shaking, some mixture between the loose and dense soils were observed at the interface, when different particle size materials were used in each zone. The dense soil displaced outwards near the surface due to loss of confinement from the loose soil. • Distribution of excess pore pressure with distance from the treatment boundary was not affected by the presence and location of a surcharge load at the surface.
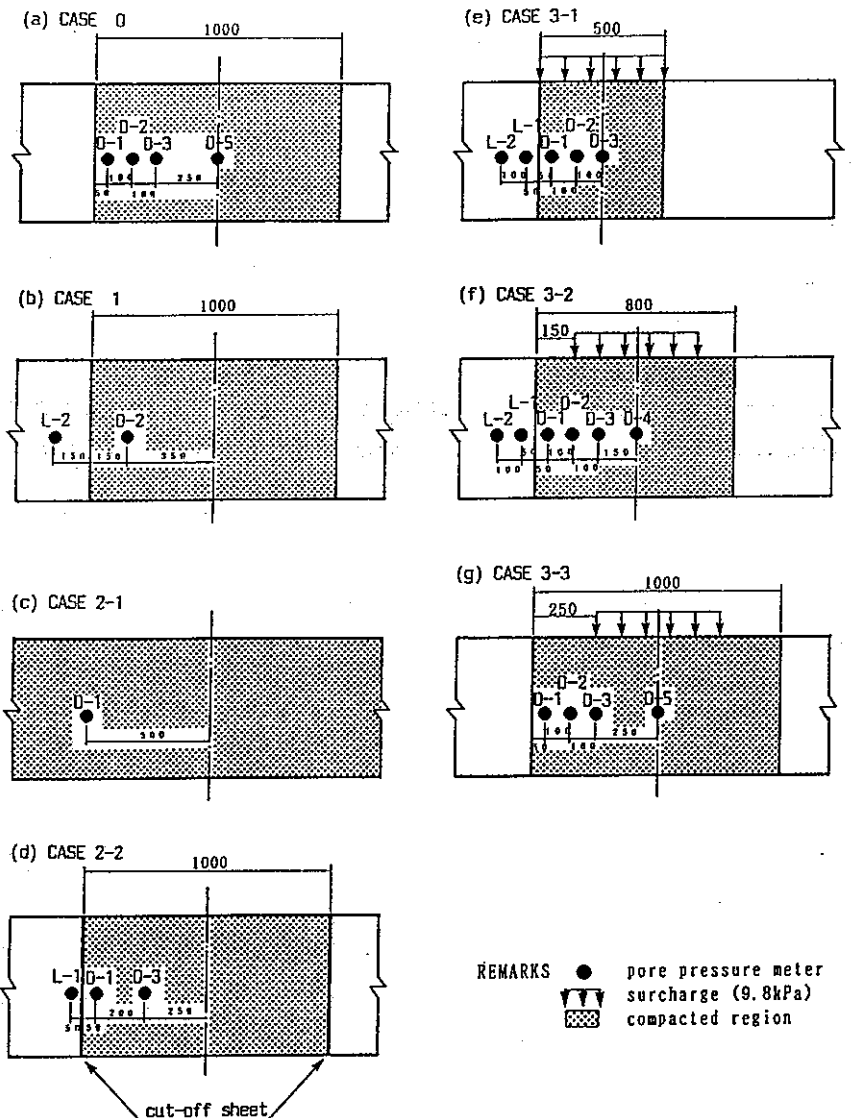
Model configuration.

test No.	compacted range	relative density(sand uesd) dense region	relative density(sand uesd) loose region	value and range of surcharge	input acceleration	comments
CASE 0	55cm x10cm x 100cm	85 % (Toyoura)	1:33% r:32% (Toyoura)		180 gal sin-wave 3 Hz 17 sec	
CASE 1	55cm x10cm x 100cm	68 % (Fuji river)	1:32% r:35% (Toyoura)		480 gal 3 Hz 47 sec	
CASE 2-1	55cm x10cm x 400cm	83 % (Toyoura)			160 gal sin-wave 3 Hz 20 sec	compacted all area
CASE 2-2	55cm x10cm x 100cm	90 % (Toyoura)	1:26% r:27% (Toyoura)		140 gal sin-wave 3 Hz 20 sec	set up rubber cut-off sheet on the boundary
CASE 3-1	55cm x10cm x 50cm	81 % (Toyoura)	1:32% r:29% (Toyoura)	9.8kPa (1.0tf/m²) 55cm x 10cm x 50cm	180 gal sin-wave 3 Hz 16 sec	
CASE 3-2	55cm x10cm x 80cm	90 % (Toyoura)	1:32% r:33% (Toyoura)	9.8kPa (1.0tf/m²) 55cm x 10cm x 50cm	170 gal sin-wave 3 Hz 15 sec	
CASE 3-3	55cm x10cm x 100cm	87 % (Toyoura)	1:33% r:32% (Toyoura)	9.8kPa (1.0tf/m²) 55cm x 10cm x 50cm	210 gal sin-wave 3 Hz 17 sec	

* : l: means left side from the front
r: means right side from the front

[_____] : changed terms against CASE 0

Figure 10.1 - Study No. 10: Taguchi et al. (1992)
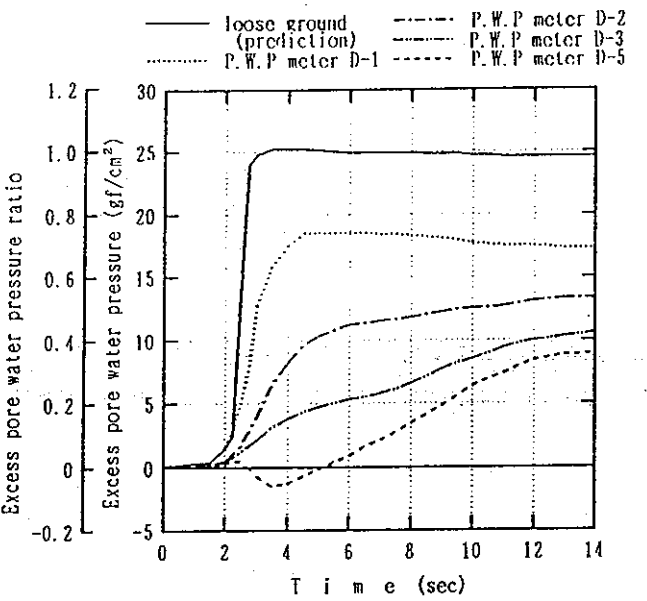
Time history of excess pore pressure for case 0.
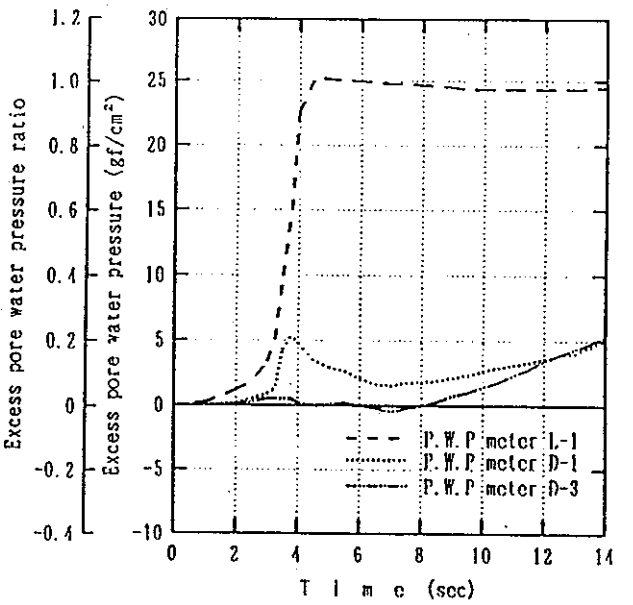
Time history of excess pore pressure for case 2-2, containing rubber sheeting to prevent water flow into dense region.

Figure 10.2 - Study No. 10: Taguchi et al. (1992)
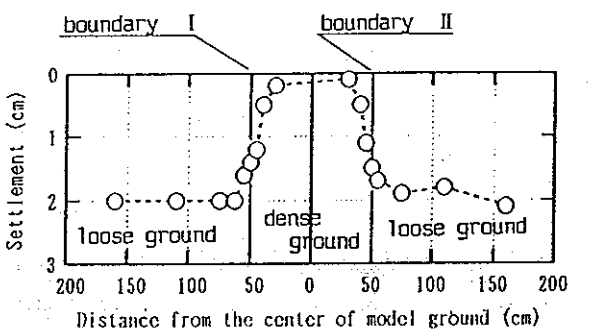
Settlement of ground surface for case 0.
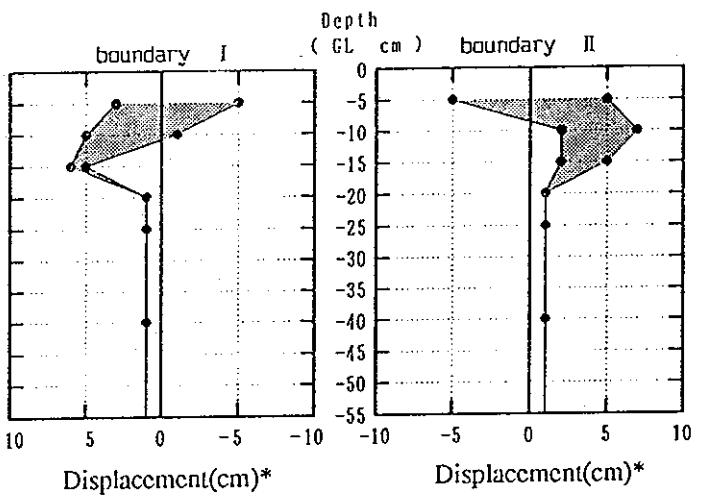
*: positive-displacement for loose ground

negative-displacement for dense ground

Displacement and soil mixing at the loose/dense boundary for case 1.

Figure 10.3 - Study No. 10: Taguchi et al. (1992)
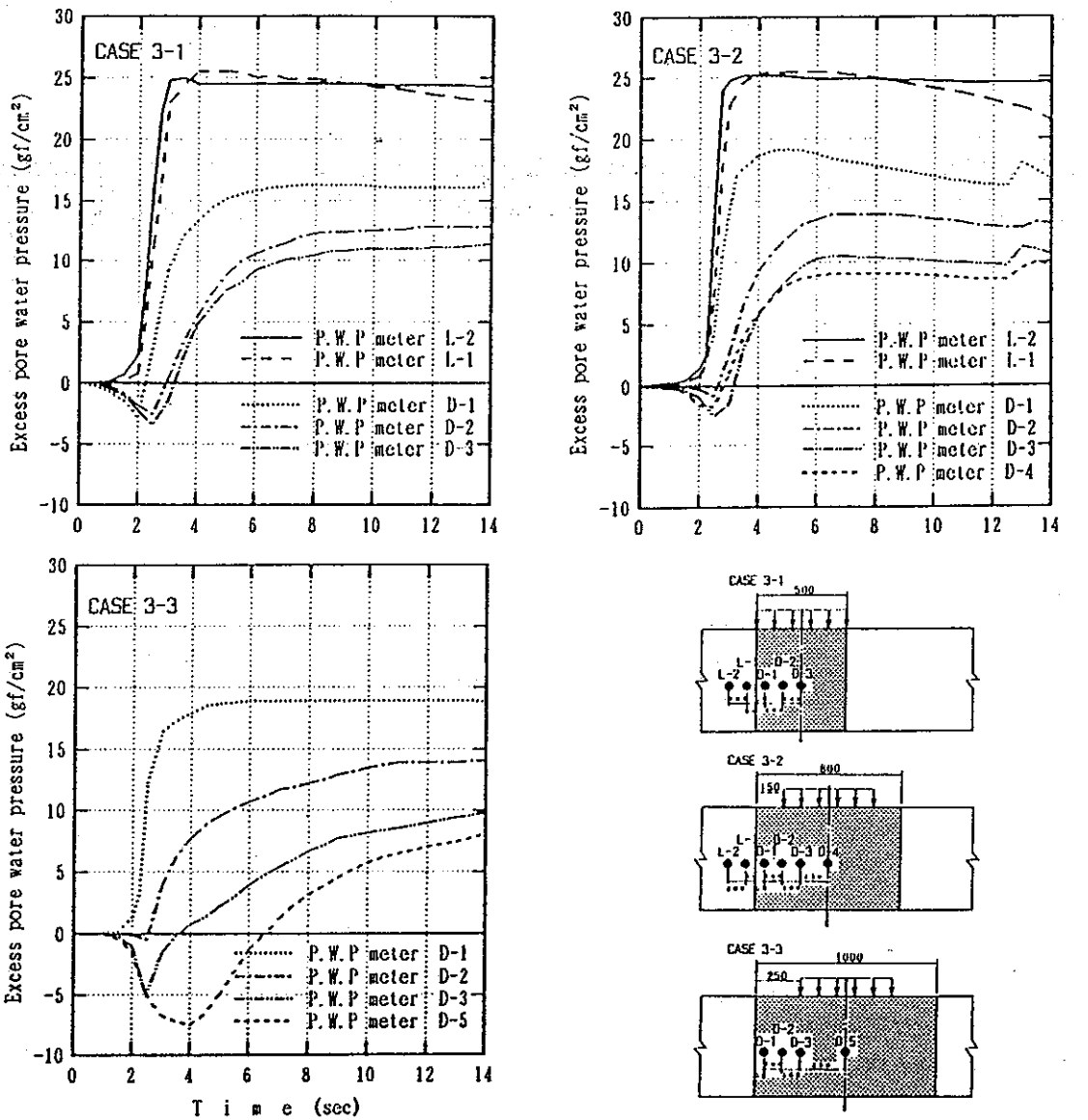
Time histories of excess pore pressure for tests with a surcharge load placed on the surface of the dense region.

Figure 10.4 - Study No. 10: Taguchi et al. (1992)

(a) 4 SECONDS AFTER SHAKING WAS STARTED

surcharge range

CASE 3-3
CASE 3-2
CASE 3-1

Excess pore water pressure (gf/cm²)

☆ — — ☆ CASE 0
○ — — ○ CASE 3-1
◇ — — ◇ CASE 3-2
▽ — — ▽ CASE 3-3

loose ground   dense ground

Distance from the boundary (cm)

(b) 12 SECONDS AFTER SHAKING WAS STARTED

surcharge range

CASE 3-3
CASE 3-2
CASE 3-1

Excess pore water pressure (gf/cm²)

☆ — — ☆ CASE 0
○ — — ○ CASE 3-1
◇ — — ◇ CASE 3-2
▽ — — ▽ CASE 3-3

loose ground   dense ground

Distance from the boundary (cm)
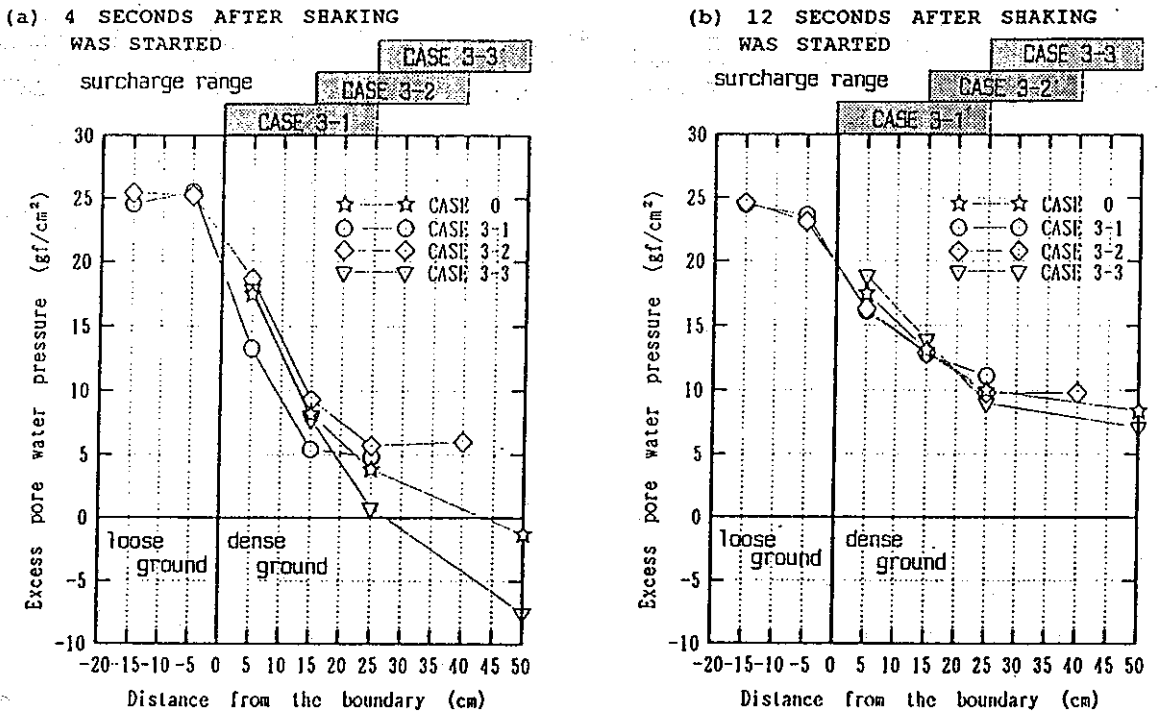
Excess pore pressure distributions near the loose/dense boundary (a) after about 5 cycles, and (b) after about 35 cycles of shaking.

Figure 10.5 - Study No. 10: Taguchi et al. (1992)

Study No. 11: Miyajima et al. (1992) and Yoshida et al. (1993)

Structure type	None and pipeline
Method(s) of treatment	Gravel drains and compaction
Modeling technique	Shaking table
Sample size, L, W, H (m)	1.5, 0.5, 0.25
Base shaking acceleration	0.06 to 0.3 g
Base shaking motion	5 Hz sinusoidal
Sand particle size	$D_{50} = 0.2$ mm
Relative density, D_r	26 % (unimproved region) 52 % (improved region)
Pore fluid	?
Testing details	Two tests on level ground models with an improved region at one the end of the sample container: (i) improved by densification, and (ii) improved region composed entirely of gravel. Seven tests with a subsurface pipeline: one of these with no improvement, and six tests with one row of gravel drains on either side of the pipeline. The spacing of the drains normal and parallel to the pipe axis was varied between tests. Permeability values: sand = 2×10^{-4} m/s, gravel = 8×10^{-2} m/s. Apparent specific gravity of pipeline = 1.7. Pipeline had two diameters cover.
Summary of results	- With level ground models when improvement was by densification, higher excess pore pressures were generated in the unimproved region, and liquefaction occurred under 0.1 g shaking. - Gravel drains led to lower generated pore pressures, and more rapid dissipation close to the improved region. - Settlement of the soil surface was similar for both treatment methods for 0.1 g shaking. For 0.08 g settlements were lower with gravel drains. - Settlements were reduced near to the improved region, out to a distance away from the improved boundary roughly equal to the depth of loose soil. - For the pipeline models, generation of excess pore pressure was slower and dissipation was accelerated by reducing the spacing of the drains. This effect was slightly more pronounced for spacing in the direction normal to the pipe axis. - Ground surface settlements were reduced by reducing the drain spacing. The effect was roughly equivalent for spacing in either direction. - Heave of the pipeline was about half a diameter when no improvement was performed. - Reduction in gravel drain spacing led to a substantial reduction in pipeline heave. The smallest heave recorded was of the order of 3 % of the pipe diameter. - Dynamic strains recorded on the pipeline were found to increase with increasing excess pore pressure ratio ($\Delta u/\sigma_v{}'$). However, permanent strains were much lower in the unimproved case.
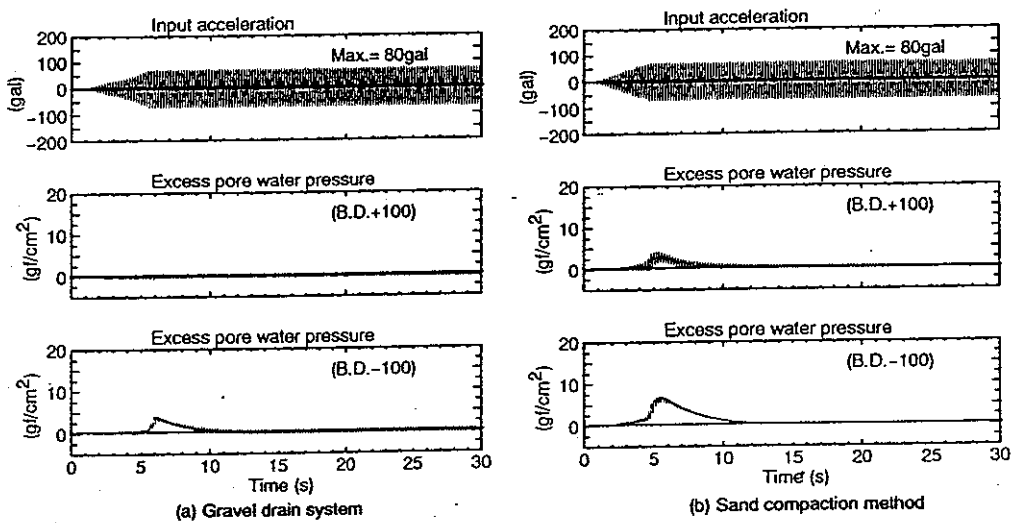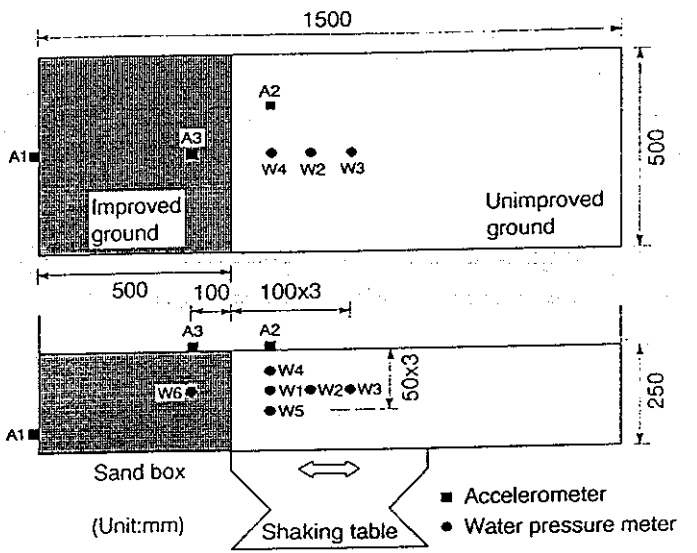
Time histories of pore pressures in a test with (a) gravel drainage and a test with (b) sand compaction. B.D.+100 is located in the improved region, B.D.-100 is located in the unimproved region.

Figure 11.1 - Study No. 11: Miyajima et al. (1992) and Yoshida et al. (1993)
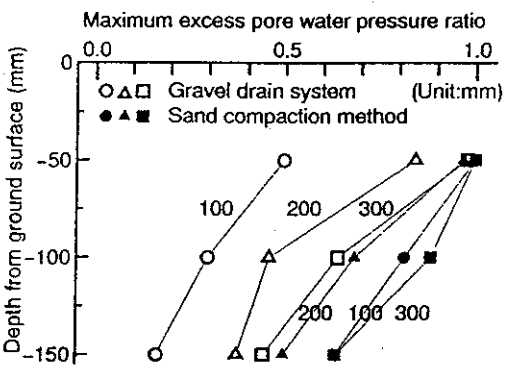
Excess pore pressure ratios at various distances away from the improved boundary
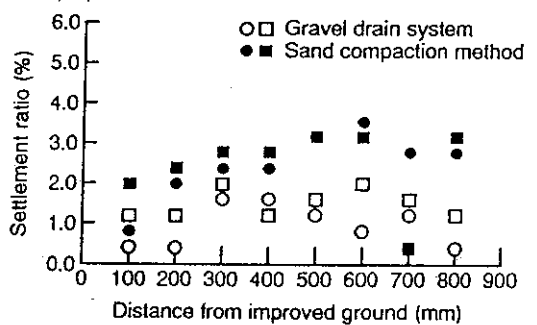
Settlement as a percentage of the liquefiable soil thickness for a 0.08 g event.
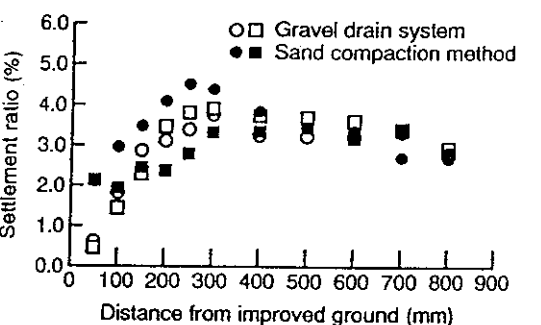
Settlement as a percentage of the liquefiable soil thickness for a 0.1 g event.
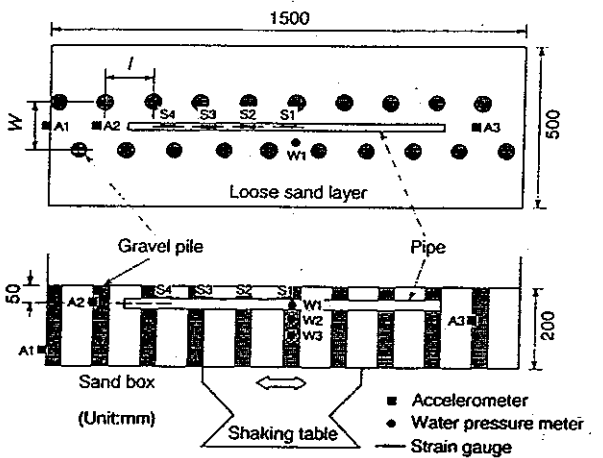
Model layout of tests incorporating gravel drains around a buried pipeline.

Figure 11.2 - Study No. 11: Miyajima et al. (1992) and Yoshida et al. (1993)
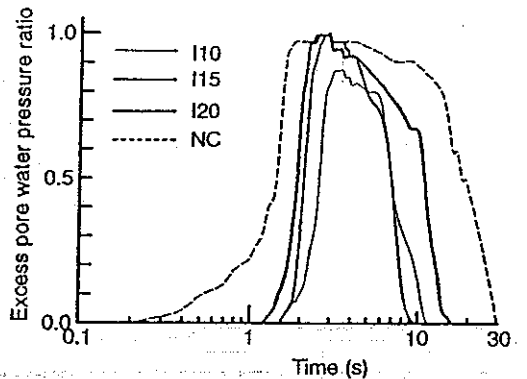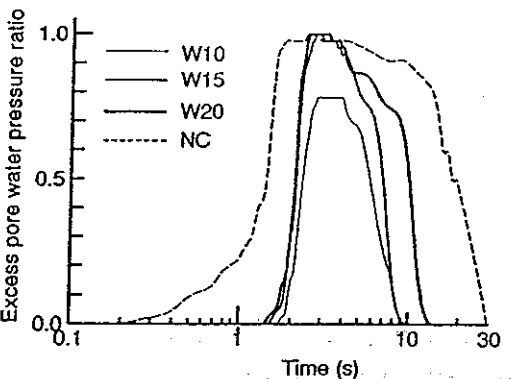
**Time histories showing variation of excess pore water pressure ratio
with variation in (a) spacing along the axis of the pipeline, and
(b) spacing perpendicular to the pipeline.**
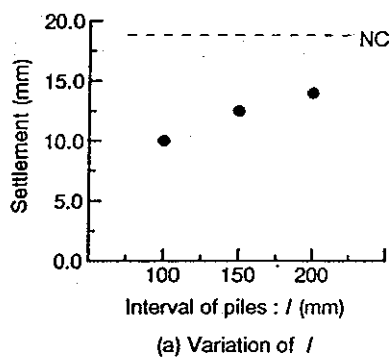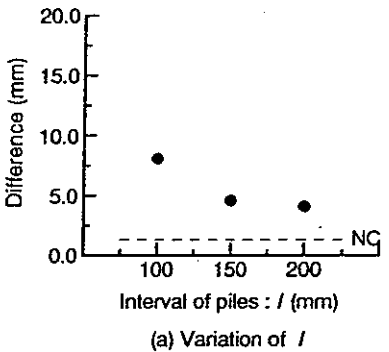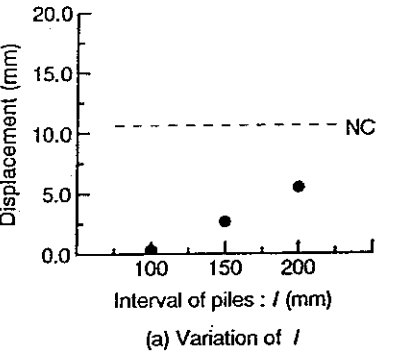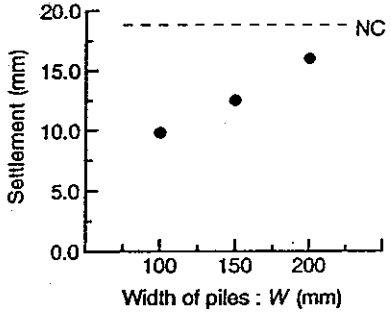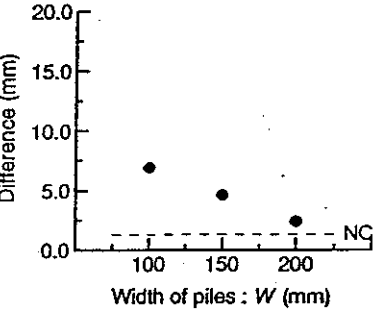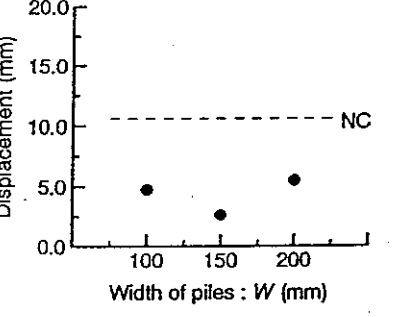
**Settlement of inner ground
surrounded by gravel drains.**

**Differential settlement
between inner and outer
ground surface surrounded by
gravel drains.**

**Vertical displacement
of pipeline.**

Figure 11.3 - Study No. 11: Miyajima et al. (1992) and Yoshida et al. (1993)

Study No. 12: Akiyoshi et al. (1993) and Fuchida et al. (1995)

Structure type	None
Method(s) of treatment	Sand compaction piles (vibrocompaction)
Modeling technique	Shaking table
Sample size, L, W, H (m)	1.5, 1.0, 0.8
Base shaking acceleration	0.1 g
Base shaking motion	5 Hz sinusoidal
Sand particle size	not stated
Relative density, D_r	22 % (unimproved ground) 40 to 50 % (sand compaction piles)
Pore fluid	not stated
Testing details	• Case 1: unimproved model. • Case 2: sand compaction piles with moderate compaction force installed to 0.5 m depth. • Case 3: sand compaction piles with high compaction force installed to 0.5 m depth. Diameter of model sand compaction piles = 70 mm, center to center spacing = 200 mm, length of piles = 500 mm. Soil depth = 800 mm.
Summary of results	• Unimproved model liquefied rapidly • Case 2 liquefied more gradually • Case 3 did not liquefy • Numerical analysis used to study generation and migration of excess pore pressures and the effect of the extent of the improved area. The analysis suggested an optimum treatment width of about 2 to 2.5 times the treated depth.
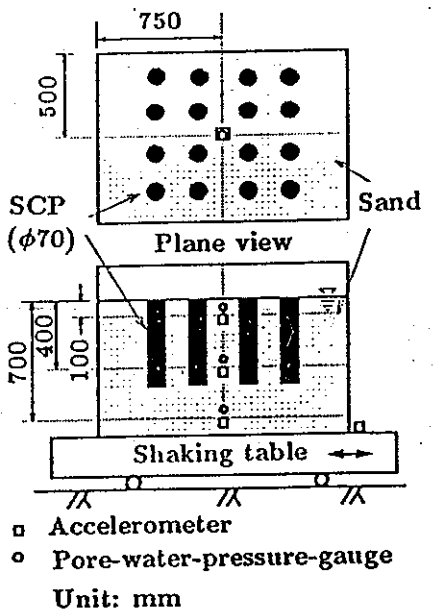
Model layout.
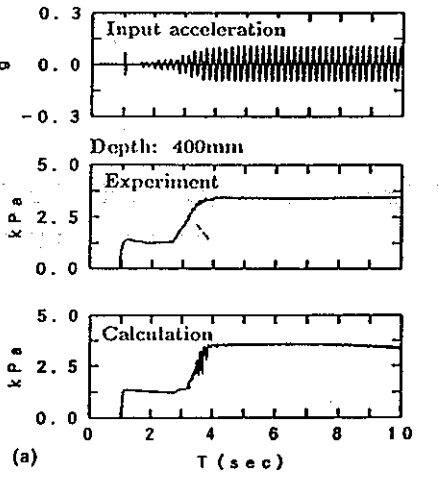
Pore pressure recorded in model with no improvement.
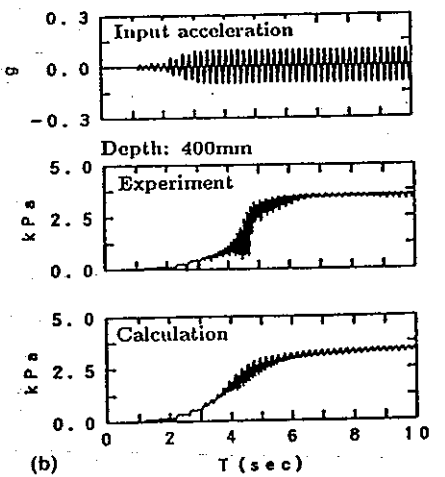
Pore pressure recorded in case 2 model with sand compaction piles with moderate compaction force.
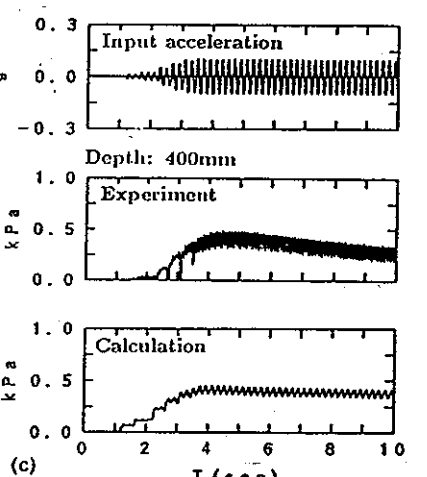
Pore pressure recorded in case 3 model with sand compaction piles with high compaction force.

**Figure 12.1 - Study No. 12: Akiyoshi et al. (1993) and Fuchida et al. (1995)**
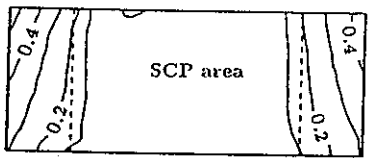
(a) T=4sec
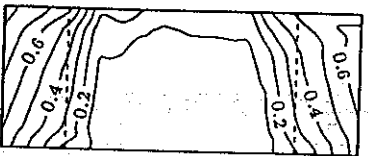
(b) T=6sec
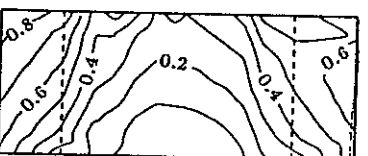
(c) T=8sec
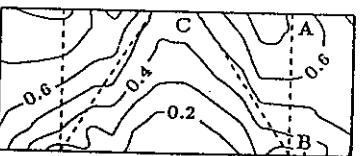
(d) T=10sec

Results of numerical analysis showing migration of pore pressure into densified region.
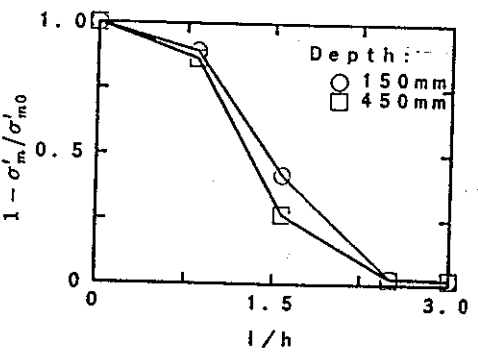
Results of numerical analysis showing reduction in excess pore pressure ratio with increasing width of densified region

Figure 12.2 - Study No. 12: Akiyoshi et al. (1993) and Fuchida et al. (1995)

Study No. 13: Ito et al. (1994)

Structure type	Embankment
Method(s) of treatment	Quick-lime consolidated briquette piles
Modeling technique	Shaking table: 1/10 scale model
Sample size, L, W, H (m)	2.0, 1.0, 0.5
Base shaking acceleration	0.2 g
Base shaking motion	2 Hz sinusoidal
Sand particle size	$D_{50} = 0.25$ mm
Relative density, D_r	60 %
Pore fluid	Water
Testing details	One test with unimproved ground. Two tests with 0.4 m diameter QCB piles installed to 4 m depth at prototype scale. Pile spacing = 2 m.
Summary of results	• Accelerations recorded on embankment reduced slightly by QCB piles. • Soil in the free field liquefied in all tests. This led to noticeable deformations near the boundary between the treated and untreated area. • QCB piles led to generated pore pressures beneath the embankment of about half those recorded in the untreated case. • QCB piles led to drastically reduced settlements: about 10 % of the untreated case. The settlements with QCB piles were about 3% of the loose sand thickness.

CASE 1

S-1 A-2

20cm

A-3

CUSHION

50cm

P-2 P-1

●NO. 1 ▽ ● No. 2 ▽

A-1

100cm 100cm

200cm

CASE 2

S-1 A-2

QCB PILE
(φ0.4cm, L40cm)
(REGULAR SQUARE
PLACEMENT)

20cm

A-3

CUSHION

50cm

P-2 P-1

●NO. 1 ▽● ▽

No. 2

A-1

@20×5=100cm

100cm 100cm

200cm
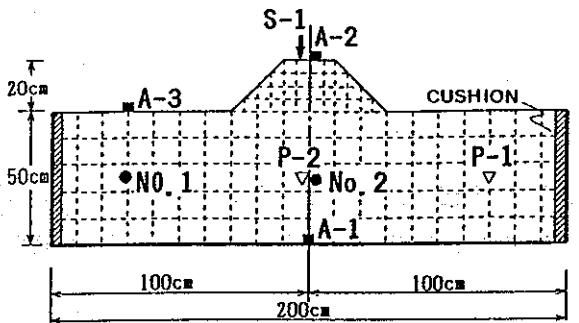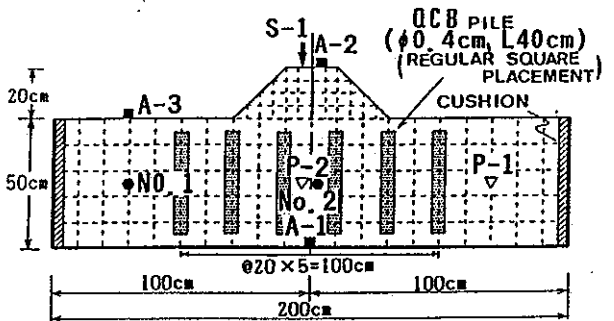
● DENSITY MEASUREMENT

▽ EXCESS PORE WATER
PRESSURE METER

■ ACCELEROMETER

↓ DISPLACEMENT METER

CASE 3

S-1 A-2

QCB PILE (REGULAR SQUARE PLACEMENT)
(φ0.4cm, L40cm) A-3

20cm

CUSHION

50cm

No. 2 NO. 1

▽● ▽ ▽ ●

P-4 P-3 P-2 P-1

@20 A-1

100cm 100cm

200cm
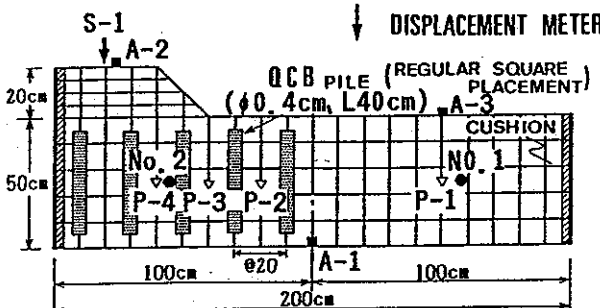
Layout of models.

Figure 13.1 - Study No. 13: Ito et al. (1994)
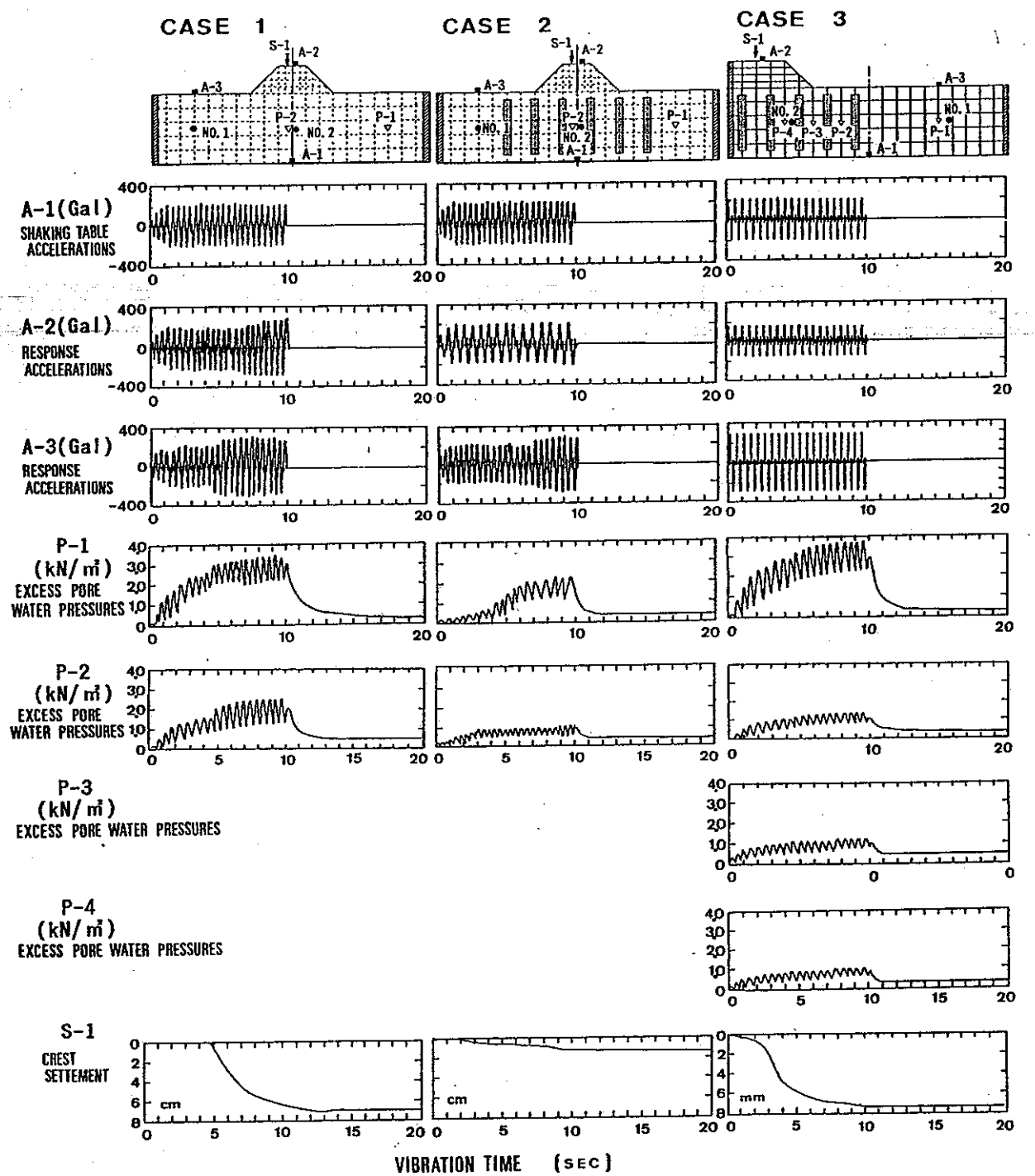
Time histories of accelerations, excess pore water pressures and settlement.

**Figure 13.2 - Study No. 13: Ito et al. (1994)**

CASE 1

10cm
|←→|

10cm

●NO. 1   ●No. 2

CASE 2

10cm
|←→|

10cm

NO. 1 ●   ●No. 2

CASE 3

10cm
|←→|

10cm

●   ●NO. 1
No. 2   30°
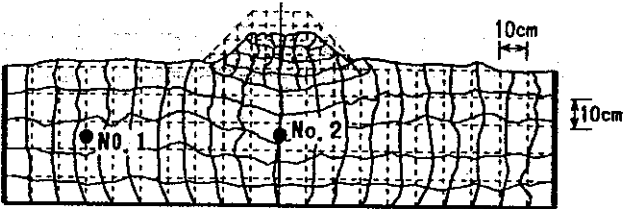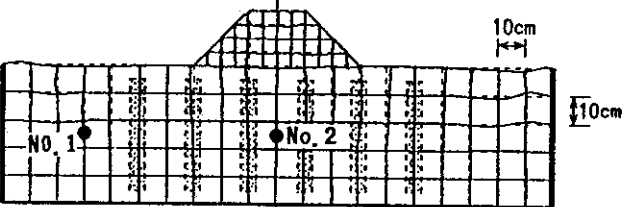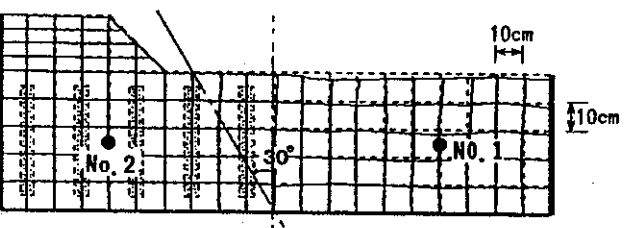
Deformed shape of models after testing.

Figure 13.3 - Study No. 13: Ito et al. (1994)

Study No. 14: Yasuda et al. (1995)

|	
Structure type	Buried pipelines and manholes
Method(s) of treatment	Variable extent of loose backfill
Modeling technique	Shaking table
Sample size, L, W, H (m)	1.0, 0.6, 0.5
Base shaking acceleration	0.25 and 0.4 g
Base shaking motion	3 Hz sinusoidal
Sand particle size	$D_{50} = 0.175$ mm
Relative density, D_r	90 % (main sample) 30 % (loose backfill)
Pore fluid	not stated
Testing details	Main samples were prepared with relatively dense sand. Several tests with the variations in the width and depth of loose backfill around pipelines and manholes. In most tests, the pipe excavation trench was lined with a plastic sheet to prevent pore pressure drainage into the surrounding soil. Two tests were conducted without this barrier sheet. Apparent specific gravity of pipeline = 0.75. Apparent specific gravity of manhole = 1.0. Also some preliminary tests illustrating the mechanism of floatation and related soil displacements for buried pipes and manholes.
Summary of results	- Preliminary tests illustrated the mechanism of floatation, with soil adjacent to the pipeline moving downward and across towards the area below the pipe. - Narrower backfilled region led to less heave of pipeline. - Over excavation and backfill with loose sand below the pipeline led to greater heave. - Placement of the pipeline directly at the base of the trench led to little heave (< 10 % of pipe diameter). - Allowing pore pressure drainage into the surrounding soil led to little heave (< 10 % of pipe diameter). - The manhole heaved virtually the same amount in all tests, by about a third of its embedment depth.

(a) Stage (1)

Pipe
φ =114mm
ρ_p=1.5
loose (Dr=34.4%)

original position — displacement up to the stage (1) or (2)

(b) Stage (2) — 10cm

Observed mechanism of uplift of a pipeline

Box
ρ_b=1.0
loose (Dr=27.3%)
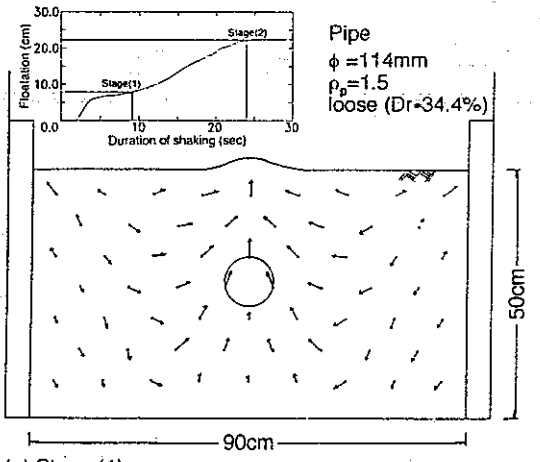
(a) Stage (1)

original position — displacement up to the stage (1) or (2)

(b) Stage (2) — 10cm

Observed mechanism of uplift of a manhole

Figure 14.1 - Study No. 14: Yasuda et al. (1995)

unit (cm)

□ piezometer
■ piezometer (small size, attached at the bottom of the pipe)
△ accelerometer
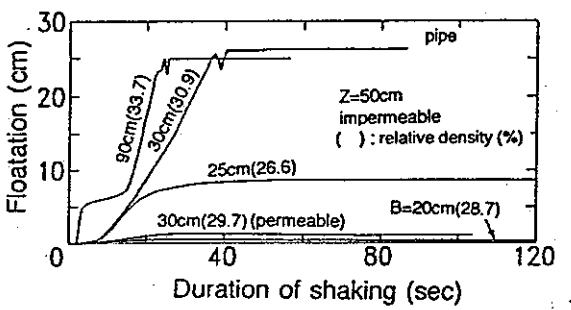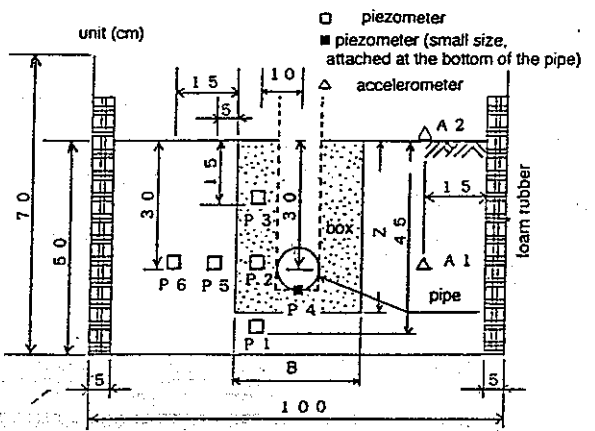
Effect of trench width on displacement of pipeline.


Effect of trench depth on displacement of pipeline.

**Figure 14.2 - Study No. 14: Yasuda et al. (1995)**
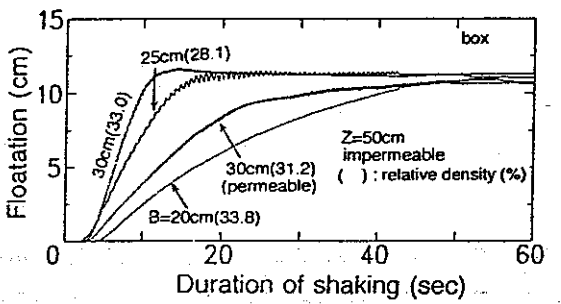
Effect of trench width on displacement of manhole.
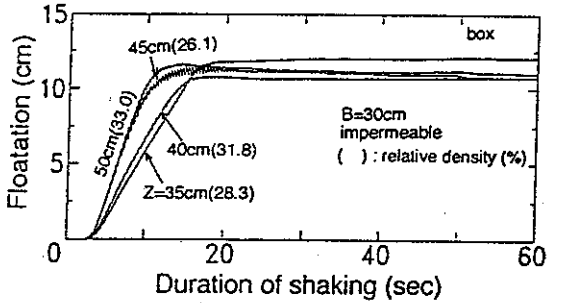
Effect of trench depth on displacement of manhole.

Figure 14.3 - Study No. 14: Yasuda et al. (1995)

Study No. 15: Kawakami (1996)

|	
Structure type	None
Method(s) of treatment	In-ground walls
Modeling technique	Shaking table
Sample size, L, W, H (m)	3.0, 1.0, 0.5
Base shaking acceleration	0.2 to 0.3 g
Base shaking motion	4 Hz sinusoidal
Sand particle size	$D_{50} = 0.2$ mm
Relative density, D_r	50%
Pore fluid	Water
Testing details	Several tests with a single in-ground wall extending across the central quarter of the testing container. Ground surface was sloped at 2 and 4%. Forces acting on the wall due to pressure from the liquefied soil were measured.
Summary of results	- Pressures from flow of liquefied soil are influenced slightly by the initial gradient of the soil surface and the depth of liquefied ground. - Differences between the pressures acting on the upstream and downstream sides of the wall were generally less than 20 %.
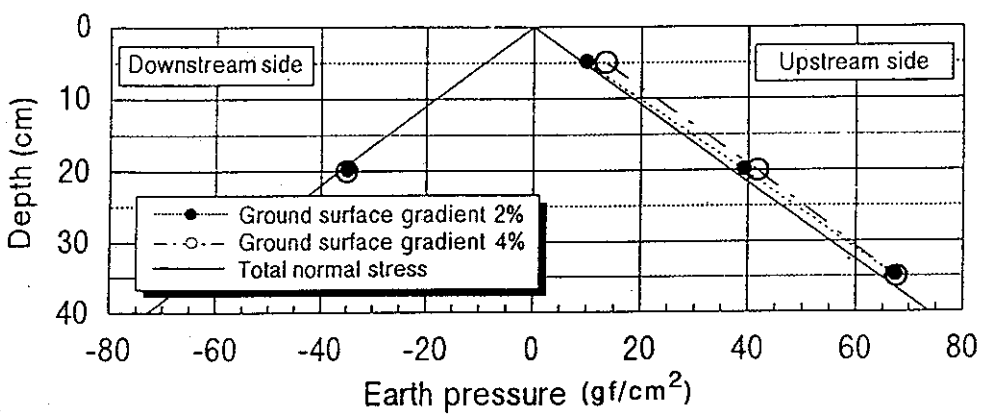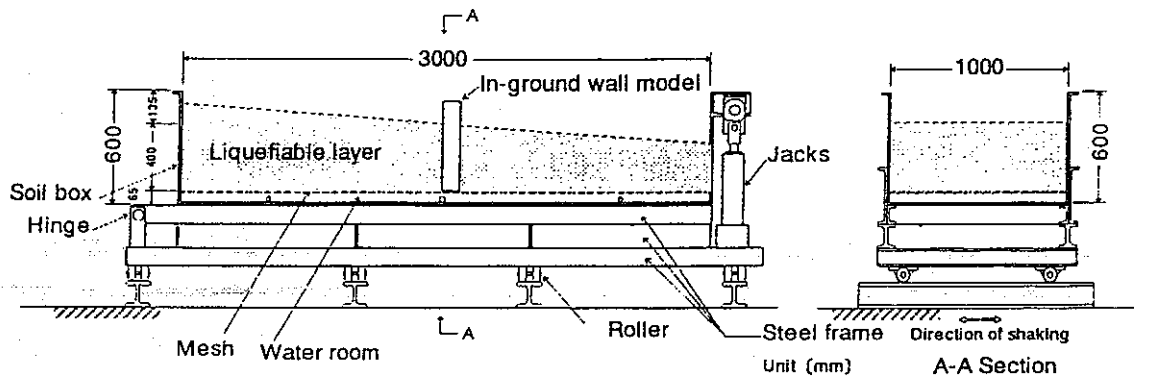
Profile of maximum earth pressure with depth.

Figure 15.1 - Study No. 15: Kawakami (1996)

Study No. 16: Tanaka et al. (1996)

Structure type	Tunnel and embankment
Method(s) of treatment	Sheet pile walls with and without drainage
Modeling technique	Shaking table
Sample size, L, W, H (m)	2.0, 1.0, 1.0
Base shaking acceleration	0.15 to 0.3 g
Base shaking motion	3 Hz sinusoidal
Sand particle size	$D_{50} = 0.38$ mm
Relative density, D_r	42 to 58 %
Pore fluid	water
Testing details	Nine tests with rectangular shaped tunnels within a loose sand deposit. Three different thicknesses of the loose sand for each of the following: (i) no improvement, (ii) sheet pile walls adjacent to the structure, and (iii) sheet pile walls with drainage. The total soil depth was 0.9 m in all cases, with loose sand depths of 0.55, 0.7 and 0.9 m. Where needed, the loose sand was underlain by a dense soil, with D_r = 90 %. Model tunnel 0.5 m wide by 0.25 m high, with 0.15 m cover, had apparent specific gravity of 0.88. Also, five tests conducted with embankments resting upon a loose sand deposit underlain by dense sand: (i) no improvement, (ii) 1.2 mm thick sheet pile walls below the toes, (iii) sheet pile walls with drainage, (iv) sheet pile walls with drains of reduced flow capacity, and (v) sheet pile walls with tie rods between the heads of the walls through the base of the embankment.
Summary of results	• Heave of the tunnel increased as the depth of the liquefiable soil increased. • Sheet pile walls reduced heave to between 30 and 40 % of that recorded without treatment. • Where the loose soil depth below the tunnel was large, sheet pile walls with drainage reduced heave to about 5 % of that recorded without treatment. • Where the loose soil depth below the tunnel was relatively small (0.15 m model scale), the addition of drainage capability to the sheet pile walls had little effect on the recorded heave. • Sheet pile walls with drainage led to reduced pore pressure generation below the tunnel. • Sheet pile wall strains were measured and used to estimate the tunnel heave assuming constant soil volume. The measured and estimated heave was similar, although depended on whether the walls incorporated drainage or not. • Settlement of the embankment was reduced to only about 75 % of the unimproved case by the addition of sheet pile walls. • Including a tie rod between the heads of the walls reduced embankment settlement to about 40 % of the unimproved case. • Drainage elements of reduced capacity led to performance mid way between the undrained sheet piles and the more freely draining sheet piles.

排水孔

(a)鋼管杭タイプ　　　(b)鋼矢板タイプ
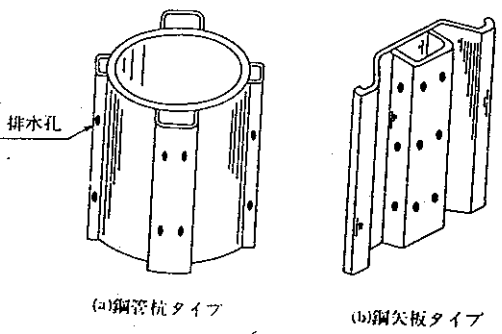
Drainage elements incorporated into a circular pile and a sheet pile.

(a)模型平面図

間隙水圧計
加速度計
変位計
ひずみゲージ
圧力センサ

(b)模型断面図

単位(mm)
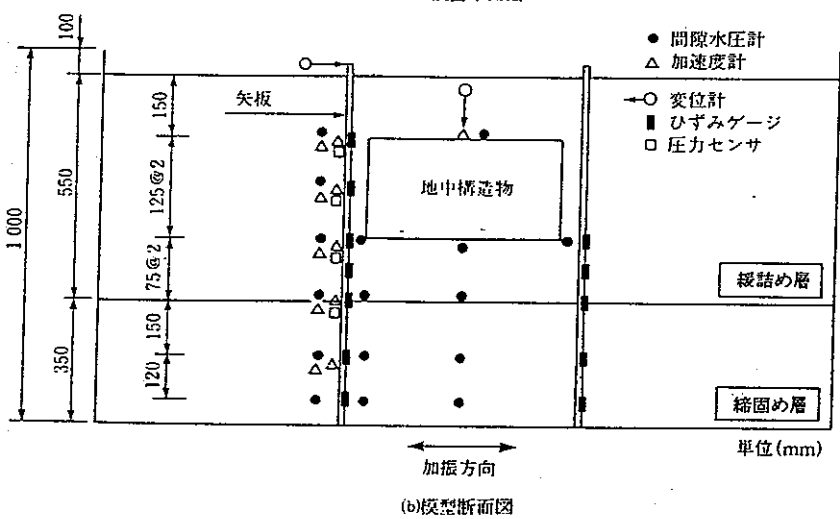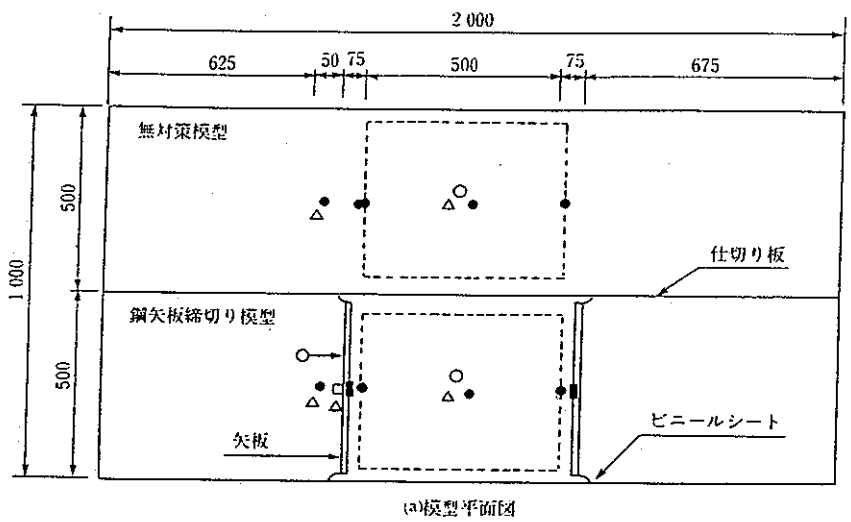
Model layout involving a tunnel.

Figure 16.1 - Study No. 16: Tanaka et al. (1996)
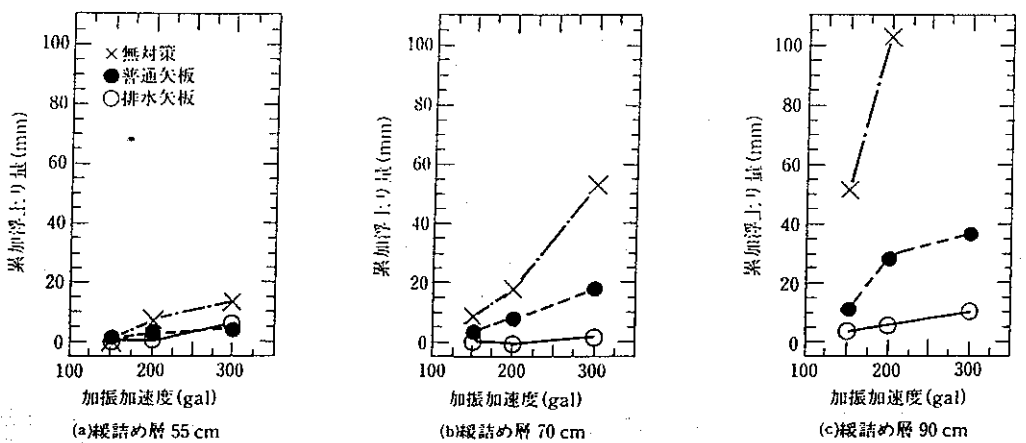
Recorded heave of the tunnel (vertical axis) versus magnitude of shaking event (horizontal axis) for different depths of liquefiable soil. Symbols: cross-unimproved; solid circle-sheet pile walls; open circle-sheet pile walls with drainage.
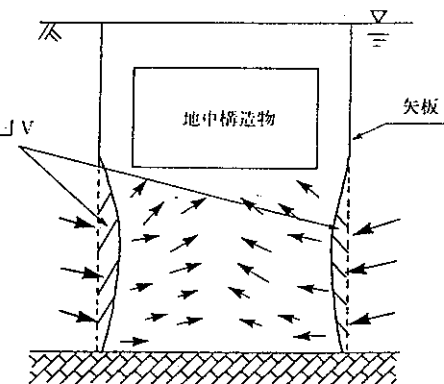

Illustration of volume change due to deflection of sheet pile walls.
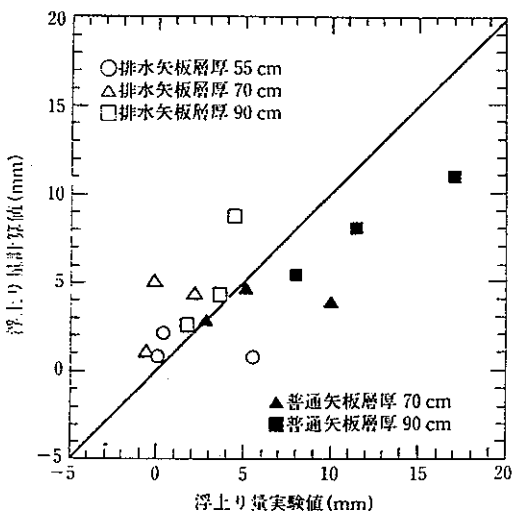
Calculated heave of tunnel from measured wall strains (vertical axis) versus measured heave (horizontal axis)
Open symbols-with drainage; solid symbols-without drainage

Figure 16.2 - Study No. 16: Tanaka et al. (1996)
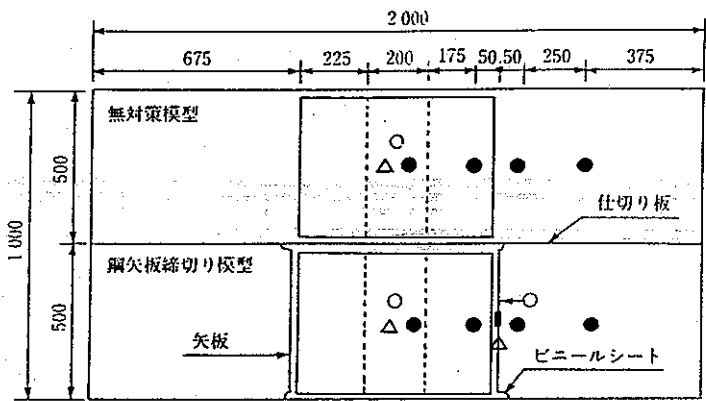
(a)模型平面図
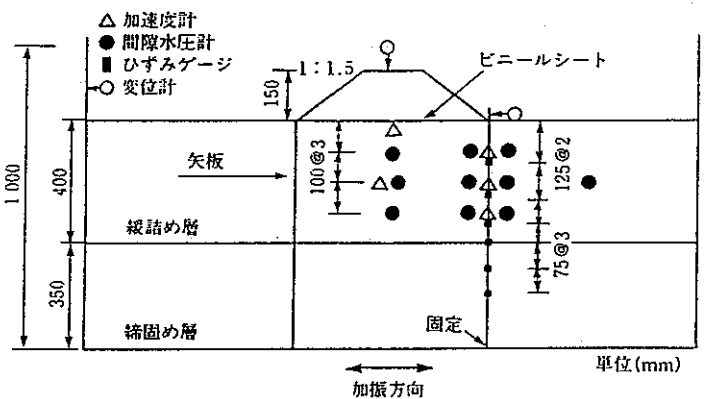
(b)模型断面図

Model layout involving an embankment.
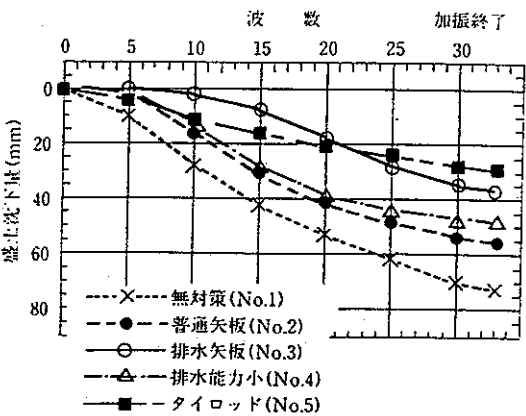
Settlement of embankment versus cycle number during shaking event.

Figure 16.3 - Study No. 16: Tanaka et al. (1996)

Study No. 17: Koga et al. (1991)

|	
Structure type	Embankment and semi-buried road structure
Method(s) of treatment	Stiff impermeable inclusions
Modeling technique	Centrifuge test at 30 g
Sample size, L, W, H (m)	0.8, ?, 0.175
Base shaking acceleration	0.18 g
Base shaking motion	2 Hz sinusoidal
Sand particle size	$D_{50} = 0.2$ mm
Relative density, D_r	60 % (unimproved ground)
Pore fluid	30 cS silicon oil
Testing details	Three tests: (i) embankment on unimproved ground, (ii) embankment with improved regions adjacent to toes, (iii) semi buried road structure with improved regions at sides of structure. Improved regions were stiff and impermeable. Apparent specific gravity of semi buried structure = 1.7.
Summary of results	• Limited data presented. • Pore pressures beneath the embankment dropped during the initial part of the shaking event then gradually rose during the event. • Liquefaction of soil adjacent to the embankment occurred, while soil below the embankment did not. • All soil liquefied in the semi buried road model. • Little heave of the road structure occurred, mainly settlement after the shaking event. • Improvement adjacent to the embankment had little impact on pore pressures, otherwise no comments given on effect of improvement.

■ acc. transducer
● pore pressure transducer
◆ level transducer

2100R

50

G A1
A2
Liquefaction Layer
P1
P2
P3 A3
A4
B5
A5
P6
Supporting Layer
P4
A_BASE
P7

56.6
38.4
270
100
75

300 200 300
800

◆ level transducer   ■ acc. transducer
                       ● pore pressure transducer

50

32.5
62.5
125
50

G A1
A2
A4
S2
S1 P1
P2
P3 A3
P4
A0.
P5
P6
A5

56.6
38.4
100
270
75

200 100 200 100 200
800

◆ level transducer   ■ acc. transducer
                       ● pore pressure transducer

G A1
A4
A6
P1
P2 A2
A3
P4
P5
P6
P7
P8
P3 A0
A5

5.30
5 90
5
140

40
160
270
60

340 10 90 10 340
5 800 5

Geometry of models.

Figure 17.1 - Study No. 17: Koga et al. (1991)
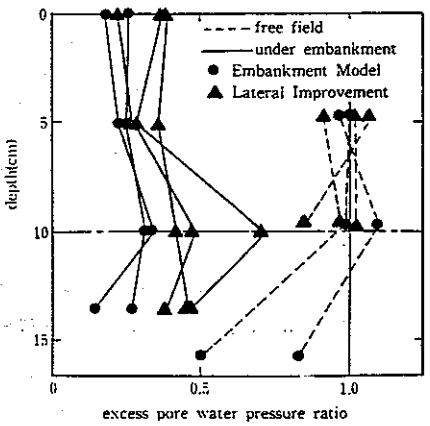
**Variation of excess pore water pressure ratio with depth for embankment model.**
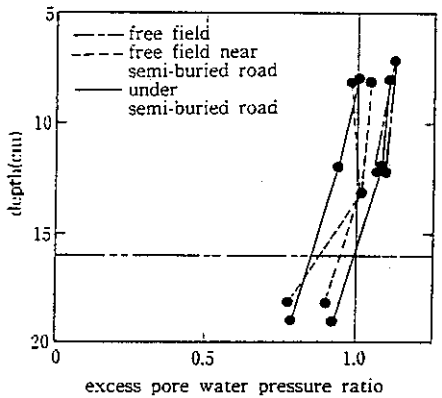
Variation of excess pore water pressure ratio with depth for semi-buried road model.
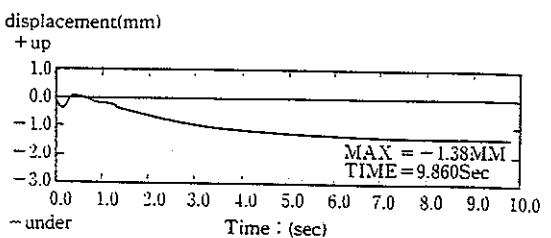
Displacement time history for semi-buried road model.

Figure 17.2 - Study No. 17: Koga et al. (1991)

Study No. 18: Suzuki et al. (1991)

Structure type	None
Method(s) of treatment	Deep cement mixing
Modeling technique	Centrifuge test at 100 g
Sample size, L, W, H (m)	0.35, 0.35, 0.22
Base shaking acceleration	0.2 g
Base shaking motion	3 - 5 Hz sinusoidal containing sharp acceleration spikes
Sand particle size	$D_{50} = 0.2$ mm
Relative density, D_r	52 % (unimproved ground)
Pore fluid	100 cS glycerin
Testing details	Four tests were performed with cellular (grid shaped) in-ground walls, with two different water levels. The width of each cell normal to the direction of shaking was varied. The walls were formed within a loose sand layer overlying a stiff free draining gravel.
Summary of results	- Primarily pore pressure data presented. - Data illustrated a relationship between the wall spacing normal to the direction of shaking across each cell and the measured excess pore pressure ratio within the cell. - For a fully submerged soil deposit, cell widths of less than the liquefiable soil depth were required to reduce pore pressures and prevent liquefaction.
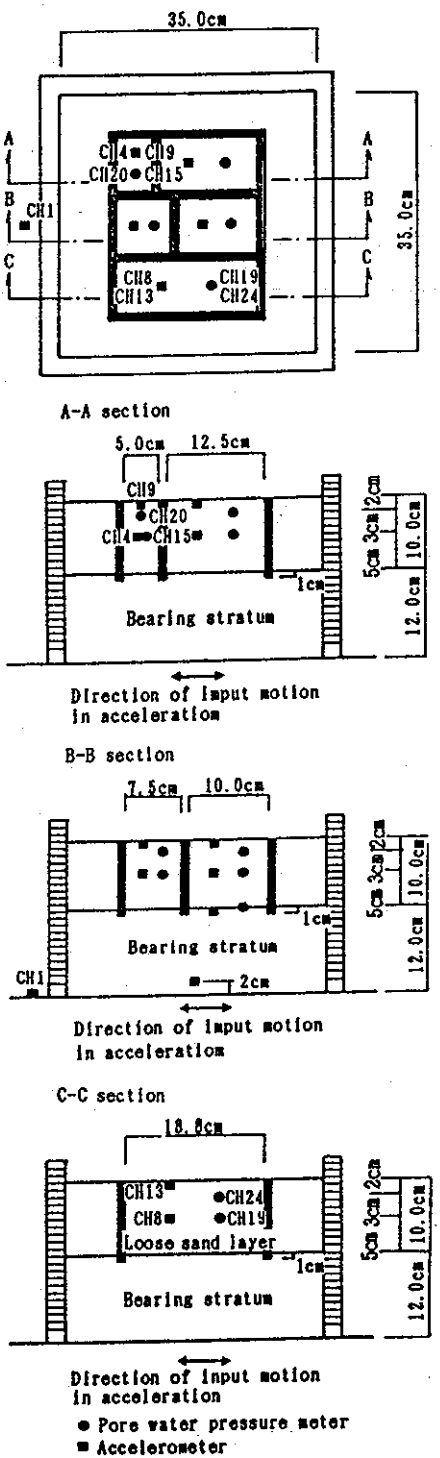
Layout of models.

Figure 18.1 - Study No. 18: Suzuki et al. (1991)
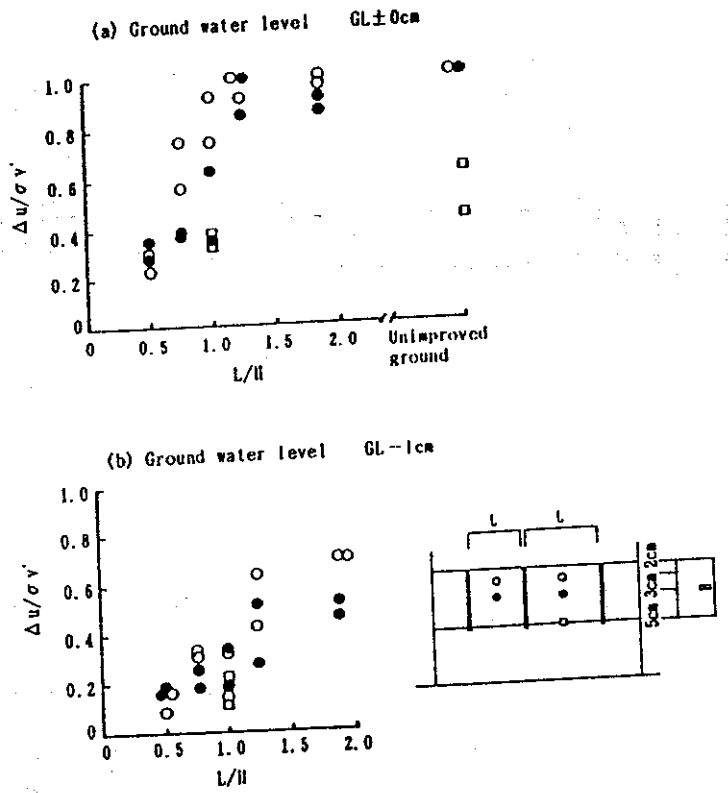
(a) Ground water level   GL±0cm

(b) Ground water level   GL--1cm

Variation of excess pore pressure ratio with ratio of wall
spacing to depth of liquefiable sand.

Figure 18.2 - Study No. 18: Suzuki et al. (1991)

Study No. 19: Babasaki et al. (1991)

Structure type	None
Method(s) of treatment	Deep cement mixing
Modeling technique	Centrifuge test at 100 g
Sample size, L, W, H (m)	0.4, 0.18, 0.18
Base shaking acceleration	0.2 g
Base shaking motion	3 - 5 Hz sinusoidal containing sharp acceleration spikes
Sand particle size	$D_{50} = 0.2$ mm
Relative density, D_r	Intact sample from field site used, SPT N < 10 in situ.
Pore fluid	100 cS glycerin
Testing details	One test on unimproved ground, one test on ground improved with cellular (grid shaped) in-ground walls. Wall spacing in each cell was varied in the direction of shaking. The cell width normal to the direction of shaking was equal to the liquefiable soil depth. The walls were formed within a loose sand layer overlying a stiff bearing stratum.
Summary of results	- Limited data presented. - The unimproved model liquefied during the 0.2 g event. - Excess pore pressures were lower within each cell, with $u/\sigma_v' =$ 0.5 to 0.6 in each cell. - No distinct relationship between wall spacing and excess pore pressure ratio was evident.

Plan   40cm

Plan   40cm

A — A   B — B

18cm

section A — A

section B — B

Loose sand
layer
(e=0.765)

Bearing stratum

5cm 5cm

10cm   7.5cm 5cm

Loose
sand
layer

Bearing stratum

5cm 5cm

8cm   10cm

Direcrion of input motion

Direction of input motion

Legend : O Pore water pressure meter
□ Accelerometer

(a) Unimproved ground

(b) Improved soil foundation

Loose sand layer

Surface of bearing
stratum

Excess pore water pressure
ration Δu/σv'

0.25   0.5   0.75   1.0   Unimproved
ground

L/H

H

Unimproved ground

L

H

Improved ground
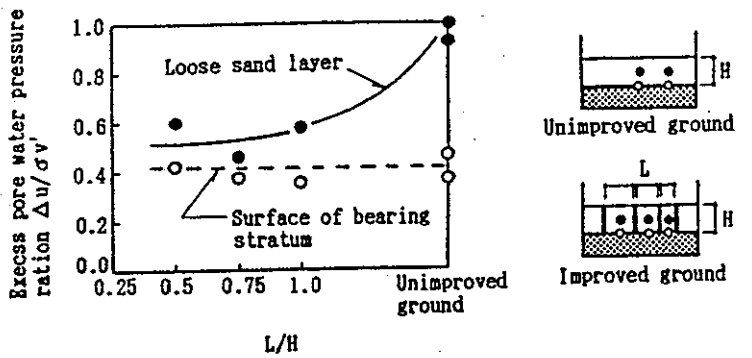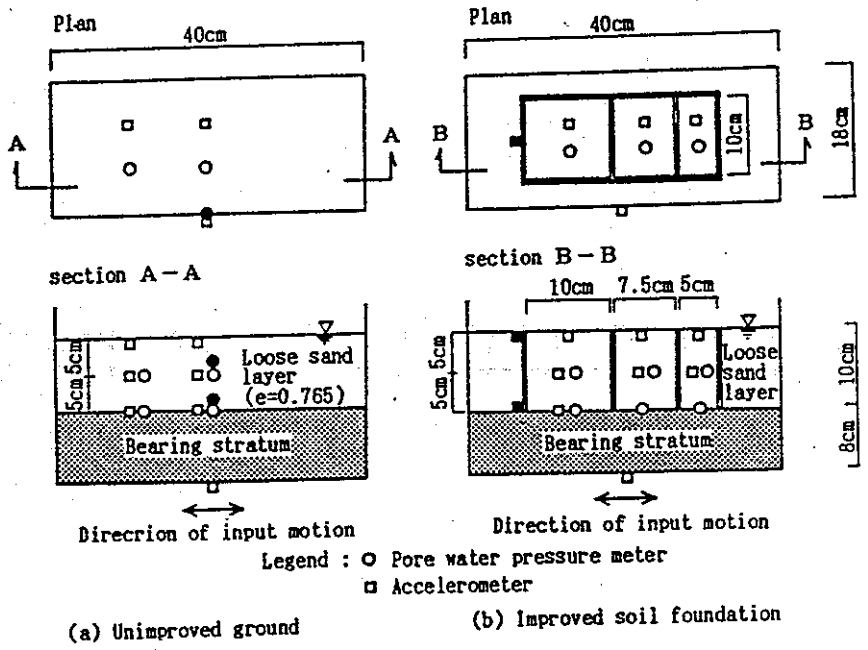
**Variation of excess pore pressure ratio with ratio of wall
spacing to depth of liquefiable sand.**

Figure 19.1 - Study No. 19: Babasaki et al. (1991)

Study No. 20: Liu and Dobry (1994) and Dobry et al. (1995)

|	
Structure type	Surface footing
Method(s) of treatment	Vibrocompaction
Modeling technique	Centrifuge test at 80 g
Sample size, L, W, H (m)	0.46, 0.25, 0.12 to 0.16
Base shaking acceleration	0.17 to 0.36 g
Base shaking motion	1.5 Hz sinusoidal
Sand particle size	$D_{50} = 0.15$ mm
Relative density, D_r	50 % (unimproved ground) 90 % (vibrocompacted area)
Pore fluid	Water
Testing details	Vibrocompaction on a square grid using different depths of compaction below a circular footing. Width of compacted zone maintained at 1.6 times footing width. Tests without ground improvement also reported where the effects of pore fluid viscosity were examined.
Summary of results	• Higher acceleration recorded on footing when ground improved. • Migration of excess pore pressures from the free field into the compacted region below the footing was observed during the shaking events. • Pore pressures at some locations continued to rise after completion of the shaking event due to stress redistribution. • Higher viscosity pore fluid led to higher positive and negative excess pore pressures during shaking.
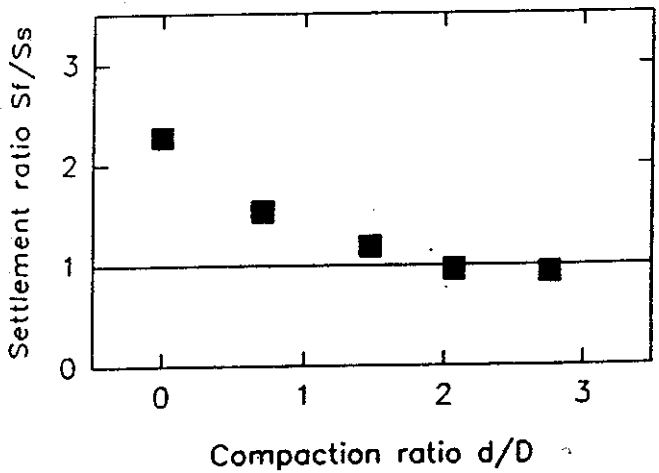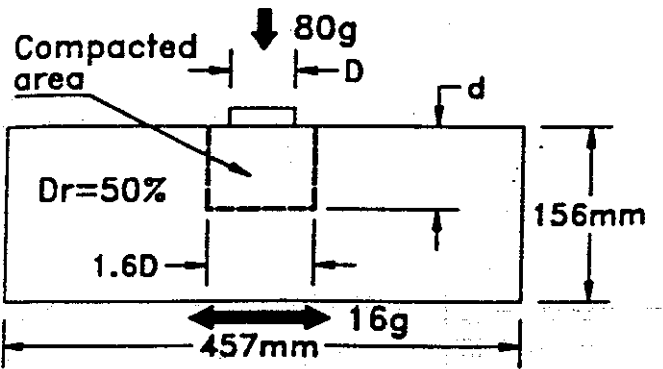
Normalized foundation settlement versus depth of compacted region.

Figure 20.1 - Study No. 20: Liu and Dobry (1994) and Dobry et al. (1995)

Study No. 21: Kimura et al. (1995)

|	
Structure type	Tunnel
Method(s) of treatment	- Gravel drains - Sheet pile walls - Sheet pile walls with drainage
Modeling technique	Centrifuge test at 50 g
Sample size, L, W, H (m)	0.44, 0.15, 0.15
Base shaking acceleration	0.2 and 0.5 g
Base shaking motion	2 Hz sinusoidal
Sand particle size	$D_{50} = 0.1$ mm (sand), 1.47 mm (drains)
Relative density, D_r	35 to 51 % (unimproved ground)
Pore fluid	Water
Testing details	Five tests on a rectangular shaped tunnel in a loose sand deposit: (i) unimproved ground, (ii) one row of gravel drains at each side of the tunnel, (iii) sheet pile walls at each side of the tunnel, (iv) two tests with sheet pile walls incorporating drainage elements. Prototype tunnel dimensions: 5 m wide, 3 m high with about 3 m cover. Apparent specific gravity of tunnel = 0.85. Permeability values: sand = 2×10^{-5} m/s, drains = 4.6×10^{-3} m/s. Drain materials contained within a filter sock. EI for the sheet pile walls = 9×10^{4} kNm^2/m prototype scale. Walls extended to 3 m below the tunnel prototype scale.
Summary of results	- Untreated ground and sheet pile wall without drainage both liquefied; tunnel acceleration was attenuated to about 10% of the input for these cases. Gravel drains led to an attenuation to about 20% of the input. Sheet pile wall with drainage attenuated initially to 40% of the input, rising during shaking to 70%. With a large shake, attenuation was 10 to 20%. - Untreated ground, sheet pile walls without drainage and gravel drains: soil below tunnel liquefied, soil above tunnel did not. Sheet pile walls with drainage: high excess pore pressures but no liquefaction below the tunnel, soil above tunnel gradually liquefies during the shaking event. With stronger shaking sheet pile walls with drainage respond similarly to untreated ground. - Ground treatment reduced upward movement of tunnel, sheet pile wall with drainage settled slightly but heaved under heavy shaking. Displacements explained by suppression of lateral flow of soil by sheet pile walls - verified by observation of lead shot markers. - Where excess pore pressure was below about 0.8 below the tunnel, no heave was observed. - Sheet pile walls without drainage lead to highest differential movement.

O pore pressure transducer

□ accelerometer

L.V.D.T 1 L.V.D.T 2 L.V.D.T 3

sheet pile

[Figure diagram with measurements: 10, 40, A2, S1, P12, 20, 50, S4, A4, P1, E2, S2, 60, E1, P22, 160, P2 P3 P4, S5, P23, 60, 60, S3, P32, 30, P31 A3, S6, A5, 70, 145, 100, 80, 20, 20, 130, 145, 440, A1(input)]
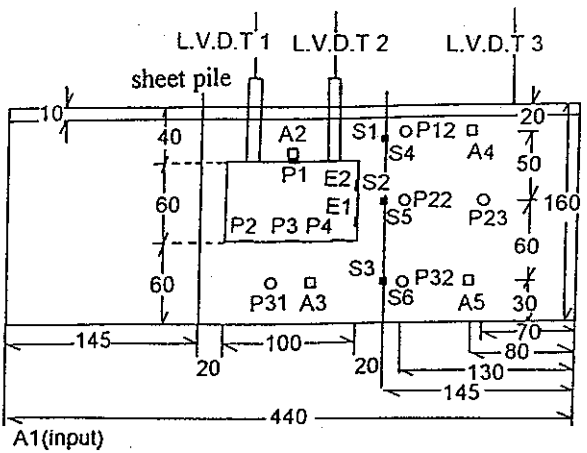
Layout of models.

| Test Codes	model condition	Input acceleration	Observed relative density	Observed degree of saturation	Observed vertical *2) movement of structure
UD0	without Structure	10.4g (208gal) *1)	42%	99%	-
UC1	No countermeasure	10.6g (212gal)	41%	99%	+3.3mm *3) +3.0mm *4)
UD2	sheet pile without drainage	10.8g (216gal)	51%	99%	+2.2mm -1.0mm
UD3	gravel drain	11.5g (230gal)	43%	99%	+1.7mm +1.3mm
UD4	sheet pile with drainage	10.6g (212gal)	46%	99%	-0.7mm -1.0mm
UD5	sheet pile with drainage	24.6g (492gal)	35%	99%	+1.9mm -1.0mm

*1) protoptype.   *2) upward positive.   *3) top : just after shaking.   *4) bottom : at final

Figure 21.1 - Study No. 21: Kimura et al. (1995)
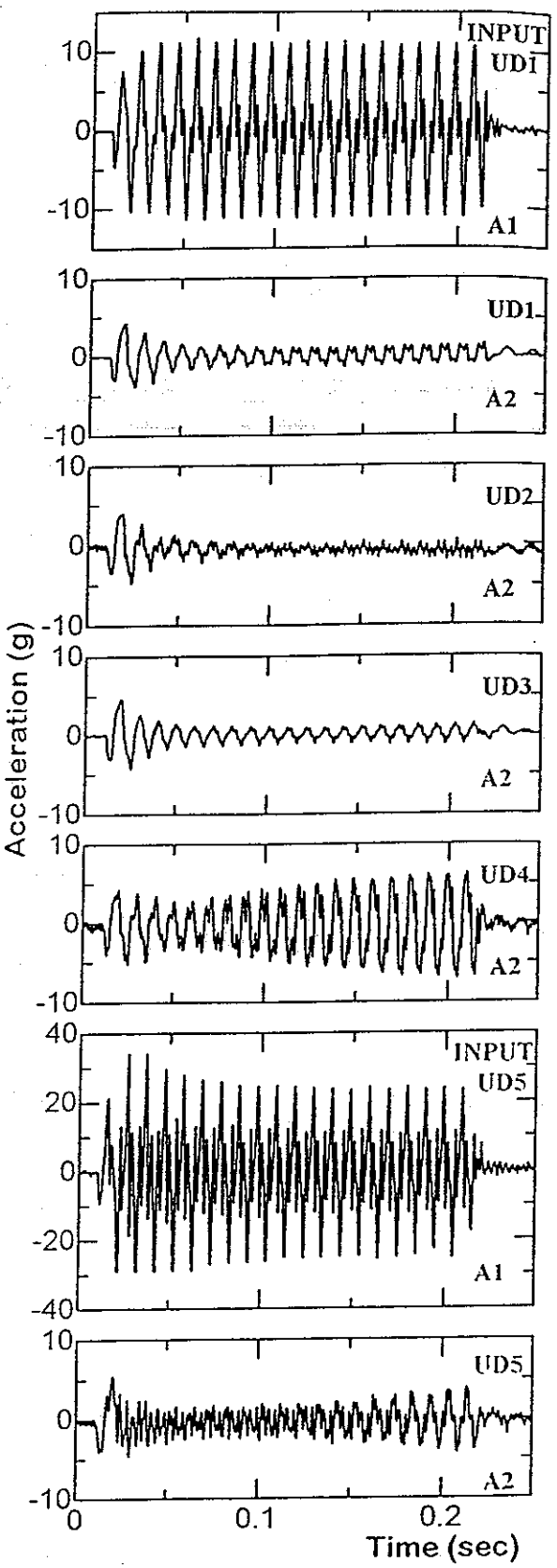
Accelerations measured on the tunnel in each test.

Figure 21.2 - Study No. 21: Kimura et al. (1995)
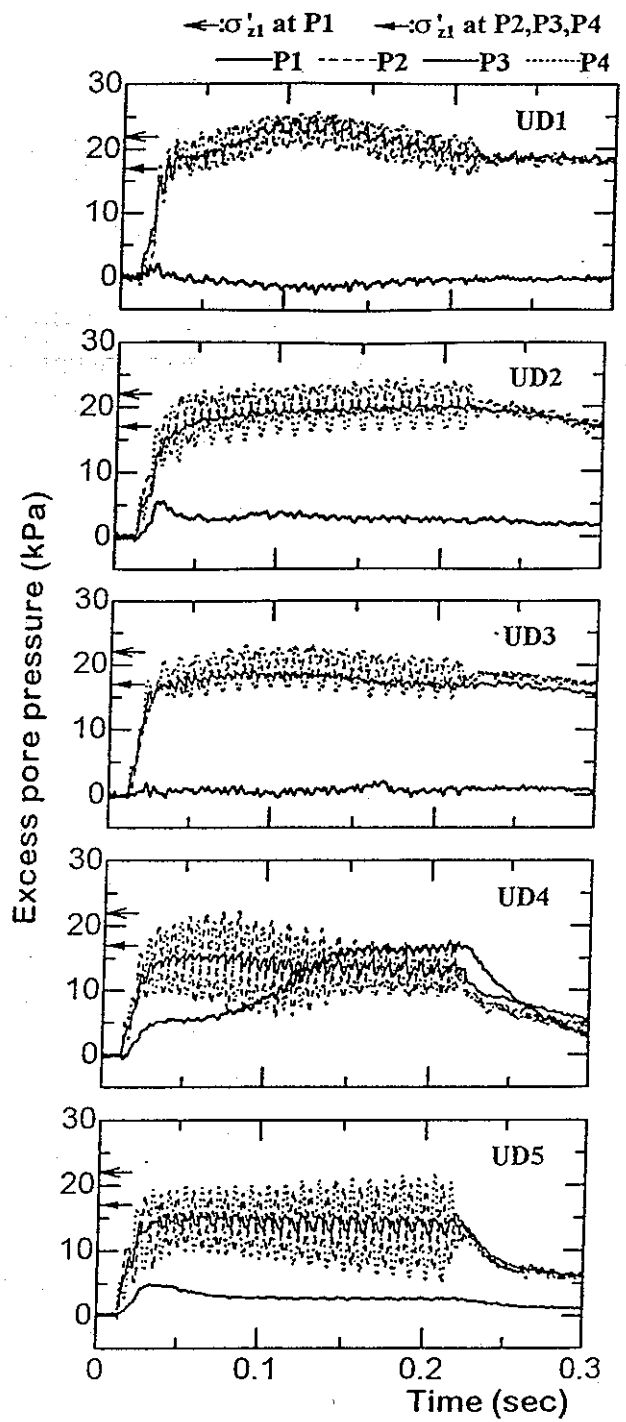
Pore pressures measured at the top (P1) and bottom (P2, P3, P4) of the tunnel in each test.

Figure 21.3 - Study No. 21: Kimura et al. (1995)
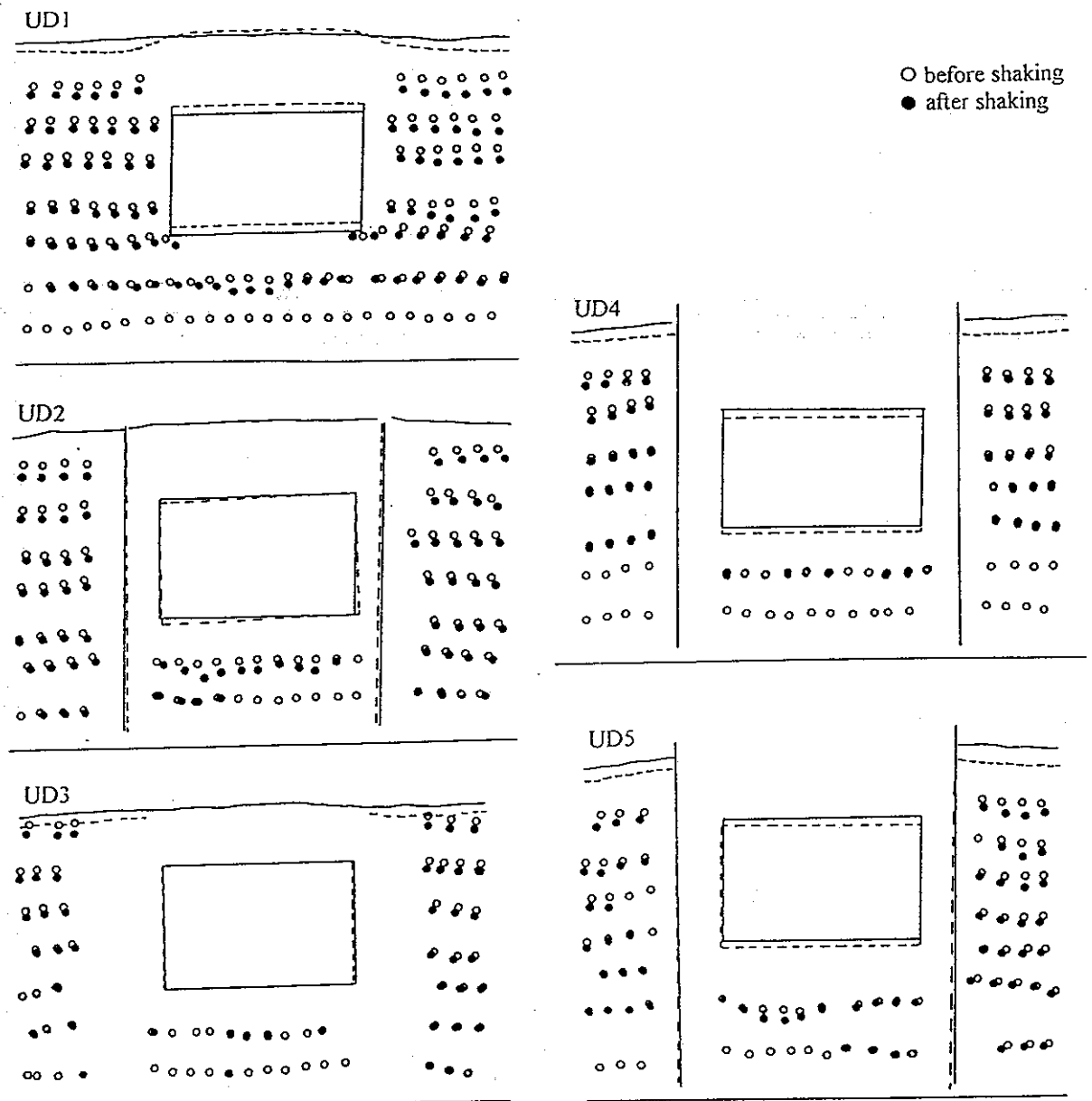
UD1

O before shaking
● after shaking

UD4

UD2

UD5

UD3

**Subsurface soil deformations measured after each test from
lead shot markers embedded in the soil.**

Figure 21.4 - Study No. 21: Kimura et al. (1995)

Study No. 22: Kimura et al. (1995)

Structure type	Oil storage tank
Method(s) of treatment	• Gravel drains • Sheet pile walls • Sheet pile walls with drainage
Modeling technique	Centrifuge test at 50 g
Sample size, L, W, H (m)	0.44, 0.15, 0.15
Base shaking acceleration	0.12 to 0.21 g
Base shaking motion	2 Hz sinusoidal
Sand particle size	$D_{50} = 0.1$ mm (sand), 1.47 mm (drains)
Relative density, D_r	43 to 49 % (unimproved ground)
Pore fluid	Water
Testing details	Seven tests on a rectangular, flexible base tank resting on a loose sand deposit comprising: (i) two tests on unimproved ground, (ii) unsaturated ground, (iii) one row of gravel drains, (iv) three rows of gravel drains, (v) sheet pile walls, and (vi) sheet pile walls with drainage. Prototype tank width = 7 m. Permeability values: sand = 2×10^{-5} m/s, drains = 4.6×10^{-3} m/s. Drain materials contained within a filter sock. EI for the sheet pile walls = 9×10^4 kNm²/m prototype scale.
Summary of results	• Higher excess pore pressures recorded adjacent to the tank than below it. • Three rows of gravel drains were significantly more effective than a single row, approximately halving the excess pore pressures beneath and adjacent to the tank. • Sheet pile walls without drainage led to the highest values of excess pore pressure developing at the side of the structure, since the wall carried load from the tank and reduced the mean stress in this area. • Sheet pile walls with drainage caused the greatest suppression of excess pore pressures, followed closely by three rows of gravel drains. • Relatively high differential settlements (80 mm) were recorded across the tank with one row of gravel drains. Three rows reduced the average settlement slightly, but virtually eliminated differential settlements. • Very similar average settlements were recorded with three rows of gravel drains, sheet pile walls and sheet pile walls with drainage. • Suppression of lateral displacements identified as important in reducing total and differential settlements.

O pore pressure transducer

□ accelerometer
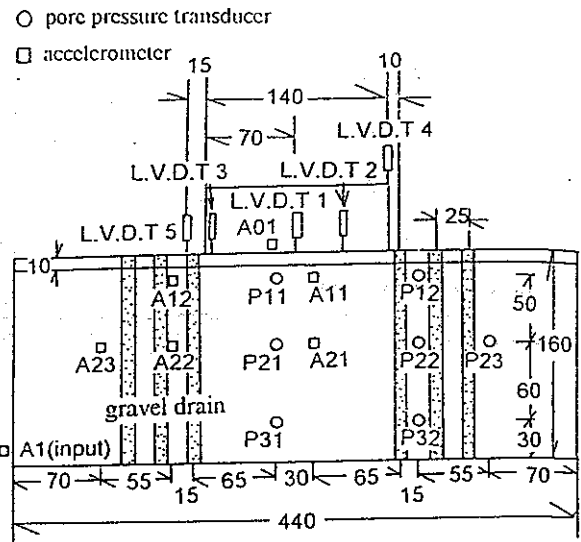
(a) reinforced with gravel drain
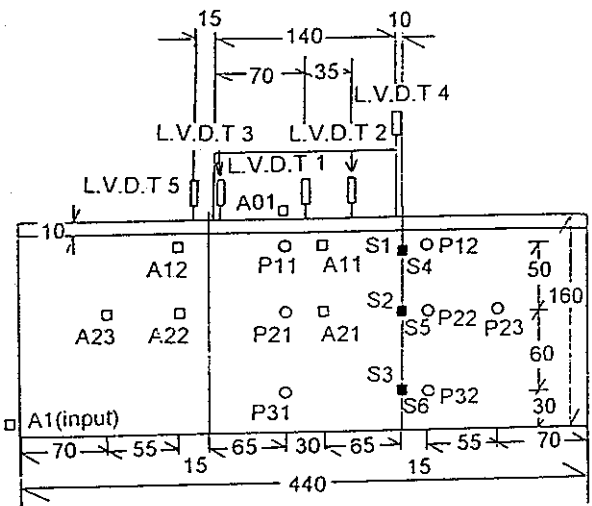
(b) reinforced with sheet pile wall

Layout of models.

Figure 22.1 - Study No. 22: Kimura et al. (1995)

Test code	Model conditions	Input acceleration	Observed relative density	Observed degree of saturation
TD1	No countermeasure	6.3g (125gal)*1)	47%	95%
TD2	No countermeasure	10.0g (200gal)	43%	91%
TD3	Non-saturated	10.7g (214gal)	44%	32%
TD4	Gravel drain 1 row	10.0g (200gal)	43%	96%
TD5	Gravel drain 3 rows	10.6* (212gal)	45%	93%
TD6	Sheet pile without drainage	10.8g (216gal)	49%	99%
TD7	Sheet pile with drainage	10.5g (210gal)	49%	99%

*1) prototype sacle,
*2) Irregular inupt motion was subjected at the early stage
of shaking: see Fig.19(b)

beneath the structure   adjacent to the structure

Excess pore pressure ratios versus depth.
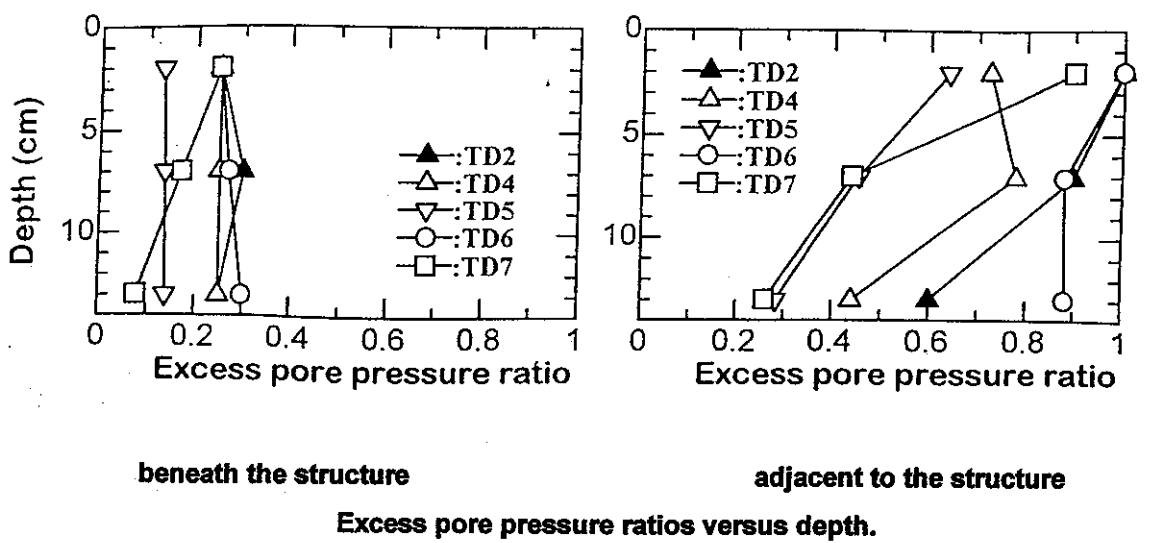
Figure 22.2 - Study No. 22: Kimura et al. (1995)

beneath the tank →:σ'_{z0} ⇒:σ'_{z1}

——:P11 ----:P21 ·······:P31

at the side of the tank

——:P12 ----:P22 —·—:P23 ·······:P32
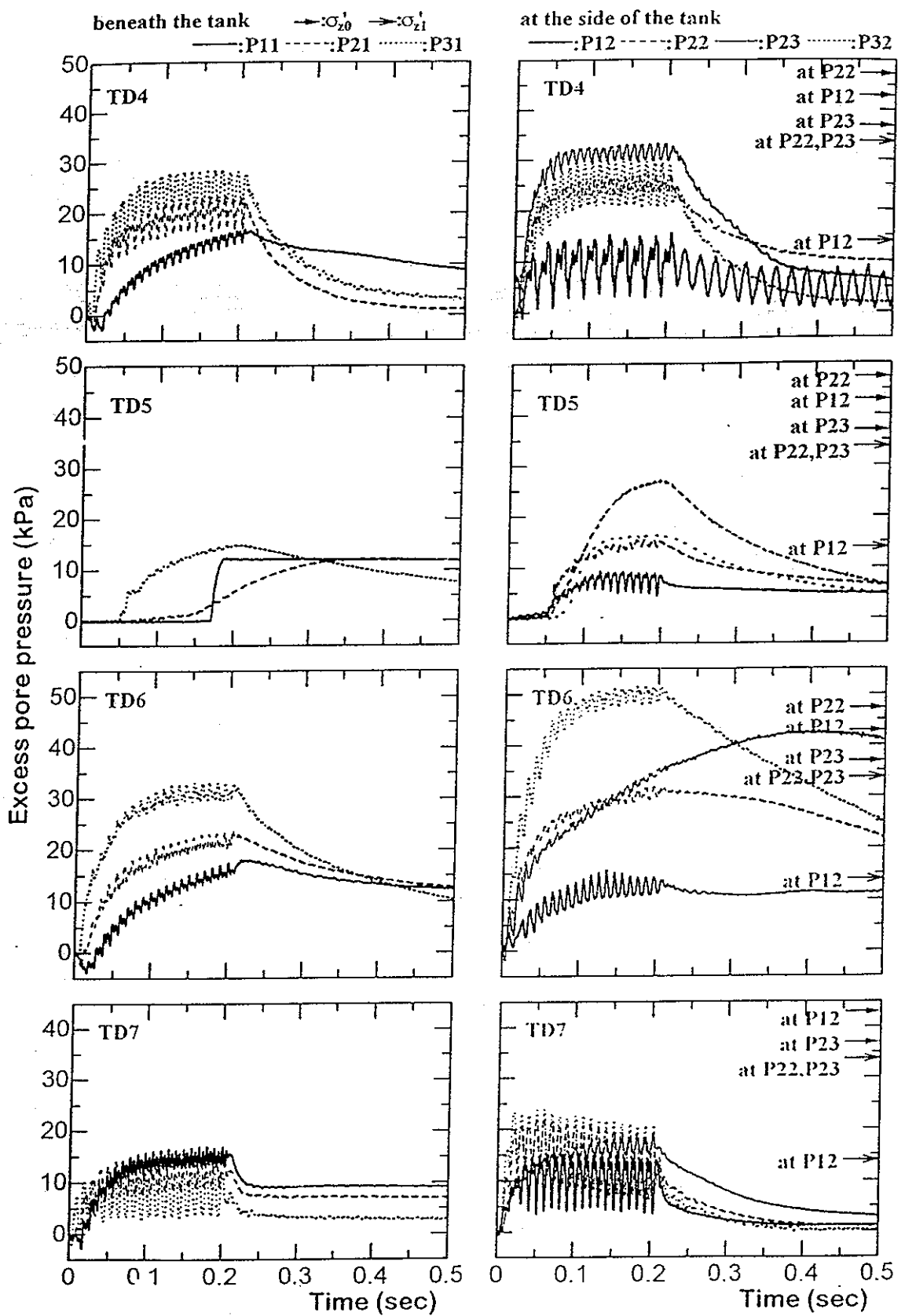
Pore pressures measured in each test.

Figure 22.3 – Study No. 22: Kimura et al. (1995)
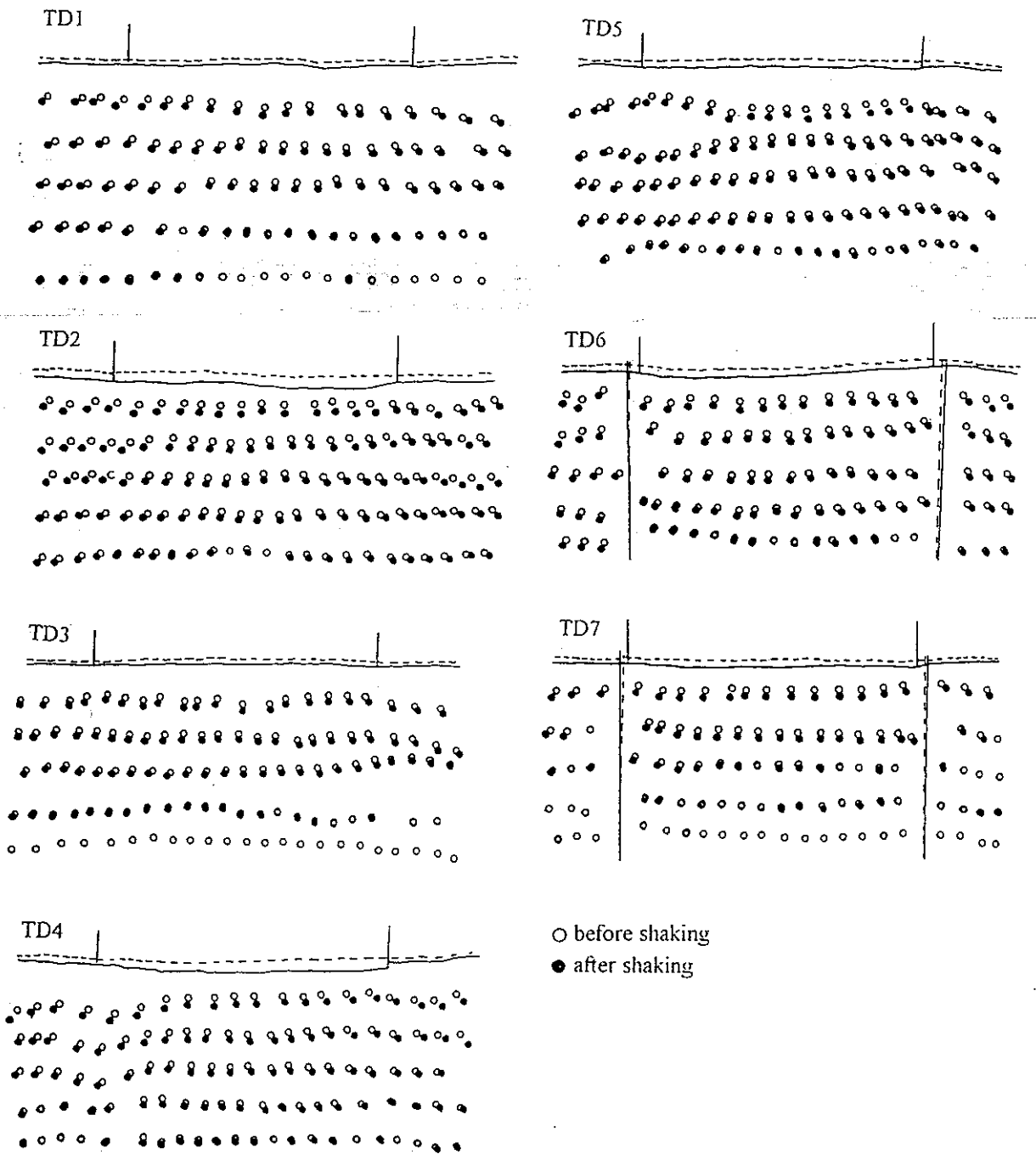
TD1

TD5

TD2

TD6

TD3

TD7

O before shaking
● after shaking

TD4

**Subsurface soil deformations measured after each test from
lead shot markers embedded in the soil.**

Figure 22.4 - Study No. 22: Kimura et al. (1995)
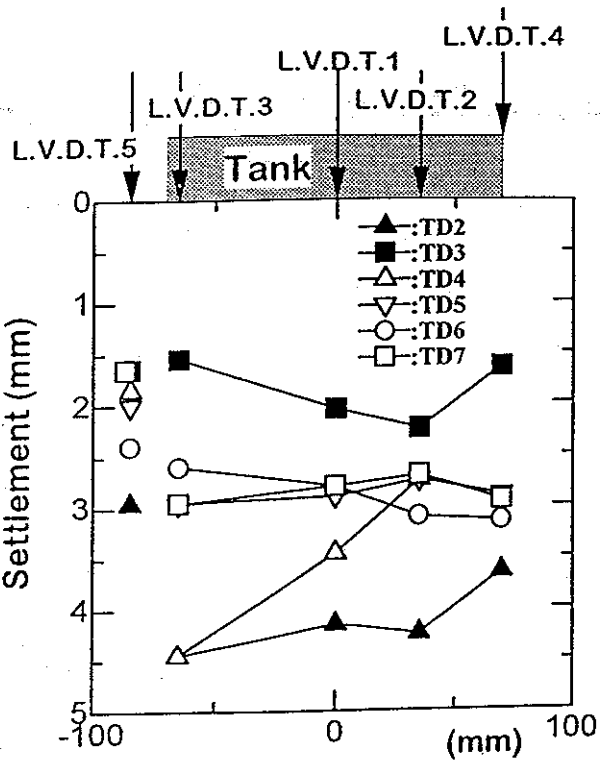
Settlement profiles measured across the base of the tank.

Figure 22.5 - Study No. 22: Kimura et al. (1995)

Study No. 23: Onoue et al. (1987)

|	
Structure type	None
Method(s) of treatment	Gravel drains
Modeling technique	Insitu test
Shaking motion	7 Hz sinusoidal
Sand particle size	$D_{50} = 0.9$ mm (sand) = 7 mm (gravel)
Relative density, D_r	SPT N = 3 to 15
Pore fluid	Water
Testing details	1.2 m diameter steel pipe driven to 11 m depth, 0.3 to 0.5 m diameter gravel drain installed in center of pipe using an auger. Filter cloth generally used around drain circumference. Steel pipe vibrated vertically to induce liquefaction in soil around drain. Permeability values: sand = 1.5×10^{-4} m/s, gravel = 6×10^{-2} m/s.
Summary of results	- Liquefaction occurred without drain. - Excess pore pressure in the soil reduced with increasing drain diameter. - At any depth, excess pore pressure observed to be virtually the same in the drain as in the surrounding soil. - Permeability of the drain was observed to reduce by about 60 % due to clogging when no filter bag was used; liquefaction of drain itself occurred in this case. - Data showed that well resistance is very significant and should be incorporated in design.

Accelerometer
at pipe head
(Z0)

Contents
P15 : pore pressure
meter
(XI5, YI5, ZI5) :
accelerometer in
(radial, tangential,
vertical) directions

Cohtents
PO5 & (XO5,
YO5, ZO5)

Contents
PI8 & (XI8,
YI8, ZI9)

Contents
PO8, (XO8,
YO8, ZO8)

Impermeable
layer

GL.+1.0m
GL.±0.0mm
GL.-1.0m
GL.-5.0m
GL.-8.0m
GL.-10.0m
GL.-11.0m

PO1 PC1
C15
CO5 PC5
C18
CO8
PC8

1200mm

Symbols
Accelerometer ,   ● Pore pressure meter
Capsule of pore pressure meter and
accelerometer (in three directions)

(a) Vertical cutaway

Before experiments
---●--- γt = 17.08KN/m³
---○--- γt = 16.31KN/m³
---×--- γt = 17.07KN/m³
After additional
experiment using Exp.4 system
(with filter cloth bag)
Before
experiments
After experiment 5
(without filter cloth bag)

Coefficient of permeability, kw (cm/sec)

Hydraulic gradient, i

Reduction in permeability of gravel drain due to clogging.

Figure 23.1 - Study 23: Onoue et al. (1987)
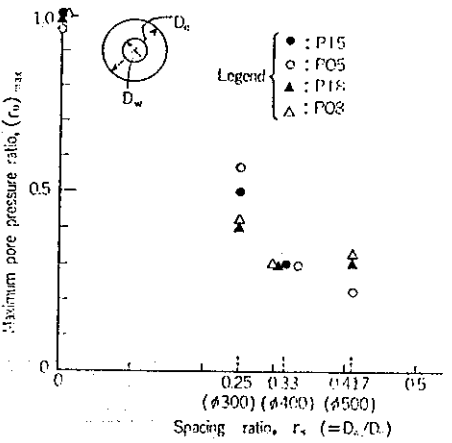
Reduction in pore pressure ratio with increasing d_w/d_e ratio
(ie. reducing tributary volume)
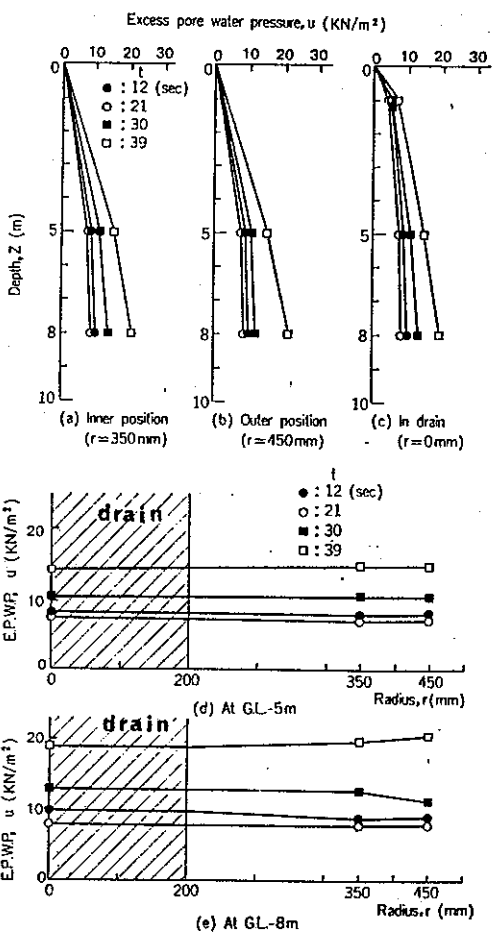
Distribution of excess pore pressures with depth and with radius.

Figure 23.2 - Study 23: Onoue et al. (1987)